TITLE: Polymeric microspheres for local delivery of proteins by administration under the kidney capsule
AUTHOR: Filis Kazazi Hyseni

ISBN: 978-94-6203-868-4

Printed by CPI - KONINKLIJKE WÖHRMANN

Cover *"Polymeric microspheres loaded with near-infrared labelled protein"*; illustration by Beni Cufi (bennycufi@gmail.com)

The printing of this thesis was financialy supported by:
Purac Biomaterials and TA Instruments

Financial support by the Dutch Kidney Foundation for the publication of this thesis is gratefully acknowledged.

The work in this thesis was funded by Project P3.02 DESIRE of the research program of the BioMedical Materials institute, co-funded by the Dutch Ministry of Economic Affairs.

Polymeric microspheres for local delivery of proteins by administration under the kidney capsule

Polymere microsferen voor lokale afgifte van eiwitten onder het nierkapsel
(met een samenvatting in het Nederlands)

Proefschrift

ter verkrijging van de graad van doctor aan de Universiteit Utrecht op gezag van de rector magnificus, prof.dr. G.J. van der Zwaan, ingevolge het besluit van het college voor promoties in het openbaar te verdedigen op maandag 28 september 2015 des ochtends te 10.30 uur

door

Filis Kazazi Hyseni

geboren op 24 november 1979 te Prizren, Kosovo

Promotor:	Prof.dr. W.E. Hennink
Copromotoren:	Dr. R.J. Kok Dr. C.F. van Nostrum

“But time is short, and science is infinite…”

Thomas Hardy (1840-1928)

Table of contents:

Chapter 1	Introduction	9
Chapter 2	Computer modeling assisted design of monodisperse PLGA microspheres with controlled porosity affords zero order release of an encapsulated macromolecule for three months	23
Chapter 3	Biocompatibility of poly(D,L-lactic-co-hydroxymethyl glycolic acid) microspheres after subcutaneous and subcapsular renal injection	59
Chapter 4	Release and pharmacokinetics of near-infrared labeled albumin from monodisperse poly(D,L-lactic-*co*-hydroxymethyl glycolic acid) microspheres after subcapsular renal injection	87
Chapter 5	A comparison of different encapsulation methods for the formulation of recombinant erythropoietin in polymeric microspheres	121
Chapter 6	Summary and future perspectives	153
Appendices	Nederlandse Samenvatting Acknowledgments List of Publications Curriculum Vitae	165

Chapter 1

Introduction

1. Renal diseases and renal replacement therapy

The kidneys play a pivotal function in the maintenance of fluid and solute homeostasis, and regulation of the acid-base balance and water-salt balance. Acute kidney injury (AKI) and chronic kidney disease (CKD) are conditions characterized by the inability of the kidneys to adequately filter waste products from the blood. These conditions are associated with high mortality rates and commonly followed by increased cardiovascular morbidity and mortality [1]. AKI occurs in 5% of hospitalized patients [2] and CKD affects an estimated 10% of the population of the world [3]. The incidence of AKI and CKD is growing rapidly as a result of increased prevalence of diabetes and obesity [4]. Effective measures to prevent and/or slow the progression of AKI [5] and CKD [3] are to a certain extent available, but patients still develop renal failure [6].

Renal replacement therapy (dialysis and renal transplantation) remains the most common therapy in the treatment of AKI and CKD. Its target is to mimic the functions and physiology of the native organ [7]. Nevertheless, patients on dialysis have mortality rates up to 50-70% within the first year of treatment. This very high percentage of mortality is mainly due to secondary complications such as infection and cardiopulmonary complications [8,9]. While renal transplantation is an intervention that leads to an improved survival rate, it is characterized by a persistent donor shortage, incompatibility issue between donor and recipient, the need of using long-term immunosuppressive drugs and patient socio-economic status [10].

2. Novel approaches in the treatment of kidney diseases

The current treatment options for AKI and CKD mainly focus on optimizing renal and cardiovascular risk factors by controlling the blood pressure, albuminuria, blood glucose and blood lipids [11]. However, these measures are not effective in a significant number of patients since the high risk for developing renal failure remains. In the recent years, this has led to increased activities in investigating novel treatment approaches [3,5].

A relatively recent and promising opportunity for the treatment of renal diseases is the use of regenerative medicine. The objective of regenerative medicine is to regrow or repair a damaged organ or tissue and as such represents an attractive alternative route for renal replacement therapy [12]. Restoration and regeneration of kidney tissue can be made with the application of stem cells or stem cell-based therapy or with bioengineering in order to restore the structure and function of the kidney [12-17]. These therapies are yet in their infancy and face many obstacles as a result of the difficulties in cell growth and expansion *in*

vitro [12]. Nevertheless, as the number of patients with renal diseases increases, there is an urgent need for new therapies that are superior to dialysis.

Drug delivery to the kidney is another emerging technique that can evolve in new pharmacotherapeutic strategies for kidney diseases. Current studies focus on local administration of therapeutics by injection of a depot in the kidney, or by using drug targeting strategy where systemically injected drugs accumulate in the kidney. Approaches for drug targeting to the kidney include carrier systems or conjugates that accumulate specifically in kidney tissue after intravenous administration [18]. Considering the administration route, intravenous injection is being used more commonly, which results in the accumulation of the therapeutics in the kidney *via* reuptake by proximal tubular cells from the urine [18]. Other targeted delivery routes include injection via renal artery [19], renal vein [20], renal infusion [21] or intraperitoneal administration [22]. A more local delivery approach is the subcapsular renal injection, where drug eluting depots are injected between the capsule and the cortex with a small needle. Recent studies have worked on the intrarenal drug delivery from hydrogel carriers that were implanted under the kidney capsule [23,24]. Primarily, the authors showed the feasibility of the subcapsular renal injection as a local delivery of therapeutics to the kidney.

3. Role of therapeutic proteins as novel drugs in the treatment of kidney related diseases

Local inflammatory processes and renal fibrosis are central in the pathogenesis of AKI and CKD and are main causes of progression towards renal failure [25-27]. Renal fibrosis represents a failed wound-healing process of the kidney tissue after chronic, sustained injury. Therefore, inhibition of profibrotic mediators might slow or arrest the progression of kidney diseases [26]. Many studies report improvement of the renal function and/or structure by inhibiting factors that promote fibrosis, such as TGF-β, connective tissue growth factor, myofibroblast activation and tumor necrosis factor-α, or enhancing factors that attenuate fibrosis, such as bone morphogenetic protein-7 (BMP-7) and hepatocyte growth factor (HGF) [26,28]. In this respect, several protein drugs are recognized as potential therapeutics for the treatment of renal diseases. Some of them are described in the next section.

The anti-inflammatory interleukin IL-10 was studied as a single intravenous dose in a rat model of renal transplantation and in mice with either ischemic or cisplatin induced or acute renal failure [29]. IL-10 significantly inhibited renal damage and showed a protective effect from renal dysfunction following injury, most probably by inhibiting the activation of genes that cause leukocyte activation and adhesion.

BMP-7 is also known for its protective role in various animal models of acute and chronic renal failure by decreasing the secretion of pro-inflammatory

cytokines and growth factors [30,31]. Intramuscular administration of interferon-γ to rats also proved to have protective effects in the kidney against the development of fibrosis in ureteral obstruction models [32].

Erythropoietin (EPO) has been recently studied in kidney related injuries for its renoprotective effects. EPO regulates the production of red blood cells and it is widely used for the treatment of anemia in chronic kidney disease and chemotherapy-induced anemia in cancer patients [33]. However, recent studies also show non-hematopoietic effects of EPO, such as cardioprotective, neuroprotective, wound healing properties [33] and renoprotective effects [34]. It was demonstrated that the intraperitoneal administration of EPO to rats with ischemic acute kidney injury significantly accelerated renal structural and functional recovery [22]. This makes EPO a promising and attractive drug candidate for the treatment of AKI and CKD.

4. Polymeric microspheres for the delivery of proteins

Due to the poor absorption from the gastrointestinal tract, proteins require administration via injection, which is usually not patient-friendly. In addition, some protein drug candidates are characterized by a short half-life and enzymatic degradation. The development of novel drug delivery systems, such as protein loaded polymeric microspheres, could overcome these shortcomings by encapsulating proteins and enabling a local and sustained release [35-39]. However, some important characteristics are required to be fulfilled by polymeric microspheres in order to achieve this. Polymers used should preferably be biocompatible, biodegradable and non-toxic. The methods for the preparation of microspheres need to be protein friendly and not cause aggregation or other structural changes to the protein. Importantly, the encapsulated protein has to maintain its biological activity and not to be immunogenic which might result from e.g. aggregation of the protein in matrices that form the delivery vehicles [40,41]. Other important characteristics required of polymeric microspheres are a high loading efficiency and high loading capacity of the loaded protein, low burst release when in contact with the release medium and preferably a continuous zero-order release of the payload.

Several natural and synthetic biodegradable polymers have been used for the preparation of drug delivery systems. A frequently studied polymer for the development of polymeric drug delivery systems is poly(lactide-*co*-glycolide acid) (PLGA) [35,42,43]. Although PLGA has been used in many studies, it also has some drawbacks, particularly for the entrapment of pharmaceutical proteins [40,44,45]. Many encapsulated proteins show incomplete release as a result of structural changes in the protein structure caused by the polymer-protein interactions [46,47], the formation of acidic degradation products in microspheres [48], methods used for preparation of microspheres [49] or storage conditions [50].

Different approaches have been investigated to overcome these drawbacks of PLGA microspheres in order to obtain protein friendly matrices for release. Researchers have focused on the modification of the polymer structure by incorporating hydrophilic groups [51-54], neutralizing acidic degradation products using additives [48,55] or the addition of stabilizers in order to protect the protein structure during preparation of the microspheres [56]. Another possibility for protecting the protein structure during formulation preparation is by application of different encapsulation methods as discussed henceforth.

Hydrophilic molecules, such as therapeutic proteins and peptides, are mainly encapsulated into polymeric microspheres with the water-in-oil-in-water (w/o/w) emulsion solvent evaporation method [57]. In the w/o/w method, an aqueous solution, in which the therapeutic protein is dissolved, is emulsified into an organic solution of the polymer. This primary w/o emulsion is then added to a second water phase containing stabilizers, such as polyvinylalcohol (PVA). Subsequently, the solvent is removed by extraction or evaporation and the microspheres are collected by filtration or centrifugation. The different formulation and processing parameters strongly influence the characteristics of the formed microspheres, such as size, porosity and the release profile of the encapsulated macromolecules [58-60]. However, when proteins are encapsulated with this method, the protein stability remains an issue. In the w/o/w method, the protein can aggregate already during the preparation of the first w/o emulsion, where proteins tend to adsorb at water/organic solvent interface which in turn can result in protein unfolding, inactivation and irreversible aggregation [49,61-63]. Recently water-free methods have been introduced as alternative methods for encapsulation of proteins into polymeric microspheres. In these methods, protein powders are suspended in an organic solution of the polymer, which is then emulsified in a water phase or in an oil phase, producing solid-in-oil-in-water (s/o/w) or solid-in-oil-in-oil (s/o/o) emulsions, respectively [64-66]. The advantage of the water-free methods is that the protein is in its solid state during the preparation of microspheres. Proteins in the dehydrated state have less conformational mobility and are therefore less likely to unfold during processing [62,67,68]. Although these methods potentially are superior to the w/o/w method, they also have some drawbacks. Aggregation of proteins has reported to occur during the s/o/w method as a result of the exposure of the dry protein powder to the polymeric organic phase. Aggregation can also occur in combination with the subsequent homogenization step and due to the exposure of protein to the o/w interface formed upon addition of the emulsifier [69]. Also, the burst release represents a major drawback for particles prepared using the s/o/o method due to the protein particles exposed to the surface leaving behind pores that may be connected to more deeply buried protein particles [67,70].

5. Aim and outline of the thesis

The project described in this thesis is part of the BioMedical Materials (BMM) project named DESIRE (Device for Smart Intervention in Renal Repair), which aims at developing polymeric delivery systems for the treatment and/or prevention of inflammation in the diseased kidney (www.bmm-program.nl). These delivery systems will be injected locally under the kidney capsule and can deliver the therapeutic cargo to the kidney over a certain time period.

The aim of this thesis is to investigate the feasibility of polymeric microspheres as injectable depot formulations for the delivery of (therapeutic) proteins to the kidney. Model macromolecules and proteins were used as well as a therapeutic protein, erythropoietin, in order to optimize the encapsulation method and to obtain insight into conditions that play role in preserving the structural integrity of the encapsulated biopharmaceutical payload. In addition, the fate of microspheres was studied after subcapsular renal injection and the release and subsequent pharmacokinetics of a model protein released from such a locally injected depot was studied in rats.

Microspheres were prepared with microsieve™ method (Nanomi B.V., Oldenzaal, The Netherlands), which affords particles with a very narrow size distribution ('monodisperse microspheres'). Monodisperse microspheres have a major advantage in syringeability compared to conventionally prepared microspheres, as they can be injected via a narrow needle causing less damage to the tissue. Most importantly, monodisperse microspheres provide more reproducible results regarding the physical properties of the microspheres and the release profile of the payload. **Chapter 2** focuses on the particle preparation method using microsieve™ technology. This chapter describes the relevance of particle porosity on the release profile of a model macromolecule, blue dextran, from PLGA microspheres. Blue dextran was used instead of proteins in order to avoid possible interactions between payload and polymer phase or degradation/modification of the payload. Different formulation parameters to prepare monodisperse microspheres were studied in relation to the particle porosity and release profile of blue dextran. The obtained results were analyzed with different artificial intelligence tools in order to obtain a microsphere batch with desired particle characteristics. These results provide valuable data on the microsphere characteristics required to obtain a zero-order sustained release of blue dextran for a prolonged time.

A novel copolymer, poly(D,L-lactic-*co*-hydroxymethyl glycolic acid) (PLHMGA), was recently developed in our department. PLHMGA microspheres and nanospheres encapsulated with model peptides and proteins showed superior performance over PLGA. However, since implanted biomaterials can evoke foreign body responses new materials should be tested for their safety after injection. **Chapter 3** describes the *in vitro* and *in vivo* results on the biocompatibility of

PLHMGA. *In vivo* biocompatibility was assessed after injection of both polydisperse and monodisperse PLHMGA microspheres subcutaneously as well as under the kidney capsule in rats. The latter represents a novel administration method for the delivery of therapeutics to the kidney.

Chapter 4 addresses the fate of PLHMGA microspheres injected under the kidney capsule and the fate of the delivered protein from the injected depot in more depth**.** Here, monodisperse PLHMGA microspheres were loaded with a near-infrared labeled model protein, NIR-BSA. These polymeric microspheres as well as free NIR-BSA protein were injected under the kidney capsule in rats. The redistribution of NIR-BSA was measured in blood and in organ homogenates. In addition, the *in vivo* release of NIR-BSA was determined after extracting the protein from the remaining microspheres in the injected kidney homogenates. The *in vivo* release profile of NIR-BSA was correlated with its *in vitro* release.

Chapter 5 reports on a study where a model therapeutic protein, erythropoietin, was encapsulated into PLHMGA microspheres, revealing the potential hurdles of encapsulating proteins susceptible to aggregation. Besides PLHMGA, another type of polymer (SynBiosys) was also used, which has shown good compatibility with protein formulations. EPO was encapsulated with w/o/w method as described earlier in previous chapters. However, since EPO is prone to dimerization and aggregation, other methods were also used for the preparation of microspheres, mainly solid-in-oil-in water or water-free solid-in–oil double emulsification methods. In these latter methods, EPO was first encapsulated by spray drying in inulin sugar glass particles, followed by encapsulation into polymeric microspheres. Next, the influence of these emulsification methods on dimerization of EPO was studied.

Chapter 6 summarizes the findings and conclusions of this thesis and discusses future perspectives.

References:

1. Eckardt KU, Coresh J, Devuyst O, Johnson RJ, Köttgen A, Levey AS, Levin A. Evolving importance of kidney disease: From subspecialty to global health burden. *The Lancet,* 382:158-169, 2013.
2. Hoste EAJ, Schurgers M. Epidemiology of acute kidney injury: How big is the problem? *Crit Care Med,* 36:S146-S151, 2008.
3. James MT, Hemmelgarn BR, Tonelli M. Early recognition and prevention of chronic kidney disease. *The Lancet,* 375:1296-1309, 2010.
4. Levey AS, Coresh J. Chronic kidney disease. *The Lancet,* 379:165-180, 2012.
5. Lameire N, Van Biesen W, Vanholder R. Acute renal failure. *Lancet,* 365:417-430, 2005.
6. Palevsky PM. Chronic-on-acute kidney injury. *Kidney Int,* 81:430-431, 2012.
7. D'Intini V, Ronco C, Bonello M, Bellomo R. Renal replacement therapy in acute renal failure. *Best Pract Res Clin Anaesthesiol,* 18:145-157, 2004.
8. Schrier RW, Wang W, Poole B, Mitra A. Acute renal failure: Definitions, diagnosis, pathogenesis, and therapy. *J Clin Invest,* 114:5-14, 2004.
9. Duran PA, Concepcion LA. Survival after acute kidney injury requiring dialysis: Long-term follow up. *Hemodial Int,* 18:S1-S6, 2014.
10. Garcia GG, Harden P, Chapman J, Martin S. The global role of kidney transplantation. *Curr Opin Organ Transplant,* 17:362-367, 2012.
11. Lambers Heerspink HJ, de Zeeuw D. Novel drugs and intervention strategies for the treatment of chronic kidney disease. *Br J Clin Pharmacol,* 76:536-550, 2013.
12. Little MH. Regrow or repair: Potential regenerative therapies for the kidney. *J Am Soc Nephrol,* 17:2390-2401, 2006.
13. Koh CJ, Atala A. Tissue Engineering, Stem Cells, and Cloning: Opportunities for Regenerative Medicine. *J Am Soc Nephrol,* 15:1113-1125, 2004.
14. Benigni A, Morigi M, Remuzzi G. Kidney regeneration. *The Lancet,* 375:1310-1317, 2010.
15. Bianchi F, Sala E, Donadei C, Capelli I, La Manna G. Potential advantages of acute kidney injury management by mesenchymal stem cells. *World J Stem Cells,* 6:644-650, 2014.
16. Papazova DA, Oosterhuis NR, Gremmels H, van Koppen A, Joles JA, Verhaar MC. Cell-based therapies for experimental chronic kidney disease: a systematic review and meta-analysis. *Dis Model Mech,* 8:281-293, 2015.
17. van Koppen A, Joles JA, Bongartz LG, van den Brandt J, Reichardt HM, Goldschmeding R, Nguyen TQ, Verhaar MC. Healthy bone marrow cells reduce progression of kidney failure better than CKD bone marrow cells in rats with established chronic kidney disease. *Cell Transplant,* 21:2299-2312, 2012.
18. Dolman MEM, Harmsen S, Storm G, Hennink WE, Kok RJ. Drug targeting to the kidney: Advances in the active targeting of therapeutics to proximal tubular cells. *Adv Drug Deliv Rev,* 62:1344-1357, 2010.
19. Takabatake Y, Isaka Y, Mizui M, Kawachi H, Shimizu F, Ito T, Hori M, Imai E. Exploring RNA inteference as a therapeutic strategy for renal disease. *Gene Ther,* 12:965-973, 2005.

20. Kim HJ, Park SJ, Koo S, Cha HJ, Lee JS, Kwon B, Cho HR. Inhibition of kidney ischemia-reperfusion injury through local infusion of a TLR2 blocker. *J Immunol Methods,* 407:146-150, 2014.
21. Knight SF, Kundu K, Joseph G, Dikalov S, Weiss D, Murthy N, Taylor WR. Folate receptor-targeted antioxidant therapy ameliorates renal ischemia-reperfusion injury. *J Am Soc Nephrol,* 23:793-800, 2012.
22. Vesey DA, Cheung C, Pat B, Endre Z, Gobé G, Johnson DW. Erythropoietin protects against ischaemic acute renal injury. *Nephrol Dial Transplant,* 19:348-355, 2004.
23. Dankers PYW, van Luyn MJA, Huizinga-van der Vlag A, van Gemert GML, Petersen AH, Meijer EW, Janssen HM, Bosman AW, Popa ER. Development and in-vivo characterization of supramolecular hydrogels for intrarenal drug delivery. *Biomaterials,* 33:5144-5155, 2012.
24. Rodell CB, Rai R, Faubel S, Burdick JA, Soranno DE. Local immunotherapy via delivery of interleukin-10 and transforming growth factor ß antagonist for treatment of chronic kidney disease. *J Control Release,* 206:131-139, 2015.
25. Silverstein DM. Inflammation in chronic kidney disease: Role in the progression of renal and cardiovascular disease. *Pediatr Nephrol,* 24:1445-1452, 2009.
26. Declèves AE, Sharma K. Novel targets of antifibrotic and anti-inflammatory treatment in CKD. *Nat Rev Nephrol, 10:257-267,* 2014.
27. Tampe D, Zeisberg M. Potential approaches to reverse or repair renal fibrosis. *Nat Rev Nephrol,* 10:226-237, 2014.
28. Lee SY, Kim SI, Choi ME. Therapeutic targets for treating fibrotic kidney diseases. *Transl Res,* 165:512-530, 2014.
29. Deng J, Kohda Y, Chiao H, Wang Y, Hu X, Hewitt SM, Miyaji T, McLeroy P, Nibhanupudy B, Li S, Star RA. Interleukin-10 inhibits ischemic and cisplatin-induced acute renal injury. *Kidney Int,* 60:2118-2128, 2001.
30. Zeisberg M. Bone morphogenic protein-7 and the kidney: Current concepts and open questions. *Nephrol Dial Transplant,* 21:568-573, 2006.
31. Vukicevic S, Basic V, Rogic D, Basic N, Shih MS, Shepard A, Jin D, Dattatreyamurty B, Jones W, Dorai H, Ryan S, Griffiths D, Maliakal J, Jelic M, Pastorcic M, Stavljenic A, Sampath TK. Osteogenic protein-1 (bone morphogenetic protein-7) reduces severity of injury after ischemic acute renal failure in rat. *J Clin Invest,* 102:202-214, 1998.
32. Yao Y, Zhang J, Tan DQ, Chen XY, Ye DF, Peng JP, Li JT, Zheng YQ, Fang L, Li YK, Fan MX. Interferon-γ improves renal interstitial fibrosis and decreases intrarenal vascular resistance of hydronephrosis in an animal model. *Urology,* 77:761.e8-761.e13, 2011.
33. Arcasoy MO. The non-haematopoietic biological effects of erythropoietin. *Br J Haematol,* 141:14-31, 2008.
34. Bahlmann FH, Fliser D. Erythropoietin and renoprotection. *Curr Opin Nephrol Hypertens,* 18:15-20, 2009.
35. Makadia HK, Siegel SJ. Poly Lactic-co-Glycolic Acid (PLGA) as biodegradable controlled drug delivery carrier. *Polymers,* 3:1377-1397, 2011.
36. Pisal DS, Kosloski MP, Balu-Iyer SV. Delivery of therapeutic proteins. *J Pharm Sci,* 99:2557-2575, 2010.
37. Brannon-Peppas L. Recent advances on the use of biodegradable microparticles and nanoparticles in controlled drug delivery. *Int J Pharm,* 116:1-9, 1995.

38. Wang L, Liu Y, Zhang W, Chen X, Yang T, Ma G. Microspheres and microcapsules for protein delivery: Strategies of drug activity retention. *Curr Pharm Des,* 19:6340-6352, 2013.
39. Schwendeman SP, Shah RB, Bailey BA, Schwendeman AS. Injectable controlled release depots for large molecules. *J Control Release,* 190:240-253, 2014.
40. van de Weert M, Hennink WE, Jiskoot W. Protein instability in poly(lactic-co-glycolic acid) microparticles. *Pharm Res,* 17:1159-1167, 2000.
41. Martín-Sabroso C, Fraguas-Sánchez AI, Aparicio-Blanco J, Cano-Abad MF, Torres-Suárez AI. Critical attributes of formulation and of elaboration process of PLGA-protein microparticles. *Int J Pharm,* 480:27-36, 2015.
42. Shi Y, Huang G. Recent developments of biodegradable and biocompatible materials based micro/nanoparticles for delivering macromolecular therapeutics. *Crit Rev Ther Drug Carrier Syst,* 26:29-84, 2009.
43. Cohen S, Yoshioka T, Lucarelli M, Hwang LH, Langer R. Controlled delivery systems for proteins based on poly(lactic/glycolic acid) microspheres. *Pharm Res,* 8:713-720, 1991.
44. Schwendeman SP. Recent advances in the stabilization of proteins encapsulated in injectable PLGA delivery systems. *Crit Rev Ther Drug Carrier Syst,* 19:73-98, 2002.
45. Ye M, Kim S, Park K. Issues in long-term protein delivery using biodegradable microparticles. *J Control Release,* 146:241-260, 2010.
46. Samadi N, Abbadessa A, Di Stefano A, van Nostrum CF, Vermonden T, Rahimian S, Teunissen EA, van Steenbergen MJ, Amidi M, Hennink WE. The effect of lauryl capping group on protein release and degradation of poly(d,l-lactic-co-glycolic acid) particles. *J Control Release, 172:436-443,* 2013.
47. Jiang G, Woo BH, Kang F, Singh J, DeLuca PP. Assessment of protein release kinetics, stability and protein polymer interaction of lysozyme encapsulated poly(D,L-lactide-co-glycolide) microspheres. *J Control Release,* 79:137-145, 2002.
48. Zhu G, Mallery SR, Schwendeman SP. Stabilization of proteins encapsulated in injectable poly (lactide-co- glycolide). *Nat Biotechnol,* 18:52-57, 2000.
49. van de Weert M, Hoechstetter J, Hennink WE, Crommelin DJA. The effect of a water/organic solvent interface on the structural stability of lysozyme. *J Control Release,* 68:351-359, 2000.
50. Lai MC, Topp EM. Solid-state chemical stability of proteins and peptides. *J Pharm Sci,* 88:489-500, 1999.
51. Leemhuis M, Van Nostrum CF, Kruijtzer JAW, Zhong ZY, Ten Breteler MR, Dijkstra PJ, Feijen J, Hennink WE. Functionalized poly(a-hydroxy acid)s via ring-opening polymerization: Toward hydrophilic polyesters with pendant hydroxyl groups. *Macromolecules,* 39:3500-3508, 2006.
52. Buske J, König C, Bassarab S, Lamprecht A, Mühlau S, Wagner KG. Influence of PEG in PEG-PLGA microspheres on particle properties and protein release. *Eur J Pharm Biopharm,* 81:57-63, 2012.
53. Tran VT, Karam JP, Garric X, Coudane J, Benoît JP, Montero-Menei CN, Venier-Julienne M-. Protein-loaded PLGA-PEG-PLGA microspheres: A tool for cell therapy. *Eur J Pharm Sci,* 45:128-137, 2012.

54. Morita T, Horikiri Y, Suzuki T, Yoshino H. Applicability of various amphiphilic polymers to the modification of protein release kinetics from biodegradable reservoir-type microspheres. *Eur J Pharm Biopharm,* 51:45-53, 2001.
55. Liu Y, Ghassemi AH, Hennink WE, Schwendeman SP. The microclimate pH in poly(D,L-lactide-co-hydroxymethyl glycolide) microspheres during biodegradation. *Biomaterials,* 33:7584-7593, 2012.
56. Blanco D, Alonso MJ. Protein encapsulation and release from poly(lactide-co-glycolide) microspheres: Effect of the protein and polymer properties and of the co-encapsulation of surfactants. *Eur J Pharm Biopharm,* 45:285-294, 1998.
57. Ogawa Y, Yamamoto M, Okada H, Yashiki T, Shimamoto T. A new technique to efficiently entrap leuprolide acetate into microcapsules of polylactic acid or copoly(lactic/glycolic) acid. *Chem Pharm Bull,* 36:1095-1103, 1988.
58. Péan JM, Venier-Julienne MC, Boury F, Menei P, Denizot B, Benoit JP. NGF release from poly(D,L-lactide-co-glycolide) microspheres. Effect of some formulation parameters on encapsulated NGF stability. *J Control Release,* 56:175-187, 1998.
59. Luan X, Bodmeier R. In situ forming microparticle system for controlled delivery of leuprolide acetate: Influence of the formulation and processing parameters. *Eur J Pharm Sci,* 27:143-149, 2006.
60. Ghaderi R, Sturesson C, Carlfors J. Effect of preparative parameters on the characteristics of poly (D,L-lactide-co-glycolide) microspheres made by the double emulsion method. *Int J Pharm,* 141:205-216, 1996.
61. Müller M, Vörös J, Csúcs G, Walter E, Danuser G, Merkle HP, Spencer ND, Textor M. Surface modification of PLGA microspheres. *J Biomed Mater Res A,* 66:55-61, 2003.
62. Perez C, Castellanos IJ, Costantino HR, Al-Azzam W, Griebenow K. Recent trends in stabilizing protein structure upon encapsulation and release from bioerodible polymers. *J Pharm Pharmacol,* 54:301-313, 2002.
63. Sah H. Protein instability toward organic solvent/water emulsification: Implications for protein microencapsulation into microspheres. *PDA J Pharm Sci Technol,* 53:3-10, 1999.
64. Al-Azzam W, Pastrana EA, Griebenow K. Co-lyophilization of bovine serum albumin (BSA) with poly(ethylene glycol) improves efficiency of BSA encapsulation and stability in polyester microspheres by a solid-in-oil-in-oil technique. *Biotechnol Lett,* 24:1367-1374, 2002.
65. Han Y, Tian H, He P, Chen X, Jing X. Insulin nanoparticle preparation and encapsulation into poly(lactic-co-glycolic acid) microspheres by using an anhydrous system. *Int J Pharm,* 378:159-166, 2009.
66. Carrasquillo KG, Stanley AM, Aponte-Carro JC, De Jésus P, Costantino HR, Bosques CJ, Griebenow K. Non-aqueous encapsulation of excipient-stabilized spray-freeze dried BSA into poly(lactide-co-glycolide) microspheres results in release of native protein. *J Control Release,* 76:199-208, 2001.
67. Leach WT, Simpson DT, Val TN, Anuta EC, Yu Z, Williams III RO, Johnston KP. Uniform encapsulation of stable protein nanoparticles produced by spray freezing for the reduction of burst release. *J Pharm Sci,* 94:56-69, 2005.
68. Partridge J, Moore BD, Halling PJ. α-chymotrypsin stability in aqueous-acetonitrile mixtures: Is the native enzyme thermodynamically or kinetically stable under low water conditions? *J Mol Catal B Enzym,* 6:11-20, 1999.

69. Castellanos IJ, Crespo R, Griebenow K. Poly(ethylene glycol) as stabilizer and emulsifying agent: A novel stabilization approach preventing aggregation and inactivation of proteins upon encapsulation in bioerodible polyester microspheres. *J Control Release,* 88:135-145, 2003.
70. Costantino HR, Firouzabadian L, Hogeland K, Wu C, Beganski C, Carrasquillo KG, Córdova M, Griebenow K, Zale SE, Tracy MA. Protein spray-freeze drying. Effect of atomization conditions on particle size and stability. *Pharm Res,* 17:1374-1383, 2000.

Chapter 2

Computer modeling assisted design of monodisperse PLGA microspheres with controlled porosity affords zero order release of an encapsulated macromolecule for three months

Filis Kazazi Hyseni[1]
Mariana Landin[2]
Audrey AR Lathuile[3]
Gert J Veldhuis[3]
Sima Rahimian[1]
Wim E Hennink[1]
Robbert Jan Kok[1]
Cornelus F van Nostrum[1]

[1.] Department of Pharmaceutics, Utrecht Institute for Pharmaceutical Sciences, Utrecht University, Utrecht, The Netherlands
[2.] Department of Pharmacy and Pharmaceutical Technology, University of Santiago, Santiago de Compostela, Spain
[3.] Nanomi B.V., Oldenzaal, The Netherlands

Pharmaceutical Research, 31:2844-2856, Oct 2014

Abstract

The aim of this study was the development of poly(D,L-lactic-*co*-glycolic acid) (PLGA) microspheres with controlled porosity, to obtain microspheres that afford continuous release of a macromolecular model compound (blue dextran). PLGA microspheres with a size of around 40 µm and narrow size distribution (span value of 0.3) were prepared with a double emulsion membrane emulsification method. Gene expression programming (GEP) analysis was applied to design and formulate a batch of microspheres with controlled porosity that shows continuous release of blue dextran. Low porous microspheres with a high loading efficiency were formed at high polymer concentrations (30% w/w in the oil phase) and were characterized with a burst release < 10% and a three-phasic release profile of blue dextran. Increasing porosity (10% w/w polymer concentrations), a sustained release of blue dextran was obtained albeit with up to 40% of burst release. The desired formulation, calculated by GEP, resulted in microspheres with 72% loading efficiency and intermediate porosity. Blue dextran was indeed released continuously in almost a zero order manner over a period of three months after an initial small burst release of 9%. By fine-tuning the porosity, the release profile of PLGA microspheres for macromolecules can be predicted and changed from a three-phasic to a continuous release.

1. Introduction

Microspheres based on biodegradable polymers such as aliphatic polyesters, e.g. poly(D,L-lactic-*co*-glycolic acid) (PLGA), are widely used for delivery of macromolecular drugs. Microspheres enable the protection and stabilization of the encapsulated drug and aim for a release profile over a desired time period [1-3]. The size and size distribution of polymeric microspheres are important factors for controlling the particle degradation [4,5] and the release profile of an entrapped drug [6-9]. In addition, the size also contributes to the *in vivo* fate of polymeric particles by affecting their cellular uptake [10-12]. Considering the above, one can comprehend that polydispersity of polymeric particles can confound the therapeutic outcome of such delivery devices. It has been shown that the production of monodisperse microspheres results in better batch-to-batch reproducibility, also in term of release kinetics [13,14]. Membrane emulsification (ME), first introduced by Nakashima *et al.* [15], is a method that makes use of a porous glass membrane with uniform pore sizes to generate monodisperse microspheres [16].

The most commonly observed release profile of macromolecular compounds from PLGA microspheres is tri-phasic, characterized by a burst release, a lag phase and a phase of sustained release [1,17-19]. For macromolecules that are insoluble in the polymer matrix, their mechanism of release is mainly governed by the particle porosity in the first two release phases and by the degradation of the polymer in the third phase [1,20,21]. Particle porosity is often associated with a sustained release after an initial, mostly high, burst release, and with a low drug loading efficiency (LE) [22]. Several studies have reported on the physical principles of the ME process [23-25] and the influence of formulation parameters on the size and monodispersity of the microspheres [26-28]. However, there is hardly information on how formulation parameters of the ME process affect the release profile of entrapped macromolecules.

In this study, the preparation of monodisperse PLGA microspheres was pursued with control of the porosity in order to fine-tune the release of a macromolecular model compound from PLGA microspheres, eventually aiming at a continuous release profile after a low burst release. Blue dextran was chosen as a model compound, as its inertness allows to investigate the intrinsic release properties of the microspheres avoiding possible interactions between payload and polymer phase or degradation/modification of the payload.

Macromolecules such as proteins are commonly formulated in PLGA microspheres by double-emulsification. With this method a primary w_1/o emulsion, that contains the macromolecular drug in the inner water phase and the polymer in the oil phase, is emulsified in a continuous water phase to obtain a $w_1/o/w_2$ emulsion [1,29,30]. In the present study, different formulation

parameters of the double emulsion ME process were varied in order to evaluate their relationship with porosity of the microspheres and the release profile of blue dextran. Subsequently, different artificial intelligence tools (Artificial Neural Networks (ANNs), fuzzy logic, gene expression programming (GEP) and genetic algorithms) were used to understand the effect of formulation parameters on the microsphere characteristics and predict the ones that generate microspheres with controlled porosity, along with other preferred properties like high monodispersity and high LE.

The relationship between formulation parameters, porosity of the microspheres and the release of blue dextran was analyzed with neurofuzzy logic, which is a hybrid computational method that combines the learning capacity of ANNs with fuzzy logic technology [31,32]. Fuzzy logic is a form of probabilistic logic which is able to manage linguistic variables. After a proper fuzzyfication process, a continuous variable can be transformed into a linguistic variable which is represented by a truth that ranges in degrees between 0 and 1. Following this process, neurofuzzy logic is able to detect complex relationships between variables and present them as simple rules [32]. GEP is an extension of genetic programming, the soft-computing method that simulates the biological evolution process to develop algorithms. This technology is able to model empirically observed values, finding equations that fit the facts within a certain error of the correct value [33]. The combination of GEP and genetic algorithms allows carrying out the process optimization to find the best selection of formulation parameters that give microspheres of preferred properties.

The aim of this study was the development of PLGA microspheres with uniform size that show sustained (preferably zero-order) release of a model macromolecule (blue dextran), while simultaneously the LE is high and the burst release is low.

2. Materials and Methods

2.1. Materials

Ester terminated (“end-capped”) poly(D,L-lactic-*co*-glycolic acid) with intrinsic viscosity (IV) of 0.2 dL/g (PLGA 5002) and 0.4 dL/g (PLGA 5004), were purchased from Purac Biochem B.V., Gorinchem, The Netherlands. Blue dextran (MW= $2 \cdot 10^6$ g/mol), sodium phosphate monobasic (NaH_2PO_4), sodium phosphate dibasic (Na_2HPO_4) and sodium azide (NaN_3) were purchased from Fluka (Zwijndrecht, The Netherlands). Polyvinyl alcohol (PVA; MW= 13,000-23,000 g/mol) and dimethylsulfoxide (DMSO) were obtained from Sigma-Aldrich (Steinheim, Germany). Sodium hydroxide (NaOH) and sodium chloride (NaCl) were supplied from Merck KGaA (Darmstadt, Germany). Dichloromethane (DCM) and

tetrahydrofuran were purchased from Biosolve B.V. (Valkenswaard, the Netherlands).

2.2. Preparation of monodisperse PLGA microspheres by Membrane Emulsification

Sixteen batches of PLGA microspheres were prepared with a cross-flow emulsification process (Figure 1A), where the continuous phase (w_2) is flowing past the membrane through which the dispersed phase (w_1/o) is pumped, resulting in the formation of emulsified droplets of uniform size. The membrane used was hydrophilic Iris-20 (microsieve^{TM} membrane technology, Nanomi B.V., Oldenzaal, The Netherlands) that generates $w_1/o/w_2$ microspheres with a mean diameter of around 40 µm. The dispersed phase, w_1/o (also known as "premix"), was prepared by mixing solutions of PLGA in DCM (1.5 mL, polymer concentrations 10, 15, 20, 25 and 30% w/w) with different volumes of blue dextran in water (0.19, 0.37 and 0.75 mL; 50 mg/mL). The inner water volumes of blue dextran are further referred to as the volume fractions, calculated as follows: inner water volume/(inner water volume + oil phase volume). The premixes were homogenized using Ultra-Turrax T8 (IKA Works, USA) with dispersing element S10N-10G, at a speed of 20,000 rpm for 30 seconds. Next, the premixes were passed through the Iris-20 membrane at a constant rate of 2 mL/h using a syringe pump (Nexus 6000, Chemyx, USA) into 30 mL of the continuous phase with different concentrations of PVA (2, 4 and 6% w/v). In selected formulations, w_2 was saturated with DCM (1.6%; [34]) or NaCl (1%) was dissolved, at a fixed PVA concentration of 4%. The continuous phase was pumped with a rate of 4.6 mL/min across the membrane.

At the end of the process, the formed dispersion of the emulsified droplets was left to stir for 2h to evaporate DCM. The hardened microspheres were collected by centrifugation at 3,000 rpm for 2 minutes, washed three times with water, froze with liquid nitrogen and freeze-dried overnight. The yield was calculated from the weight of the microspheres recovered versus the weight of blue dextran and PLGA used to prepare the microspheres. The stability of the premix was evaluated using separate premix samples that were incubated at room temperature, to observe possible phase separation. The stability is expressed as the time until phase separation was visually observed. The stability was also measured with an Ostwald capillary viscometer and a rheometer. However, as a result of the rapid evaporation of dichloromethane, the obtained results were not reliable.

2.3. Microsphere size and size distribution analysis

The size and size distribution of the obtained microspheres were measured with an optical particle sizer (Accusizer 780, Santa Barbara, California, USA). At least 5,000 microspheres of each formulation were analyzed. The volume-weight mean microsphere diameter (vol-wt mean) is reported as particle size and the span value was calculated with the following formula: $sp = (d_{90} - d_{10})/d_{50}$, where d_x is the diameter corresponding to x vol.% on a cumulative microsphere size distribution curve. The size distribution is narrow for span values < 0.45 [23].

2.4. Porosity analysis

The morphology of the microspheres was investigated with scanning electron microscopic (SEM) analysis (Phenom, FEI Company, The Netherlands). Lyophilized microspheres were transferred onto 12-mm diameter aluminum specimen stubs (Agar Scientific Ltd., England) using double-sided adhesive tape. Prior to analysis, the microspheres were coated using an ion coater with platinum under vacuum. To determine the porosity of the microspheres, SEM pictures with similar magnification (~5000 ×) were used and the porosities were visually graded by three independent individuals according to the grading scale given in Supplemental Table SI. For each formulation, at least six microspheres were scored. Representative SEM pictures of microspheres with porosity grade 1 to 5 are shown in Supplemental Figure S1.

2.5. Blue dextran content of microspheres

The blue dextran content of the microspheres was determined by dissolving 50 mg of microspheres in 1 mL of DMSO. The absorption of the solution was measured with a UV microplate reader (Spectrostar Nano, BMG Labtech, Germany) at 620 nm, with a blue dextran calibration curve (from 0.01 to 3 mg/mL in DMSO). The theoretical loading (TL) of blue dextran was calculated from the amount of blue dextran in the feed divided by the sum of the amount of blue dextran and PLGA times 100%. The loading capacity (LC) was calculated from the weight of entrapped blue dextran divided by the dry weight of the microspheres times 100%. The loading efficiency (LE) was calculated as the percentage of the amount of blue dextran entrapped in the microspheres divided by the amount added during the preparation of microspheres times 100%.

2.6. In vitro degradation and release studies

Around 10 mg of the different microsphere formulations was suspended in 1.5 mL of 100 mM phosphate buffered saline (pH 7.4) containing 56 mM NaCl, 33

mM Na_2HPO_4, 66 mM NaH_2PO_4 and 0.05% (w/v) NaN_3 (added to prevent bacterial growth). The microspheres were incubated at 37°C while gently shaking. At different time-points, vials were removed and centrifuged (4,000 rpm for 5 minutes). The microspheres were washed three times with water, lyophilized and analyzed for residual dry weight and PLGA molecular weight.

The molecular weight of PLGA in degraded microspheres was measured with GPC (Waters Alliance system), consisting of a Waters 2695 separations module and a Waters 2414 refractive index detector. Two PL-gel 5 µm Mixed-D columns fitted with a guard column (Polymer Labs, Mw range 0.2 – 400 kDa) were used. For calibration, polystyrene standards (PS-2, Easi Cal, Varian, USA) with narrow molecular weight distributions (MW = 580 – 377,400 g/mol) were used. Tetrahydrofuran was used as the mobile phase at a flow rate of 1 mL/min. Standards and samples were dissolved in tetrahydrofuran overnight and filtered through 0.2 µm filters prior to the analysis. The data acquisitions and analysis were performed using Empower Pro software (Waters Corporation).

The release of blue dextran was studied in triplicate. At indicated time points, samples were centrifuged and 0.5 mL of the supernatant was removed and replaced with the same volume of fresh buffer. The amount of released blue dextran was measured with a UV microplate reader at 620 nm. Two main points were applied for characterization of the release curves: *the burst release*, calculated as the percentage of the loaded blue dextran released within 24h, and the slope of the release curve from day 1 till day 20 referred to as the *release rate*$_{(1\text{-}20\ d)}$ (expressed in % of the loading released per day (%/day)).

2.7. The software tools: neurofuzzy logic and GEP

The database of 16 formulations was modeled using two different artificial intelligence approaches. A commercial neurofuzzy logic software, FormRules® v3.31 (Intelligensys Ltd, 2008, UK), was used to generate information and knowledge related to the influence of different parameters to the particle outcome, and a commercial software, INForm ® v4.11 (Intelligensys Ltd, 2008, UK), implementing GEP and genetic algorithms, was used to model and optimize the system obtaining suitable ingredients and process conditions to achieve a microsphere batch with the desirable characteristics. The polymer type, polymer concentration in the oil phase, inner water volume and excipients in the continuous phase were introduced as *input* parameters, whereas size of the microspheres, span value, LE and porosity were selected as *output* parameters (Table I). In order to model release properties (i.e. burst release and release rate$_{(1\text{-}20d)}$), two extra inputs were included: porosity and theoretical loading. The common training parameters used by FormRules v3.31 were the following: ridge regression factor of 1 e^{-6}, number of set densities: 2, set densities: 2.3, maximum

inputs per submodel: 4, maximum nodes per input: 15, adapt nodes: true. Specific training parameters selected for each property are given in Supplemental Table SII. FormRules v3.31 contains various statistical fitness criteria including Cross Validation (CV), Minimum Description Length (MDL), Structural Risk Minimization (SRM), Leave One Out Cross Validation (LOOCV) and Bayesian Information Criterion (BIC). All were investigated to obtain the model that gave the best predictability together with the simplest and more intelligible rules [35].

GEP training parameters selected with INForm v4.11 for modeling included Mean Squared Error as fitness criteria and the following general operation parameters: number of populations: 10, number of generations: 1000-10000, gene headlength: 5-7, number of genes: 2-3 and random seed: 1-10). Equations included the mathematical functions +, - , x, /, *exp* when necessary [33].

Separate models were developed with FormRules and INForm for each property, the accuracy of which was assessed using correlation coefficient (R^2) and ANOVA *f*-ratios for each output:

$$R^2 = \left(1 - \frac{\sum_{i=1}^{n} \left(y_i - y_i' \right)^2}{\sum_{i=1}^{n} \left(y_i - y_i'' \right)^2} \right) \times 100\% \qquad (1)$$

where, *y* is the actual point in the data set, *y*' is the value calculated by the model and *y*" is the mean of the dependent variable. The larger the value of the train set R^2, the more the model captured the variation in the training data. Values for R^2 > 70% are indicative of reasonable model predictabilities [35]. The ANOVA is used to assess whether the values of a quantitative variable predicted by the model within several pre-defined groups differ from the corresponding experimental values. The ANOVA *f*-ratio is calculated with the variation due to an experimental treatment or effect divided by the variation due to an experimental error. ANOVA *f*-ratios higher than *f*-critical values [36] for the degrees of freedom of the model mean that there are not statistical significant differences between those groups.

3. Results and Discussion

3.1. Membrane emulsification process: general features

In this study, different PLGA microspheres with a narrow size distribution, loaded with blue dextran, were prepared by a membrane emulsification (ME) process. The ME module consists of a specially developed microsieve™ membrane with uniform pore sizes that acts as an emulsifying element (Figure 1). In ME, the dispersed phase (premix) is pressed through the membrane pores with a diameter d_p (m) into the continuous phase which flows past the membrane in a recirculating

loop. Small droplets are formed at the pore openings near the membrane surface, which are detached once they reach a certain size d_d (m). The minimum pressure that has to be applied in order to make the dispersed phase flow through the porous membrane is known as the critical transmembrane pressure, P_{ctm} (Pa), or the capillary pressure. Calculated from the Laplace equation, P_{ctm} is proportional to the interfacial tension γ ($N \cdot m^{-1}$) between the oil phase (W_1/O) and the water phase (W_2) divided by d_p, $P_{ctm}=4\gamma/d_p$ [16,37-39]. The transmembrane pressure, ΔP_{tm} (Pa), is used to overcome flow resistances in the pores and interfacial tension forces and is defined as the difference between the pressure of the dispersed phase, P_d (Pa), and the average pressure of the continuous phase $\overline{P_c}$ (Pa), $\Delta P_{tm} = P_d - \overline{P_c}$, where $\overline{P_c} = (P_{c,in} + P_{c,out})/2$ ($P_{c,in}$ and $P_{c,out}$ refer to the pressure of the continuous phase at the inlet and outlet of the main channel) [40-42]. For the production of monodisperse emulsions, ΔP_{tm} should be 2-10 times higher than P_{ctm} *[43]*.

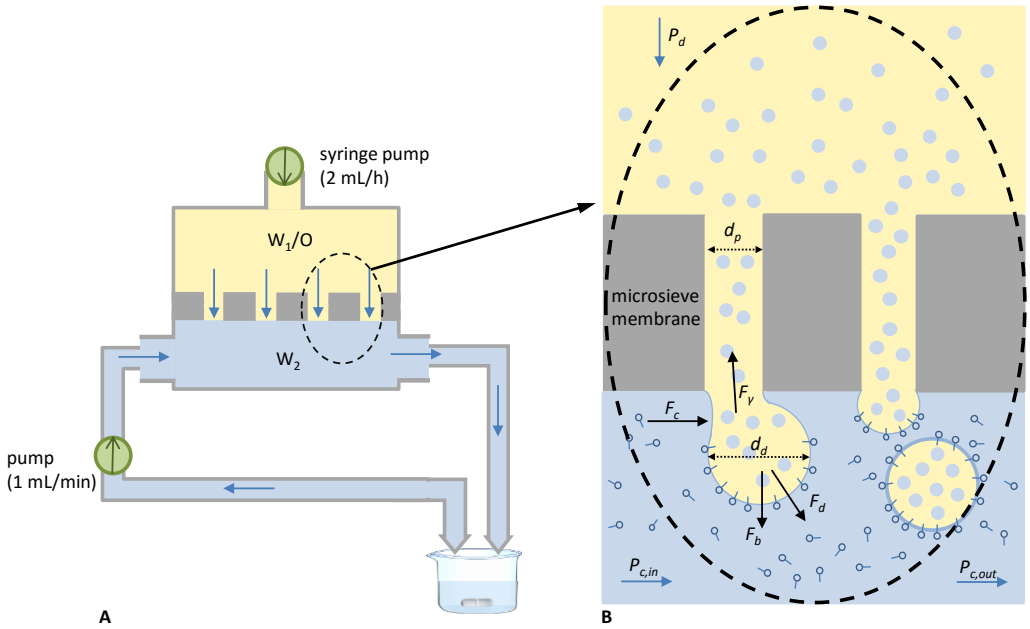

Figure 1. Schematic diagram of the membrane emulsification method. **A.** Membrane module; **B.** Principle of particle preparation with microsieve membrane; (w_1/o – dispersed phase (premix), w_2 – external water phase, P_d – pressure applied on the dispersed phase, $P_{c,in}$ and $P_{c,out}$ –pressure on the flowing continuous phase at both ends of the membrane modulus, d_p – diameter of the membrane pore, d_d – diameter of the droplet formed at the membrane pore, F_γ – the interfacial tension force, F_b – the buoyancy force, F_c – the drag force of the continuous phase flow, F_d – the inertial force caused by the flow of the dispersed phase.

The flux with which the dispersed phase flows through the membrane, J_d ($m \cdot s^{-1}$) can be calculated from the Hagen-Poiseuille law [44,45], $J_d = \Delta P_{tm}/(\eta_d R_m)$, where, η_d (Pa·s) is the viscosity of the premix and R_m (m^{-1}) is the hydraulic membrane resistance. The hydraulic membrane resistance is a constant that can be calculated using the formula $R_m = \Delta P_{tm} / \eta_w J_w$, in which J_w is the clean water flux through the membrane and η_w is the viscosity of water [44,45]. The flow rate through a pore, q, can be related to the period of drop detachment, t_d (s) using the following equation [38]

$$q = \frac{\eta_d r_p}{\gamma t_d} \qquad (2)$$

where, r_p (m) is the radius of the membrane pore ($d_p = 2r_p$). According to equation (2), with increasing η_d the formed droplets retain longer at the membrane before they detach resulting in an increase in size. The droplet formation time can be expressed as a function of J_d and d_d using the following equation [46],

$$t_d = \frac{2}{3} \frac{k\varepsilon}{d_p^2} \frac{d_{4,3}^3}{J_d} \qquad (3)$$

where, k is the fraction of active pores, ε is the membrane porosity and $d_{4,3}$ (m) [47] is the volume-weighted mean droplet diameter. The factor k is introduced as during ME not all pores are permeated with liquid. It has been shown that between 2-40% of the pores are active [39,40,46].

Once a droplet is formed at the membrane pore, the d_d upon detachment is governed by the balance between four different hydrodynamic forces (Figure 1 B): the drag force generated by the continuous phase flow (F_c), the interfacial tension force (F_γ), the inertial force caused by flow of the dispersed phase (F_d) and the buoyancy or gravitational force (F_b) [37,40,42]. In microfluidics flow, the buoyant force is insignificant as it is very small compared to F_c and F_γ [37]. From these forces, F_γ is the attaching force while the others are detaching forces. Hence the droplet is detached from the pore when the detaching forces are greater than the attaching force [42].

The drag force of the continuous phase flow affects the size and the size distribution of the formed emulsion droplets by generating a shear stress along the membrane surface, which detaches the formed droplet. An increase in flow velocity of the continuous phase causes a larger shear force along the membrane which in turn results in deformed droplets with increased polydispersity [37]. The surfactant (PVA) in the continuous phase has an important effect on particle size as it reduces the interfacial tension force (F_γ) by adsorbing onto the interface between the immiscible water and oil phases. The adsorption kinetics determines

the size of the droplets because when PVA adsorbs quickly onto the interface of the formed droplets and the continuous aqueous phase, it causes a quick reduction of the interfacial surface tension which in turn results in earlier droplet detachment from the membrane surface and thus in smaller droplets [40,44].

In this study, different formulation parameters were varied, mainly polymer molecular weight, polymer concentration in the oil phase, inner water volume and excipients in the continuous phase. The dispersed phase flux and the continuous phase flow rate were kept constant at 2 mL/h and 4.6 mL/min, respectively. The yield of the microspheres was around 60% for most of the formulations and 40% for formulations with high viscosity of the dispersed phase (Table I: 30% PLGA 5002 and all formulations with PLGA 5004). In these latter formulations, as a result of higher viscosity, a significant amount of the premix remained in the module as a void volume.

Formulation parameters and the obtained microsphere characteristics that were used as training parameters for the computational modeling are shown in Table I. Values of training parameters used by FormRules v3.31 are given in Supplemental Table SII together with R^2 values and their corresponding ANOVA *f* values, and the inputs selected as significant by the fuzzy logic software to express the variability of each parameter. From this table it can be seen that the values of R^2 are higher than 77% and the *f*-ratios are higher than the critical *f*-values [36] for the corresponding degrees of freedom, indicating a successfully developed model. A more detailed discussion regarding the observed microsphere properties of the different formulations is given below.

3.2. Stability of the premix

The stability of the premix plays an important role in generating monodisperse microspheres with ME [27]. For most formulations given in Table I the premix was stable during the processing time. The premixes of formulation 1 with 10% of PLGA 5002 in the oil phase and formulations 11 and 12 with 11% and 33% of the inner water volume had marginal stability, as phase separation occurred in less than 40 minutes. This may have affected droplet formation especially at the end of the processing period, and thus can explain the relatively higher polydispersity of the obtained microspheres (span value > 0.8) [27]. Neurofuzzy logic showed a good correlation between the formulation parameters and premix stability with R^2 of 97% (Supplemental Table SII). The most important parameter contributing to the premix stability was the concentration of PLGA in the oil phase, by yielding more stable premixes with increased concentrations. Likely, high PLGA concentrations in the oil phase result in high viscosity of the premix that in turn retards phase separation.

Table I. Selected formulation parameters studied and the results obtained. Fields in grey indicate the parameters varied in those particular formulations which were used as inputs for statistical analyzes with ANN and GEP, whereas the results were used as outputs.

Formulation #	PLGA	PLGA in the oil phase (%)	w_1[a] (%)	Continuous phase (w_2)	PVA (%)	TL (wt%)	Stability[b] W_1/O (min)	Yield (%)	Vol-wt mean diameter (μm)	Span value	LC (%)	LE (%)	Porosity[c]	Burst release[d] (%)	Release rate$_{(1\text{-}20d)}$[e] (%/day)
1	5002	10	20	PVA	4	7.8	30	72	40 ±13	0.9	1.5	19	4	0	0
2	5002	15	20	PVA	4	5.0	60	65	43 ±8	0.4	2.0	58	4	25	1.25
3	5002	20	20	PVA	4	3.5	80	67	40 ±6	0.3	1.9	52	2	9	0.08
4	5002	25	20	PVA	4	2.7	120	60	47 ±7	0.2	2.0	71	3	5	0.43
5	5002	30	20	PVA	4	2.1	120	31	59 ±5	0.1	1.9	88	1	0.4	0
6	5004	10	20	PVA	4	7.8	90	44	41 ±9	0.5	5.1	64	5	39	0.98
7	5004	15	20	PVA	4	5.0	100	45	45 ±9	0.3	2.6	50	5	21	1.16
8	5004	20	20	PVA	4	3.5	130	40	63 ±15	0.6	2.6	71	3	11	0.32
9	5004	25	20	PVA	4	2.7	180	40	75 ±19	0.7	2.5	91	3	11	0.55
10	5004	30	20	PVA	4	2.2	185	39	76 ±15	0.5	2.2	100	2	10	0.33
11	5002	20	11	PVA	4	1.8	40	46	58 ±23	1.1	1.0	55	2	0	0
12	5002	20	33	PVA	4	6.8	20	64	46 ±14	0.8	3.1	45	3	34	0.30
13	5002	20	20	PVA	2	3.5	80	65	45 ±6	0.2	1.9	53	3	39	0.50
14	5002	20	20	PVA	6	3.5	80	68	48 ±12	0.5	2.1	60	3	27	0.83
15	5002	20	20	PVA + 1% NaCl	4	3.5	80	63	52 ±20	1.0	2.2	60	1	0	0
16	5002	20	20	PVA + 1.6% DCM	4	3.5	80	59	42 ±10	0.4	1.5	43	2	26	0.32

[a] inner water volume is calculated as the percentage of the following: inner water volume / (inner water volume + oil phase volume); [b] time after which visual phase separation occurred, [c] porosity was graded by three independent individuals according to the procedure given in Supplemental Table SI. The results do not differ for more than one point; [d] release of blue dextran in 24h; [e] slope of the release curve calculated between days 1 and 20; PVA-polyvinyl alcohol; TL-theoretical drug loading; LC-loading capacity; LE-loading efficiency; DCM-dichloromethane.

3.3. *Effect of formulation parameters on the size characteristics of microspheres*

Table I shows that using the same pore-size membrane, microspheres ranging from 40 to 76 μm were produced, with different size distributions (span value between 0.1 and 1.1) and different porosities. The size of the droplet that detaches from the membrane depends on several factors, as discussed above. However, as during the preparation of the formulations in this study the flow rate of the dispersed phase and the flux of the continuous phase were kept constant, the size of the droplet depended mainly on the composition of the dispersed phase and the continuous phase. Thus, the final microsphere size depended on the size of the detached droplets as well as the polymer concentration, as presented in Figure 2 and 3. In accordance with neurofuzzy logic analysis (Supplemental Table SII), the mean diameter of the microspheres is dependent on the PLGA type and concentration in the oil phase, both influencing the viscosity of the dispersed phase (η_d). The diameter of the microspheres doubled with an increase of PLGA molecular weight and its concentration, reaching 76 μm for formulation 10. This is in accordance with equation (2) that when η_d increases the t_d increases as well and consequently the droplets retain longer at the membrane pores before detaching, leading to an increased size of the final droplets, which in turn will yield bigger microspheres after evaporation of the solvent. For the formulations with low or intermediate viscosities, the t_d was < 1 sec, as observed by microscope, whereas a longer time (t_d > 3 sec) was noted for the droplets with the highest viscosities of the premixes. Bigger droplets at the membrane pores can give coalescence when present at neighboring pores resulting in bigger particles and broadening of the distribution (Table I, formulations 8, 9, 10) [38,48]. In addition to the size, the distribution became bimodal with increased viscosity of the dispersed phase (Figure 2) as a result of the coalescence of the formed droplets [48].

The span value was also affected by the inner water volume and the PVA concentration in the continuous phase (Figure 3), as supported by the neuroffuzy logic analysis (Supplemental Table SII). Indeed the narrowest size distribution of microspheres (span value of 0.3) was obtained for the formulation with 20% inner water phase (Table I, compare formulations 3, 11, 12). The external phase with 2 and 4% PVA resulted in almost monodisperse microspheres with span value < 0.3 (formulations 13 and 3). Increased span value of 0.5 was seen for 6% PVA (formulation 14) likely as a result of increased viscosity of the continuous phase which decreases the diffusion rate of PVA molecules from the bulk to the newly formed droplets leading to slow reduction rate of the interfacial tension [44]. This in turn results in an increase of the coalescence probability of the droplets formed at the membrane surface causing broader size distribution and slightly larger microspheres (48 μm compared to 40 μm; formulations 14 and 3) [44]. Lower PVA

concentrations (< 1%) were previously shown by Liu *et al*. [24] to yield insufficiently stable emulsion droplets and were therefore not used in this study. The addition of 1% NaCl to the continuous phase (formulation 15), increased the mean microsphere size to 52 μm and the span value to 1.0, most likely because NaCl reduces the zeta-potential of the emulsified droplets resulting in their fusion which in turn yields microspheres of increased average size and broader size distribution [28]. Saturation of the continuous phase with DCM slightly increased the span value from 0.3 to 0.4, while the mean microsphere size remained around 41 μm (compare formulations 3 and 16).

3.4. Effect of formulation parameters on the porosity of the microspheres

Microsphere porosity was dependent on the PLGA molecular weight, PLGA concentration in the oil phase and the composition of the continuous phase, with PLGA concentration being the most important variable (Table I, and Supplemental Figure S2A). Highly porous microspheres with grade 4 and 5 were formed with 10 and 15% of PLGA in the oil phase (Table I; formulations 1, 2, 6, 7). Likely, in these formulations with relatively low viscosity, the inner water phase moves relatively easily through the emulsified droplet during solidification and comes in contact with the external phase, resulting in a more porous structure [49,50]. On the contrary, increase of the PLGA concentration to 30% resulted in microspheres with low porosity, grade 1 and 2 (Table I; formulations 5 and 10). Increasing the inner water volume to 33% resulted in microspheres with porosity grade 3 (formulation 12) and with additional presence of fissures on their surface (Supplemental Figure S3). During the formation of these microspheres, there is a higher volume fraction of inner water droplets which results in less dense and thus more porous microspheres upon solidification [49,51]. The addition of 1% NaCl to the continuous phase (formulation 15) resulted in the formation of denser microspheres (porosity grade 1), likely because of the reduced outflow of the inner water phase to the continuous phase of higher osmotic pressure [52]. The addition of DCM to the continuous phase had no influence on the microsphere porosity (formulation 16). However, the SEM pictures of this formulation showed the presence of a fissured surface, similar to formulation 12, probably as a result of a slower solidification process when the continuous PVA phase was saturated with DCM.

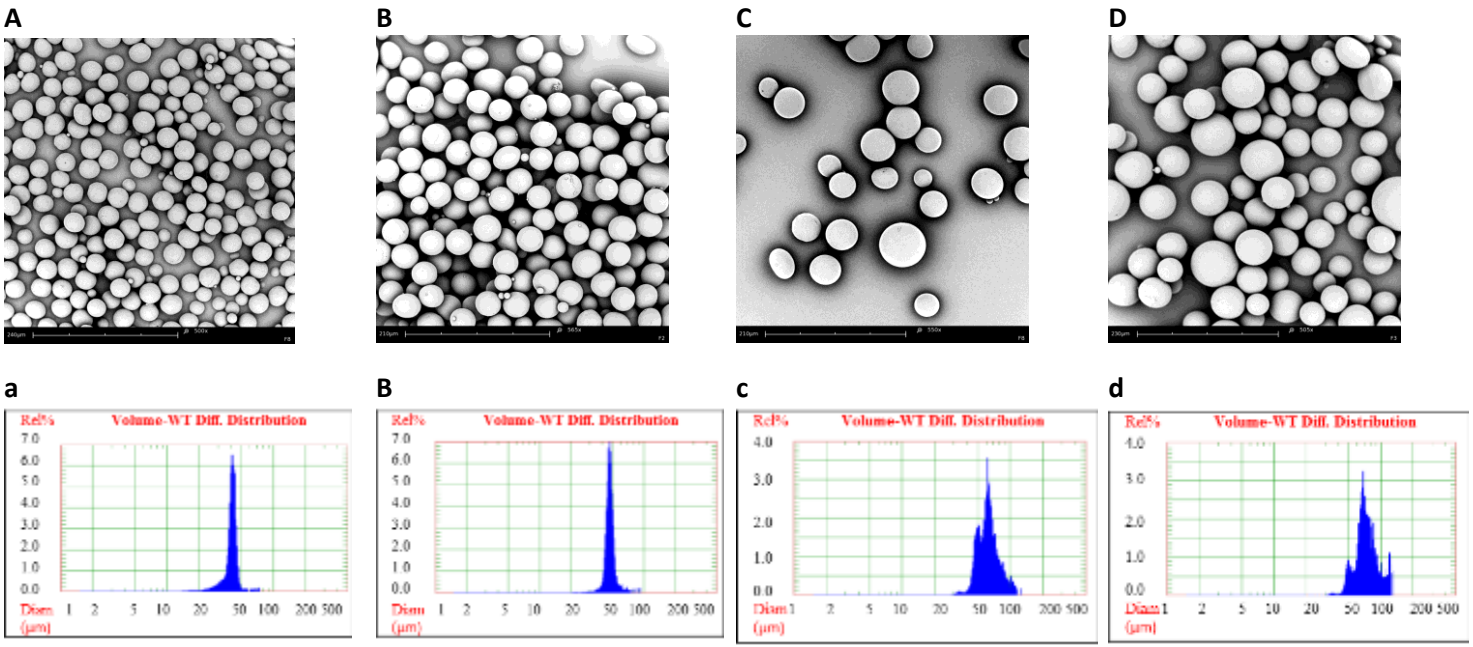

Figure 2. SEM photographs and volume weight mean diameter of microspheres from different formulations showing the influence of the dispersed phase viscosity; **A** and **a.** Formulation 3 (20% PLGA 5002, 20% w_1, 4% PVA); **B** and **b.** Formulation 4 (25% PLGA 5002, 20% w_1, 4% PVA); **C** and **c.** Formulation 8 (20% PLGA 5004, 20% w_1, 4% PVA) and **D** and **d.** Formulation 9 (25% PLGA 5004, 20% w_1, 4% PVA) (magnification 500x).

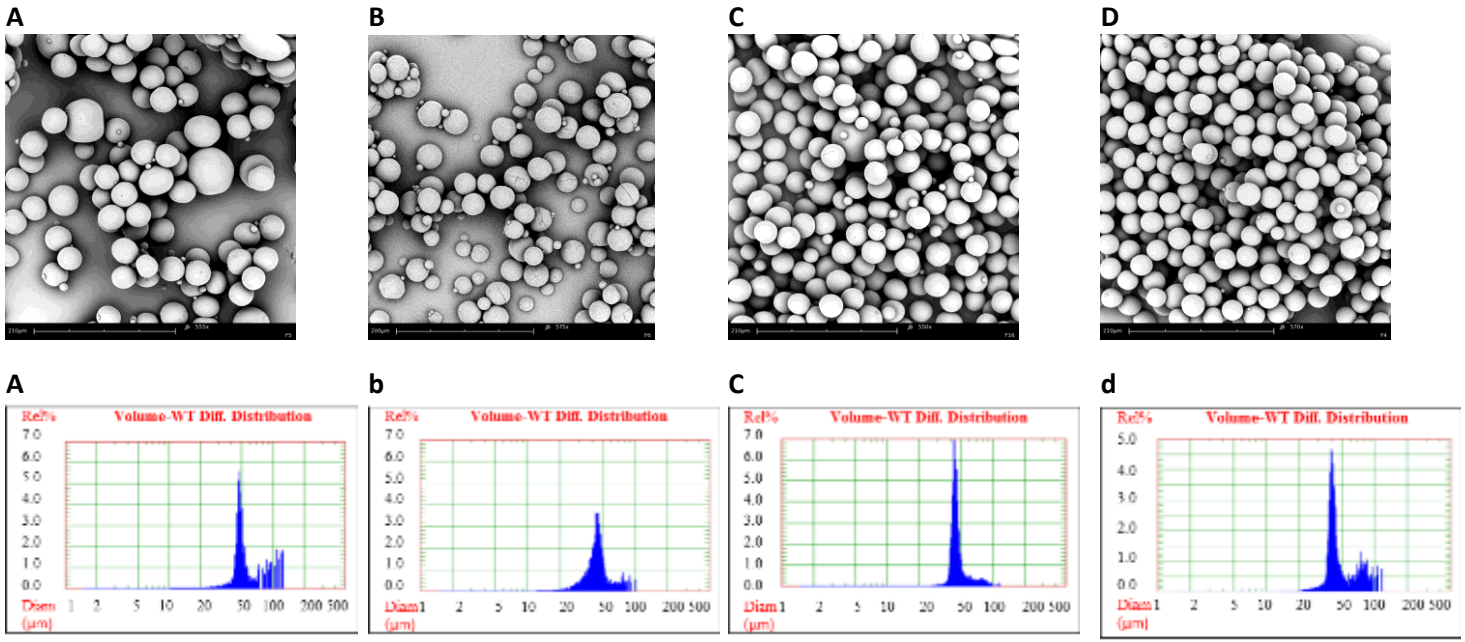

Figure 3. SEM photographs and volume weight mean diameter of microspheres from different formulations showing the influence of the inner water phase and external phase content; **A** and **a.** Formulation 11 (20% PLGA 5002, 11% w_1, 4% PVA); **B** and **b**. Formulation 12 (20% PLGA 5002, 33% w_1, 4% PVA); **C** and **c.** Formulation 14 (20% PLGA 5002, 20 % w_1, 6% PVA) and **D** and **d**. Formulation 15 (20% PLGA 5002, 20% w_1, 4% PVA and 1% NaCl) (magnification 500x).

3.5. Effect of formulation parameters on LC and LE

Table I and Supplemental Table SII show that both LC and LE were dependent on the PLGA molecular weight and concentration in the oil phase. With PLGA 5002 and a polymer concentration of 10% in the oil phase, the LC was relatively low (1.5%, formulation 1), whereas with 10% of PLGA 5004 in the oil phase the LC increased to 5.1% (formulation 6). The variability of LE is due to PLGA concentration and molecular weight, with PLGA concentration having the highest effect. A maximum LE of 100% was obtained with a high concentration of high molecular weight PLGA (30% PLGA 5004; formulation 10), whereas the lowest LE of 19% was obtained with low concentration of the low molecular weight PLGA (10% PLGA 5002; formulation 1). Microspheres prepared with higher PLGA concentration have shorter solidification times of the emulsified droplets and thus a lower probability that the inner water droplets come in contact with the external phase which in turn results in a higher LE. In addition, a higher viscosity of the oil phase decreases the transport of the blue dextran from the inner aqueous phase to the outer phase leading to the formation of microspheres with high LE [21].

A slight increase from 53 to 60% in LE was seen with increasing PVA concentration from 2 to 6% (formulation 13 and 14, respectively). An increase from 52 to 60% was seen with the addition of 1% NaCl (compare formulations 3 and 15), in line with previous experiments [27,28,52]. The addition of NaCl to the continuous phase changes the osmotic pressure between the inner and the outer water phase, suppressing the leakage of blue dextran [28]. Higher concentrations than 1% of NaCl were not tested in this study, as it was previously shown that this did not improve the LE [27].

3.6. Effect of formulation parameters on degradation and release profile

The microspheres of Table I were evaluated for their release and degradation characteristics by incubating them at 37°C in 150 mM phosphate pH 7.4 buffer. Figure 4 shows the degradation characteristics (molecular weight and weight loss) of the microspheres prepared with different concentrations of PLGA (either 5002 or 5004) in the oil phase. It is shown that the microspheres degrade via bulk degradation, characteristic for end-capped PLGA [53,54], as no weight loss occurred during the first 20 days followed by a decrease thereafter, while the weight average molecular weight (M_w) gradually decreased in time. The degradation was followed for 90 days, in which period 90% weight loss occurred. Figures 5-8 show the release of blue dextran from the different microsphere formulations. During degradation, a total release of blue dextran was reached, albeit with striking differences in the release profiles between different formulations. Microspheres with low porosity presented a three-phasic release

profile characterized by (I) burst release, (II) lag phase and (III) sustained release, which is frequently observed for the release of macromolecules from PLGA microspheres [22]. For this type of microspheres, as exemplified by formulation 5 in Figure 5, the burst release was rather low (0.4%) and there was no blue dextran release during phase II (a typical lag phase from day 1-20). The release of blue dextran started around day 20 together with the onset of microsphere erosion that was shown in Figure 4. In contrast, the microspheres with porosity grade 4 and 5 showed a different release pattern, characterized by a high burst release (up to 39%) and continuous release of blue dextran from day 1 until day 90, with a release rate (day 1-20) of around 1.0%/day (see, for example Figure 6, formulation 6).

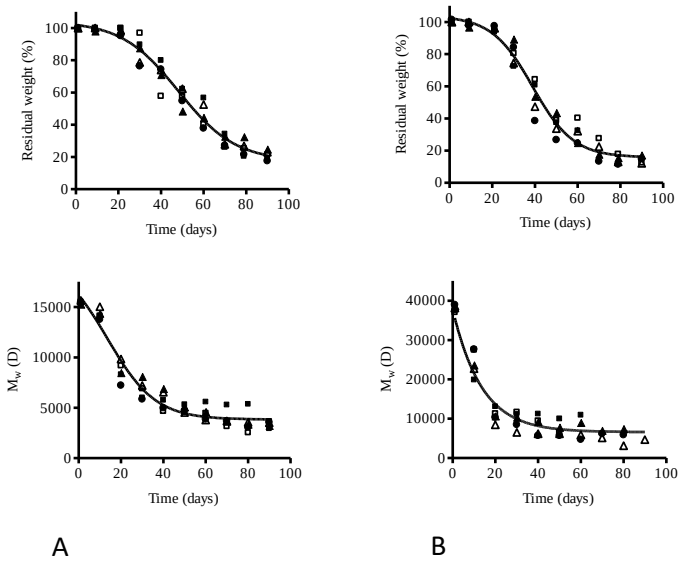

Figure 4. Residual weight of the microspheres (%) and PLGA weight average molecular weight (M_w) over time. The microspheres were prepared with different polymer concentration in the oil phase. **A.** PLGA 5002 (formulations 1-5) and **B.** PLGA 5004 (formulations 6-10); (PLGA 10%, closed squares; PLGA 15%, open squares; PLGA 20%, closed triangles; PLGA 25%, open triangles; PLGA 30%, closed circles).

Porosity of PLGA microspheres has been shown to play a major role for the burst release by creating a pathway for diffusion of the loaded macromolecules present in pores that are connected with the external medium [55]. As the hydrodynamic radius of blue dextran with molecular weight of $2 \cdot 10^6$ Da is substantially smaller (~27 nm) [56] than the radius of the pores in microspheres

with porosity grade 4 and 5 (>1µm), this may give rise to the initial burst release of blue dextran in highly porous microspheres. One exception was seen for formulation 1 (Figure 5) which showed a three-phasic release profile with no burst, although the porosity grade was 4. This formulation had a low LE of 19%, and most probably the majority of the payload was lost during the washing while the remaining blue dextran was localized in the core of the microspheres rather than in pores near the surface [17,57]. It has been shown that pore closure occurs in PLGA microspheres and films, once they are hydrated during degradation studies [58-60]. The kinetics of closure depends on the size of the pores, the temperature of the degradation medium and the glass transition temperature of the matrix. In line with the results published, the pore closure is rather slow for the PLGA microspheres of this study (T_g in dry state is around 45°C and when hydrated it is depressed to about 30°C [9,61,62]), allowing diffusion of entrapped blue dextran through these water-filled pores.

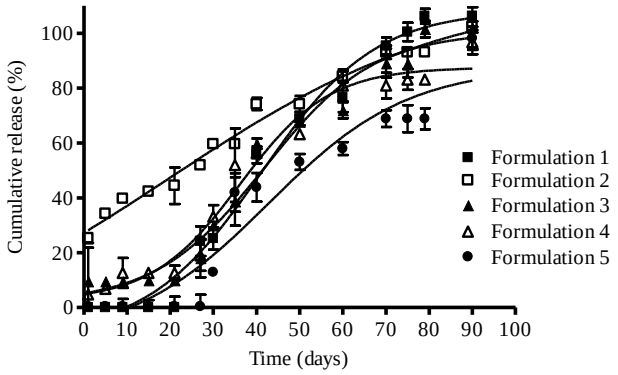

Figure 5. Cumulative release of blue dextran from microspheres prepared with PLGA 5002 and different polymer concentrations in the oil phase. Formulation 1: PLGA 10%, Formulation 2: PLGA 15%, Formulation 3: PLGA 20%, Formulation 4: PLGA 25% and Formulation 5: PLGA 30%. The detailed formulation variables are listed in Table I.

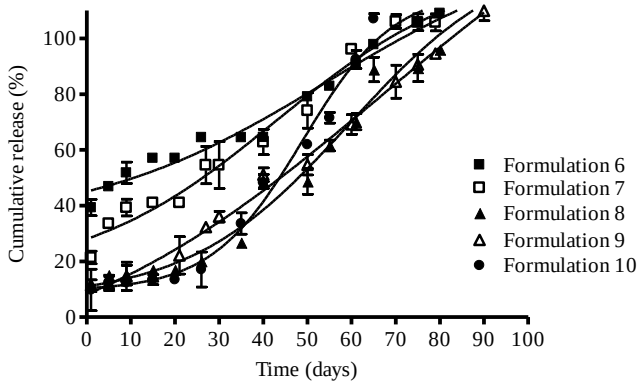

Figure 6. Cumulative release of blue dextran from microspheres prepared with PLGA 5004 and different polymer concentrations in the oil phase. Formulation 6: PLGA 10%, Formulation 7: PLGA 15%, Formulation 8: PLGA 20%, Formulation 9: PLGA 25% and Formulation 10: PLGA 30%. The detailed formulation variables are listed in Table I.

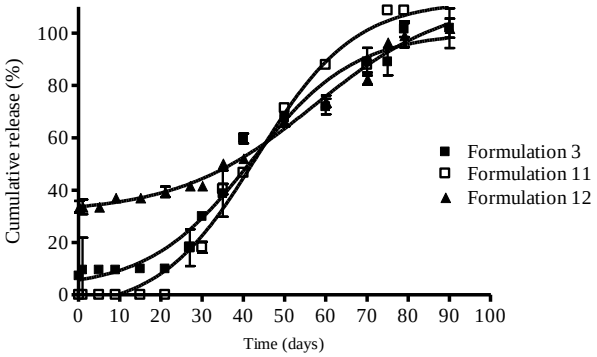

Figure 7. Cumulative release of blue dextran from microspheres prepared with PLGA 5002 and different inner water phase volumes. Formulation 3: 20%, Formulation 11: 11% and Formulation 12: 33%. The detailed formulation variables are listed in Table I.

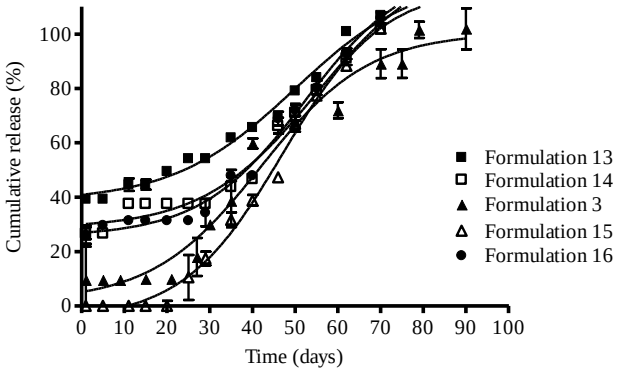

Figure 8. Cumulative release of blue dextran from microspheres prepared with PLGA 5002 and different excipients in w_2. Formulation 13: 2% PVA, Formulation 3: 4% PVA, Formulation 14: 6% PVA, Formulation 15: 4% PVA and 1% NaCl and Formulation 16: 4% PVA and 1.6% DCM. The detailed formulation variables are listed in Table I.

The 3D graphs in Supplemental Figure S2 (B and C) present the relationship between porosity and inner water volume as input parameters, and burst release and release rate$_{(1\text{-}20d)}$ as output parameters. The inner water volume has the most significant effect on the burst release, whereas porosity has a significant role on the release rate$_{(1\text{-}20d)}$ (Supplemental Table SII). Increasing the inner water volume from 11% to 33%, substantially increased the burst release from 0% up to 34% (see Table I, formulations 3, 11, 12) as a result of more porous structure of the microspheres formed with the increased inner water volume, as explained earlier. A continuous release of blue dextran was obtained from the formulation prepared with an inner water volume of 33% (Figure 7, formulation 12) as a result of increased porosity and presence of fissures on the surface of microspheres (Supplemental Figure S3).

Figure 8 shows that the release characteristics also depended on the composition of the continuous phase. The burst release increased to 39 and 27% for formulations prepared with 2% and 6% PVA, respectively, as compared to the formulation with 4% PVA which had only a 9% burst (Table I, compare formulations 13 and 14 with 3). Formulations 13 and 14 with porosity grade 3 had a continuous release of blue dextran with release rate$_{(1\text{-}20d)}$ of 0.5 and 0.8%/day, respectively. Interestingly, the addition of 1% NaCl to the continuous phase resulted in microspheres with no burst release (9% for the formulation without NaCl; compare formulation 15 with 3).

3.7. Preparation and characterization of the formulation with controlled porosity and desired release profile

For controlled release applications, a zero-order release of macromolecular drugs from microspheres is often desired [1]. In addition, the presence of the initial burst release is also undesirable as it is often not reproducible, and it can also be associated with toxic side effects due to the resulting high drug plasma levels [19]. Further, a high encapsulation efficacy of the particularly expensive biotherapeutics is required. In order to achieve a formulation that has a low burst release and a continuous release without a lag phase, the input and output parameters given in Table I were modeled by GEP and genetic algorithms technology, to find the best combination of inputs for producing microspheres with the desired properties. The following constrains were used in the model to calculate the optimal formulation: mean microsphere size of 40 µm, span value lower than 0.70, LE higher than 60%, burst release lower than 20% and release rate$_{(1\text{-}20)}$ higher than 0.7 %/day. The training R^2 obtained for the outputs were greater than 70% (Supplemental Table SII), indicating an acceptable prediction for each of the output parameters [35]. For a continuous release of blue dextran a controlled and intermediate porosity is needed, and thus porosity grade equal or higher than three was used for modeling. GEP combined with genetic algorithm analysis proposed the following formulation characteristics: 15% PLGA 5004 in the oil phase with the inner water volume of 16% and 3% PVA in the continuous phase. This premix was stable for 85 minutes (GEP predicted a value of 88.2 min). This formulation was processed with ME and three independent batches were prepared. Figure 9 shows the release profiles of these microspheres and Table II reports the predictions of the output parameters and the resulting values obtained for these batches. Advantageously, the prepared batches showed a smaller span value (0.25) and higher LE (70 ±8%) compared to the prediction (0.53 and 54%, respectively). Microsphere size was around 41 µm and the average porosity grade was 3.6 ±0.4. By controlling the porosity of this formulation, a zero-order release profile was achieved for blue dextran with a complete release in a period of three months. A low burst of only 9 ±2% was achieved together with a continuous release of blue dextran from day 1 till 20 (release rate$_{(1\text{-}20d)}$ = 0.8 ±0.1 %/day), a period during which the release is mainly governed by the porosity of microspheres. The continuous release from day 20 till day ~90 is governed by degradation of the microspheres. Thus, these prepared nearly monodisperse microspheres showed the desired continuous release profile of blue dextran with high LE and low burst release, demonstrating the power of GEP and genetic algorithm to design microspheres with predictable and tailorable characteristics.

Table II. Results of the defined formulation (microsphere size 40µm, span value < 0.7, porosity ≥ 3, LE > 60%, burst release < 20% and release rate$_{(1\text{-}20d)}$ > 0.7 %/day) predicted with GEP. The formulation was produced in triplicate with the following formulation parameters: PLGA 5004, 15% PLGA in oil phase, inner water volume of 16% and 3% PVA in w_2.

Output parameters	Predicted values	Batch 1	Batch 2	Batch 3
Stability w_1/o (min)	88.2	85	nd	nd
Vol-wt mean diameter (µm)	47	41 ±9	40 ±5	43 ±7
Span value	0.53	0.24	0.25	0.25
Porosity	4	4	4	3
Loading efficiency (%)	54	62	78	75
Burst release (%)	9	11	10	7
Release rate$_{(1\text{-}20d)}$ (%/day)	0.8	0.9	0.8	0.7

nd-not determined

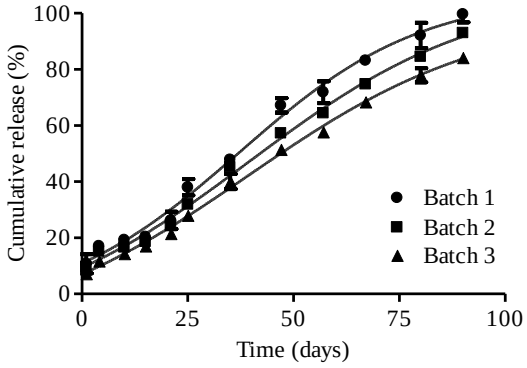

Figure 9. Cumulative release of blue dextran from microspheres prepared using the formulation parameters calculated by GEP (see Table II) to yield microspheres with the following predicted release characteristics: porosity grade 4, burst release of 9% and release rate$_{(1\text{-}20d)}$ of 0.8 %/day.

Conclusion

This article reports a systematic approach for preparation of PLGA microspheres with controlled porosity that showed continuous and almost zero-order release of a macromolecular model compound for three months together with a high LE and low burst release. To understand the relation between formulation parameters (polymer molecular weight, polymer concentration in the oil phase, inner water volume and excipients in the continuous phase) and microsphere characteristics, an experimental design approach was followed in which the porosity was correlated to the release profiles of blue dextran. This study successfully predicted the formulation conditions that are required to prepare microspheres that release the macromolecular model compound in a sustained manner, with low burst release.

Acknowledgments

This research forms part of the Project P3.02 DESIRE of the research program of the BioMedical Materials institute, co-funded by the Dutch Ministry of Economic Affairs. ML thanks the Spanish Government for financial support (SAF 2012- 39878-C02-01).

Abbreviations

ANNs	Artificial Neural Networks
GEP	Gene expression programming
LC	Loading capacity
LE	Loading efficiency
ME	Membrane emulsification
PLGA	Poly(D,L-lactic-*co*-glycolic acid)
PVA	Polyvinyl alcohol
TL	Theoretical loading
$d_{4,3}$	Volume-weighted mean droplet diameter
d_d	Droplet diameter
d_p	Membrane pore diameter
ε	Membrane porosity
F_b	The buoyancy force
F_c	The drag force of the continuous phase flow
F_d	The inertial force of the dispersed phase flow
F_γ	The interfacial tension force
Γ	Interfacial tension
J_d	Dispersed phase flux
k	Fraction of active membrane pores
η_d	Viscosity of the dispersed phase
$\overline{P_c}$	Continuous phase pressure
$P_{c,in}$; $P_{c,out}$	Pressure of the continuous phase at the inlet and outlet of the main channel
P_{ctm}	Critical transmembrane pressure
P_d	Dispersed phase pressure
ΔP_{tm}	Transmembrane pressure
q	Dispersed phase flow rate
R^2	Correlation coefficient
R_m	Hydraulic membrane resistance
r_p	Radius of the membrane pore
t_d	Period of drop detachment

References:

1. Ye M, Kim S, Park K. Issues in long-term protein delivery using biodegradable microparticles. *J Control Release,* 146:241-260, 2010.
2. Giteau A, Venier-Julienne MC, Aubert-Pouëssel A, Benoit JP. How to achieve sustained and complete protein release from PLGA-based microparticles? *Int J Pharm,* 350:14-26, 2008.
3. Sinha VR, Trehan A. Biodegradable microspheres for protein delivery. *J Control Release,* 90:261-280, 2003.
4. Dunne M, Corrigan OI, Ramtoola Z. Influence of particle size and dissolution conditions on the degradation properties of polylactide-co-glycolide particles. *Biomaterials,* 21:1659-1668, 2000.
5. Vert M, Schwach G, Engel R, Coudane J. Something new in the field of PLA/GA bioresorbable polymers? *J Control Release,* 53:85-92, 1998.
6. Berchane NS, Carson KH, Rice-Ficht AC, Andrews MJ. Effect of mean diameter and polydispersity of PLG microspheres on drug release: Experiment and theory. *Int J Pharm,* 337:118-126, 2007.
7. Varde NK, Pack DW. Influence of particle size and antacid on release and stability of plasmid DNA from uniform PLGA microspheres. *J Control Release,* 124:172-180, 2007.
8. Dawes GJS, Fratila-Apachitei LE, Mulia K, Apachitei I, Witkamp G, Duszczyk J. Size effect of PLGA spheres on drug loading efficiency and release profiles. *J Mater Sci Mater Med,* 20:1089-1094, 2009.
9. Samadi N, Abbadessa A, Di Stefano A, van Nostrum CF, Vermonden T, Rahimian S, Teunissen EA, van Steenbergen MJ, Amidi M, Hennink WE. The effect of lauryl capping group on protein release and degradation of poly(d,l-lactic-co-glycolic acid) particles. *J Control Release,* 172:436-443, 2013.
10. Desai MP, Labhasetwar V, Walter E, Levy RJ, Amidon GL. The mechanism of uptake of biodegradable microparticles in Caco-2 cells is size dependent. *Pharm Res,* 14:1568-1573, 1997.
11. Schmidt C, Lautenschlaeger C, Collnot E-, Schumann M, Bojarski C, Schulzke J-, Lehr C-, Stallmach A. Nano- and microscaled particles for drug targeting to inflamed intestinal mucosa-A first in vivo study in human patients. *J Control Release,* 165:139-145, 2013.
12. Carr KE, Smyth SH, McCullough MT, Morris JF, Moyes SM. Morphological aspects of interactions between microparticles and mammalian cells: Intestinal uptake and onward movement. *Prog Histochem Cytochem,* 46:185-252, 2012.
13. Berkland C, King M, Cox A, Kim K, Pack DW. Precise control of PLG microsphere size provides enhanced control of drug release rate. *J Control Release,* 82:137-147, 2002.
14. Tran VT, Benoît JP, Venier-Julienne MC. Why and how to prepare biodegradable, monodispersed, polymeric microparticles in the field of pharmacy? *Int J Pharm,* 407:1-11, 2011.
15. Nakashima T, Shimizu M, Kukizaki M. Membrane emulsification by microporous glass. *Key Eng Mat,* 61-62:513-516, 1991.
16. Nakashima T, Shimizu M, Kukizaki M. Particle control of emulsion by membrane emulsification and its applications. *Adv Drug Deliv Rev,* 45:47-56, 2000.

17. Hora MS, Rana RK, Nunberg JH, Tice TR, Gilley RM, Hudson ME. Release of human serum albumin from poly(lactide-co-glycolide) microspheres. *Pharm Res,* 7:1190-1194, 1990.
18. Wang X, Venkatraman SS, Boey FYC, Loo JSC, Tan LP. Controlled release of sirolimus from a multilayered PLGA stent matrix. *Biomaterials,* 27:5588-5595, 2006.
19. Allison SD. Analysis of initial burst in PLGA microparticles. *Expert Opin in Drug Del,* 5:615-628, 2008.
20. Ghassemi AH, van Steenbergen MJ, Talsma H, van Nostrum CF, Jiskoot W, Crommelin DJA, Hennink WE. Preparation and characterization of protein loaded microspheres based on a hydroxylated aliphatic polyester, poly(lactic-co-hydroxymethyl glycolic acid). *J Control Release,* 138:57-63, 2009.
21. Ghaderi R, Sturesson C, Carlfors J. Effect of preparative parameters on the characteristics of poly (D,L-lactide-co-glycolide) microspheres made by the double emulsion method. *Int J Pharm,* 141:205-216, 1996.
22. Fredenberg S, Wahlgren M, Reslow M, Axelsson A. The mechanisms of drug release in poly(lactic-co-glycolic acid)-based drug delivery systems - A review. *Int J Pharm,* 415:34-52, 2011.
23. Vladisavljević GT, Williams RA. Recent developments in manufacturing emulsions and particulate products using membranes. *Adv Colloid Interfac,* 113:1-20, 2005.
24. Liu R, Ma GH, Wan YH, Su ZG. Influence of process parameters on the size distribution of PLA microcapsules prepared by combining membrane emulsification technique and double emulsion-solvent evaporation method. *Colloid Surface B,* 45:144-153, 2005.
25. Vladisavljević GT, Shimizu M, Nakashima T. Production of multiple emulsions for drug delivery systems by repeated SPG membrane homogenization: Influence of mean pore size, interfacial tension and continuous phase viscosity. *J Membr Sci,* 284:373-383, 2006.
26. Doan TVP, Olivier JC. Preparation of rifampicin-loaded PLGA microspheres for lung delivery as aerosol by premix membrane homogenization. *Int J Pharm,* 382:61-66, 2009.
27. Liu R, Ma G, Meng FT, Su ZG. Preparation of uniform-sized PLA microcapsules by combining Shirasu Porous Glass membrane emulsification technique and multiple emulsion-solvent evaporation method. *J Control Release,* 103:31-43, 2005.
28. Ito F, Fujimori H, Honnami H, Kawakami H, Kanamura K, Makino K. Control of drug loading efficiency and drug release behavior in preparation of hydrophilic-drug-containing monodisperse PLGA microspheres. *J Mater Sci Mater Med,* 21:1563-1571, 2010.
29. van de Weert M, Hennink WE, Jiskoot W. Protein instability in poly(lactic-co-glycolic acid) microparticles. *Pharm Res,* 17:1159-1167, 2000.
30. Schwendeman SP. Recent advances in the stabilization of proteins encapsulated in injectable PLGA delivery systems. *Crit Rev Ther Drug Carrier Syst,* 19:73-98, 2002.
31. Landín M, Rowe RC, York P. Advantages of neurofuzzy logic against conventional experimental design and statistical analysis in studying and developing direct compression formulations. *Eur J Pharm Sci,* 38:325-331, 2009.
32. Gallego PP, Gago J, Landin M. Artificial neural networks technology to model and predict plant biology process. In: Suzuki K, editor. Artificial neural networks -

Methodological advances and biomedical applicationsCroatia: InTech, 2011. p. 197-216.
33. Ferreira C. Gene expression programming: Mathematical modeling by an artificial intelligence. second ed. Germany: Springer-Verlag, 2006.
34. Sadek PC. Illustrated pocket dictionary of chromatography. first ed. New Jersey: Wiley-Interscience, 2004.
35. Colbourn E, Rowe RC. Neural computing and pharmaceutical formulation. In: Swarbrick J, Boylan JC, editors. Encyclopaedia of Pharmaceutical Technology. third ed. 2005.
36. NIST/SEMATECH e-Handbook of Statistical Methods, 01/02/2013. Available from: http://www.itl.nist.gov/div898/handbook/
37. Peng SJ, Williams RA. Controlled production of emulsions using a crossflow membrane. Part I: Droplet formation from a single pore. *Chem Eng Res Design,* 76:894-901, 1998.
38. Christov NC, Danov KD, Danova DK, Kralchevsky PA. The drop size in membrane emulsification determined from the balance of capillary and hydrodynamic forces. *Langmuir,* 24:1397-1410, 2008.
39. Abrahamse AJ, Van Lierop R, Van der Sman RGM, Van der Padt A, Boom RM. Analysis of droplet formation and interactions during cross-flow membrane emulsification. *J Membr Sci,* 204:125-137, 2002.
40. Schröder V, Behrend O, Schubert H. Effect of Dynamic Interfacial Tension on the Emulsification Process Using Microporous, Ceramic Membranes. *J Colloid Interface Sci,* 202:334-340, 1998.
41. Joscelyne SM, Trägårdh G. Membrane emulsification - A literature review. *J Membr Sci,* 169:107-117, 2000.
42. Pathak M. Numerical simulation of droplet dynamics in membrane emulsification systems. In: Andriychuk M, editor. Numerical simulation - From theory to industry In Tech; 2012. p. 415.
43. Williams RA, Peng SJ, Wheeler DA, Morley NC, Taylor D, Whalley M, Houldsworth DW. Controlled Production of Emulsions Using a Crossflow Membrane: Part II: Industrial Scale Manufacture. *Chem Eng Res Design,* 76:902-910, 1998.
44. Kukizaki M. Shirasu porous glass (SPG) membrane emulsification in the absence of shear flow at the membrane surface: Influence of surfactant type and concentration, viscosities of dispersed and continuous phases, and transmembrane pressure. *J Membr Sci,* 327:234-243, 2009.
45. Vladisavljević GT, Shimizu M, Nakashima T. Permeability of hydrophilic and hydrophobic Shirasu-porous-glass (SPG) membranes to pure liquids and its microstructure. *J Membr Sci,* 250:69-77, 2005.
46. Vladisavljevic GT, Schubert H. Preparation and analysis of oil-in-water emulsions with a narrow droplet size distribution using Shirasu-porous-glass (SPG) membranes. *Desalination,* 144:167-172, 2002.
47. Xu R. Particle characterization: Light scattering methods. : New York: Kluwer Academic, 2002.
48. Lepercq-Bost É, Giorgi M, Isambert A, Arnaud C. Estimating the risk of coalescence in membrane emulsification. *J Membr Sci,* 357:36-46, 2010.

49. Crotts G, Park TG. Preparation of porous and nonporous biodegradable polymeric hollow microspheres. *J Control Release,* 35:91-105, 1995.
50. Chaisri W, Ghassemi AH, Hennink WE, Okonogi S. Enhanced gentamicin loading and release of PLGA and PLHMGA microspheres by varying the formulation parameters. *Colloid Surf B,* 84:508-514, 2011.
51. Yushu H, Venkatraman S. The effect of process variables on the morphology and release characteristics of protein-loaded PLGA particles. *J Appl Polym Sci,* 101:3053-3061, 2006.
52. Liu R, Huang SS, Wan YH, Ma GH, Su ZG. Preparation of insulin-loaded PLA/PLGA microcapsules by a novel membrane emulsification method and its release in vitro. *Colloid Surf B,* 51:30-38, 2006.
53. Göpferich A. Mechanisms of polymer degradation and erosion. *Biomaterials,* 17:103-114, 1996.
54. Grizzi I, Garreau H, Li S, Vert M. Hydrolytic degradation of devices based on poly(DL-lactic acid) size dependence. *Biomaterials,* 16:305-311, 1995.
55. Batycky RP, Hanes J, Langer R, Edwards DA. A theoretical model of erosion and macromolecular drug release from biodegrading microspheres. *J Pharm Sci,* 86:1464-1477, 1997.
56. Armstrong JK, Wenby RB, Meiselman HJ, Fisher TC. The hydrodynamic radii of macromolecules and their effect on red blood cell aggregation. *Biophys J,* 87:4259-4270, 2004.
57. Allison SD. Effect of structural relaxation on the preparation and drug release behavior of poly(lactic-co-glycolic) acid microparticle drug delivery systems. *J Pharm Sci,* 97:2022-2035, 2008.
58. Mazzara JM, Balagna MA, Thouless MD, Schwendeman SP. Healing kinetics of microneedle-formed pores in PLGA films. *J Control Release,* 171:172-177, 2013.
59. Fredenberg S, Wahlgren M, Reslow M, Axelsson A. Pore formation and pore closure in poly(D,L-lactide-co-glycolide) films. *J Control Release,* 150:142-149, 2011.
60. Kang J, Schwendeman SP. Pore closing and opening in biodegradable polymers and their effect on the controlled release of proteins. *Mol Pharm,* 4:104-118, 2007.
61. Blasi P, D'Souza SS, Selmin F, DeLuca PP. Plasticizing effect of water on poly(lactide-co-glycolide). *J Control Release,* 108:1-9, 2005.
62. Passerini N, Craig DQM. An investigation into the effects of residual water on the glass transition temperature of polylactide microspheres using modulated temperature DSC. *J Control Release,* 73:111-115, 2001.

Supplemental Information

Supplemental Table SI. Grading procedure for the porosity assignment of the PLGA microspheres using SEM pictures.

Grade	< 1 µm size pores (mean nr/ ~6 particles)	> 1µm size pores (mean nr/ ~6 particles)
1	None	None
2	Few (1-5)	None
3	Few (5-10)	Few (1-3)
4	Moderate (10-20)	Moderate (3-5)
5	Many > 20	Many > 5

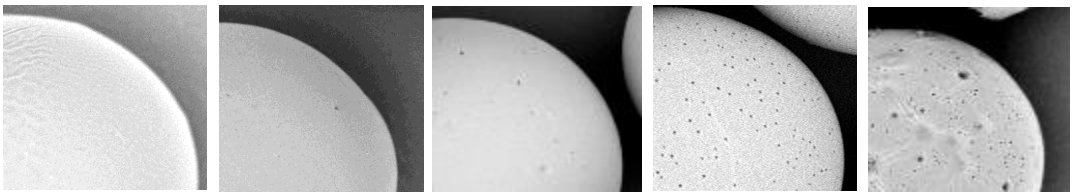

Supplemental Figure S1. Representative SEM photographs of PLGA microspheres for porosity grading (magnification 5000x). From left to right: porosity grade 1 (Formulation 15), grade 2 (Formulation 3), grade 3 (Formulation 9), grade 4 (Formulation 1) and grade 5 (Formulation 7). Formulation characteristics are given in Table I.

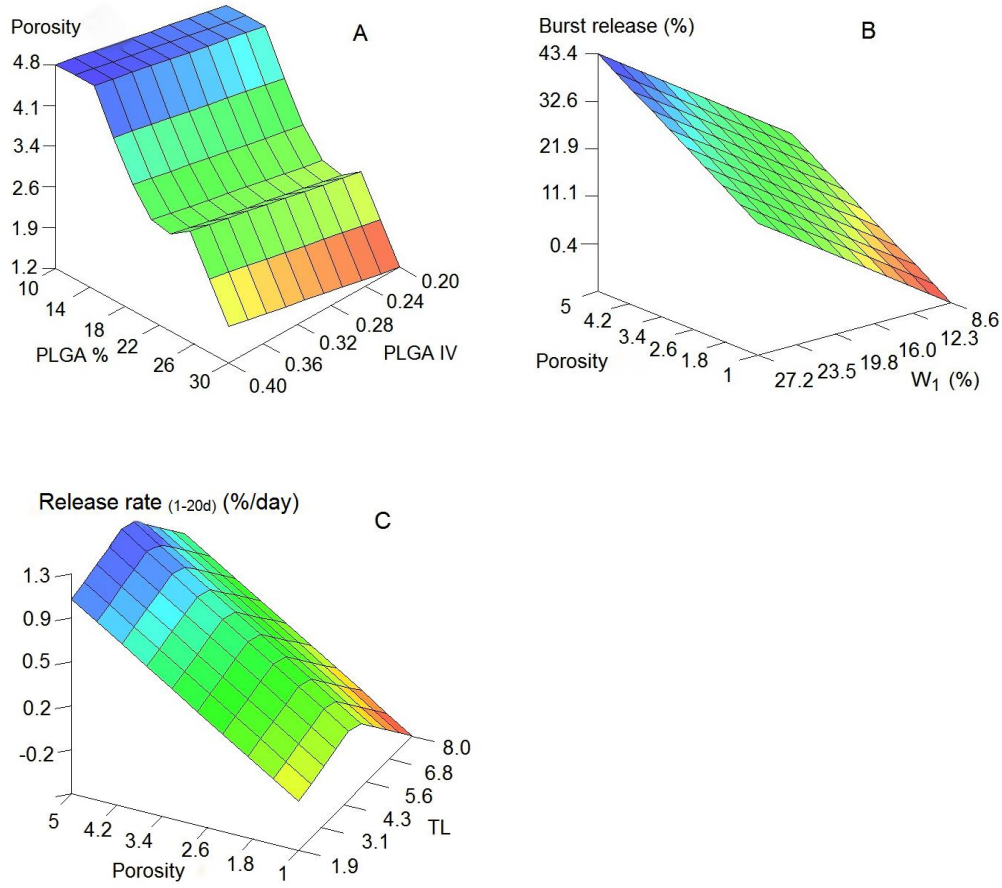

Supplemental Figure S2. Results of microsphere porosity as an input and output parameter calculated by neurofuzzy logic: A. Porosity as an output parameter (z-axis) depending on the PLGA concentration in the oil phase (% w/w) and PLGA molecular weight (expressed as intrinsic viscosity (IV)) (x and y-axis); B. Influence of porosity and W_1 as input parameters (x and y-axis) on the burst release (%) (z-axis); C. Influence of porosity and theoretical drug loading (TL) as input parameters (x and y-axis) on the release rate$_{(1\text{-}20)}$ (z-axis).

Supplemental Table SII. Values of training parameters used by FormRules v3.31 for modeling; model assessment parameters including *R*-squared and ANOVA *f* computed ratio; and the significant inputs selected by Neurofuzzy Logic as the ones that explain the variation of each output (the input with the strongest effect is printed in bold); and the GEP predictability results for each output parameter.

	Stability[a] W_1/O (min)	Yield (%)	Vol-WT mean diameter (μm)	Span value	Porosity[b]	LE (%)	LC (%)	Burst release[c] (%)	Release rate$_{(1\ 20d)}$[d] (%/day)
TRAINING PARAMETER SETTING WITH FormRules v3.31									
Minimization parameter[e]									
Model Selection Criteria[f]	SRM (C_1=0.832)	SRM (C_1=0.67)	MDL	SRM (C_1=0.72)	MDL	MDL	MDL	SRM (C_1=0.74)	SRM (C_1=0.75)
NEUROFUZZY LOGIC MODEL ASSESSMENT PARAMETERS									
R^2 (%)	97.37	96.51	81.86	95.35	92.58	87.54	91.06	77.07	78.26
Computed *f* ratio[g]	74.27*	16.61*	13.54*	3.47**	16.04*	30.45*	10.19*	2.94**	9.90*
SIGNIFICANT INPUTS FROM THE NEUROFUZZY LOGIC SUBMODELS									
	PLGA type **PLGA %** W_1	**PLGA type*** **PLGA %** W_1	**PLGA type*** **PLGA %**	PLGA type* PLGA % **W_1** W_2 PVA %	PLGA type **PLGA %** W_2	PLGA type **PLGA %**	**PLGA type*** **PLGA %**	Porosity **W_1** W_2 PVA %	**Porosity** TL
GEP Predictability Train set R^2 (%)			87.15	91.31	75.19	88.18		75.65	72.89

[a] time after which visual phase separation occurred, [b]porosity was graded according to the procedure given in Supplemental Table SI, [c]release of blue dextran in 24h, [d]slope of the release curve calculated between days 1 and 20, [e]for other training parameters refer to paragraph 2.7, [f]SRM-Structural Risk Minimization, MDL-Minimum Description Length, [g] *significant model with $\alpha<0.01$, **significant model with $\alpha<0.05$; LE-loading efficiency, LC-loading capacity, PLGA type (PLGA 5002 or 5004), PLGA %-percentage of PLGA in the oil phase,W_1- percentage of inner water volume, W_2-excipients in the continuous phase, PVA %-percentage of PVA in the continuous phase, TL-theoretical drug loading.

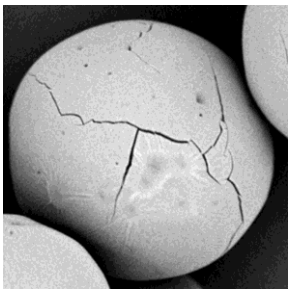

Supplemental Figure S3. SEM photograph of formulation 12 prepared with 20% PLGA 5002, 33% inner water volume and 4% PVA in the continuous phase (magnification 4000x).

Chapter 3

Biocompatibility of poly(D,L-lactic-co-hydroxymethyl glycolic acid) microspheres after subcutaneous and subcapsular renal injection

Filis Kazazi Hyseni[1]
Jurjen Zandstra[2]
Eliane R Popa[2]
Roel Goldschmeding[3]
Audrey AR Lathuile[4]
Gert J Veldhuis[4]
Cornelus F van Nostrum[1]
Wim E Hennink[1]
Robbert Jan Kok[1]

[1.] Department of Pharmaceutics, Utrecht Institute for Pharmaceutical Sciences, Utrecht University, Utrecht, The Netherlands
[2.] Department of Pathology and Medical Biology, Medical Biology Section, University Medical Centre Groningen, University of Groningen, Groningen, The Netherlands
[3.] Department of Pathology, University Medical Center Utrecht, Utrecht, The Netherlands
[4.] Nanomi B.V., Oldenzaal, The Netherlands

International Journal of Pharmaceutics, 482:99-109, Mar 2015

Abstract

Poly(D,L-lactic-*co*-hydroxymethyl glycolic acid) (PLHMGA) is a biodegradable copolymer with potential as a novel carrier in polymeric drug delivery systems. In this study, the biocompatibility of PLHMGA microspheres (PLHMGA-ms) was investigated both *in vitro* in three different cell types (PK-84, HK-2 and PTECs) and *in vivo* at two implantation sites (by subcutaneous and subcapsular renal injection) in rats. Both monodisperse (narrow size distribution) and polydisperse PLHMGA-ms were prepared with volume weight mean diameter of 34 and 17 µm, respectively. Mono and polydisperse PLHMGA-ms showed good cytocompatibility properties upon 72h incubation with the cells (100 µg microspheres/600 µL/cell line). A mild foreign body reaction was seen shortly after subcutaneous injection (20 mg per pocket) of both mono and polydisperse PLHMGA-ms with the presence of mainly macrophages, few foreign body giant cells and myofibroblasts. This transient inflammatory reaction diminished within 28 days after injection, the time-point at which the microspheres were degraded. The degradation profile is comparable to the *in vitro* degradation time of the microspheres (*i.e.*, within 35 days) when incubated at 37°C in phosphate buffered saline. Subcapsular renal injection of monodisperse PLHMGA-ms (10 mg) in rats was characterized with similar inflammatory patterns compared to the subcutaneous injection. No cortical damage was observed in the injected kidneys. In conclusion, this study demonstrates that PLHMGA-ms are well tolerated after *in vivo* injection in rats. This makes them a good candidate for controlled delivery systems of low-molecular weight drugs as well as protein biopharmaceuticals.

1. Introduction

Poly(D,L-lactic-*co*-glycolic acid) (PLGA) is a biodegradable aliphatic polyester that has been investigated for controlled delivery of low molecular weight drugs [1], peptides [2,3], proteins [4-6] and vaccine antigens [7,8]. PLGA is degraded by hydrolytic cleavage of ester bonds that connect the monomer units, and the final degradation products are lactic and glycolic acid, both endogenous compounds [9,10]. An important drawback of PLGA matrices, however, is the formation of acidic degradation products which are detrimental for the stability and integrity of entrapped (therapeutic) proteins [11,12]. Denaturation of the formulated protein or structural modifications due to acid-catalyzed reactions will affect both therapeutic efficacy and can cause potential immunological responses to the formulated protein [13,14].

A novel copolymer, poly(D,L-lactic-*co*-hydroxymethyl glycolic acid) (PLHMGA) [15] has a similar molecular structure as PLGA with additional pendant hydroxyl groups on the polymer backbone (Figure 1). The degradation of this co-polymer and the release of entrapped proteins can be tailored by its copolymer composition [16-18]. Furthermore, PLHMGA based microspheres are peptide and protein friendly [17-19]. Owing to the more hydrophilic nature of PLHMGA compared to PLGA, it has been demonstrated that the water-soluble acidic degradation products of PLHMGA are rapidly released from degrading microspheres into the external medium [20]. As PLHMGA is intended for use of delivering drugs *in vivo*, characterization of the *in vivo* biodegradation as well as biocompatibility properties of these copolymeric microspheres is required.

The aim of this study is to evaluate the *in vitro* cytotoxicity and *in vivo* biocompatibility of PLHMGA microspheres (PLHMGA-ms). These tests are mandatory according to the International Organization for Standardization (ISO) guidelines for biological evaluation of implantable medical devices [21]. PLHMGA-ms were prepared with two different methods, a conventional single emulsion solvent evaporation method for preparation of polydisperse microspheres and by membrane emulsification method for generating uniform size microspheres. Previously, we have shown that microspheres prepared by this method of emulsification have high batch-to-batch reproducibility in terms of particle characteristics and release kinetics [22]. Moreover, due to the uniform size, monodisperse microspheres also have better injectability and hence allow the use of smaller needles for the administration of microsphere suspensions. This is of special attention in the present study, in which we investigated the feasibility of injecting PLHMGA microspheres under the renal capsule. Subcapsular renal injection is a relatively new method for local delivery of therapeutics to the kidneys which was earlier tested for the injection of hydrogels [23]. We created a small pocket between the capsule and the soft cortex tissue with a small blunt needle

and used the same needle to inject a concentrated dispersion of the microspheres, to study their biocompatibility at this injection site. In addition, we studied the biocompatibility of PLHMGA microspheres after subcutaneous injection.

The *in vitro* cytocompatibility was assessed in three different cell types, namely dermal fibroblasts (PK-84), proximal tubular epithelial cells (HK-2) and primary tubular epithelial cells (PTECs). For the *in vivo* biocompatibility assessment, both monodisperse and polydisperse PLHMGA-ms were injected subcutaneously in rats. The inflammatory response was studied along with the influence of particle size and polydispersity on the foreign body reaction. Furthermore, the degradation profile of PLHMGA-ms was studied *in vitro* and correlated to the *in vivo* degradation as observed in histopathology tissue samples.

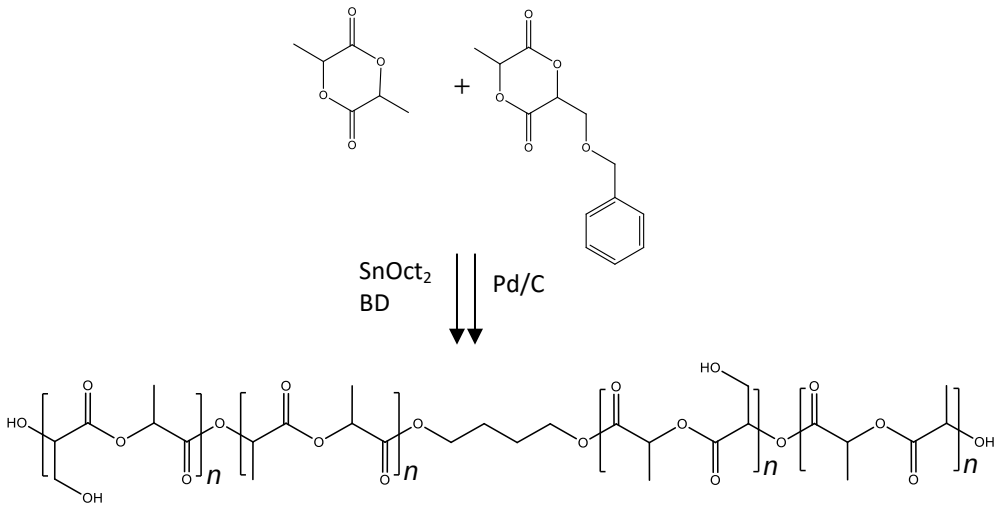

Figure 1. Synthesis of poly(lactic-co-hydroxymethyl glycolic acid) (PLHMGA) from **D,L**-Lactide and 3*S*-(benzyloxymethyl)–6*S*–methyl–1,4–dioxane-2,5–dione (BMMG) by melt copolymerization with $SnOct_2$ as catalyst and 1,4-butanediol (BD) as initiator. The protective benzyl groups were removed by hydrogenation using palladium on activated carbon (Pd/C) as a catalyst.

2. Materials and Methods

2.1. Materials

O-Benzyl-L-serine was purchased from Senn Chemicals AG (Dielsdorf, Switzerland). DL-Lactide was purchased from Purac (The Netherlands). Tin(II) 2-ethylhexanoate ($SnOct_2$), poly(vinyl alcohol) (PVA; M_w= 13,000-23,000 g/mol), palladium 10 wt% (dry basis) on activated carbon, hematoxylin solution and dimethylsulfoxide (DMSO) were obtained from Sigma–Aldrich (Germany). 1,4-Butanediol, 99+% was obtained from Acros Organics (Belgium). Carboxymethylcellulose (CMC, with viscosity of 2,000 mPa s of a 1% solution in water) was obtained from Bufa B.V. (255611, The Netherlands). Sodium phosphate dibasic (Na_2HPO_4) and sodium azide (NaN_3) were purchased from Fluka (The Netherlands). Dichloromethane (DCM) and tetrahydrofuran were purchased from Biosolve BV (The Netherlands). Sodium dihydrogen phosphate (NaH_2PO_4), sodium hydroxide (NaOH) and sodium chloride (NaCl) were supplied from Merck (Germany). Mouse anti rat CD68 monoclonal antibody (clone ED-1) was obtained from AbD Serotec (MCA341R, Germany). Monoclonal mouse anti-human Actin (α-SMA) was obtained from Dako (Clone 1A4, Denmark).

2.2. Polymer synthesis and characterization

Poly(D,L-lactic-*co*-hydroxymethyl glycolic acid) (PLHMGA) was synthesized as previously described [15], using butanediol as an initiator, to obtain a hydroxyl terminated co-polymer. In brief, BMMG (3*S*-(benzyloxymethyl)-6*S*-methyl-1,4-dioxane-2,5-dione) was synthesized from *O*-benzyl-L-serine [15]. In the second step BMMG (35 mol%) and D,L-lactide (65 mol%) were copolymerized in the melt at 130°C using butanediol and tin(II) 2-ethylhexanoate as initiator and catalyst, respectively, to yield poly(D,L-lactic-*ran*-benzyloxymethyl glycolic acid) (PLBMGA). Next, the resulting PLBMGA was dissolved in chloroform and subsequently precipitated in cold methanol, and dried *in vacuo*. In the third step, the protective benzyl groups of PLBMGA were removed by hydrogenation of the polymer dissolved in tetrahydrofuran, using 10% w/w palladium on activated carbon (Pd/C) as a catalyst, for 16 h at room temperature. The catalyst was removed by filtration through 0.2 µm nylon filters (Alltech Associates) and the formed copolymer, PLHMGA, was dried *in vacuo* (Figure 1).

The molecular weight of the polymer was determined by GPC (Waters Alliance System) with a Waters 2695 separating module and a Waters 2414 refractive index detector, using tetrahydrofuran as solvent at a flow rate of 1 mL/min; polystyrene standards (PS-2, M_w = 580–377,400 Da, EasiCal, Varian) were used for calibration. Two PL-gel 5 µm Mixed-D columns fitted with a guard column

(Polymer Labs, M_w range 0.2 – 400 kDa) were used. The composition of the copolymer was determined by NMR (Gemini-300 MHz) in chloroform-*d*, 99.8 atom% (Sigma-Aldrich) as a solvent [15].

PLHMGA- ^1H NMR ($CDCl_3$): δ = 1.4-1.6 (m, 3H, -CH_3), 3.8-4.1 (m, 2H, -CH_2-OH), 5.0-5.3 (m, 2H, -CH-CH_2-OH and –CH-CH_3)

The thermal properties of the copolymer were measured with differential scanning calorimetry (DSC - Q 2000, TA Instruments). Approximately 5 mg of copolymer was transferred into an aluminum pan (T zero pan/lid set, TA Instruments) and the sample was scanned with a modulated heating method in three cycles [17]. The sample was heated until 120°C (5°C/min) and then cooled down to -50°C, followed by a heating until 120°C (5°C/min). The temperature modulation was ±1°C/min. The glass transition temperature (T_g) was determined from the second heating scan. Residual palladium in PLHMGA, used as a catalyst during the de-protection step, was measured with instrumental neutron activation analysis (Technical University of Delft). Around 100 mg of PLHMGA was packed in high purity polyethylene capsules and was irradiated at a neutron flux of 4.5 x10^{16} m^{-2} s^{-1}. The *γ* ray spectra were acquired using various independently calibrated detectors. The spectra obtained were interpreted using the nuclear data set [24]. The detection limit of palladium with this method is 2.4 ppm.

2.3. Preparation of polydisperse and monodisperse PLHMGA-ms

Monodisperse PLHMGA-ms were prepared using a membrane emulsification method with a single emulsion (o/w) as described in detail elsewhere [22,25]. The particles were prepared aseptically in a flow cabinet using autoclaved equipment and sterile water. The oil phase (o) contained 3 g of polymer dissolved in 20.3 mL DCM (10%; w/w). This solution was then pushed through the microsieve^{TM} membrane (Iris-20, Nanomi B.V., The Netherlands) at a rate of 12 mL/h by using a syringe pump (Nexus 6000, Chemyx, USA) into the continuous phase (w) containing 400 mL of 4% PVA (the ratio of the oil phase and the continuous phase was 1:20). Polydisperse PLHMGA-ms were prepared with conventional single emulsion (o/w) method. Two grams of polymer were dissolved in 13.5 mL DCM (10%; w/w) and 67.5 mL of 0.5% PVA solution was added. The mixture was homogenized with Ultra-Turrax T8 (Ika Works, USA) with dispersing element S10N-10G, at a speed of 20,000 rpm for 30s, and then added dropwise to 270 mL of 4% PVA solution. For both methods, the collected droplets were stirred for three hours at room temperature to evaporate DCM. The hardened microspheres were washed three times with water by centrifuging at 3,000 rpm for 2 min (Rotina 380, Hettich, Germany) and subsequently collected after freeze-

drying (Alpha 1-2, Martin Christ, Germany). Single batches were used for *in vitro* cytocompatibility and *in vivo* biocompatibility testing.

2.4. Characterization of PLHMGA-ms

The size of the particles was measured with an optical particle sizer (Accusizer 780, California, USA). At least 5,000 microspheres were analyzed and the volume-weight mean particle diameter is reported as the mean particle size. The morphology of the microspheres was analyzed with scanning electron microscope (SEM, Phenom, FEI Company, The Netherlands). Lyophilized microspheres were transferred onto 12-mm diameter aluminum specimen stubs (Agar Scientific Ltd., England) using double-sided adhesive tape. Prior to analysis, the microspheres were coated with platinum using an ion coater under vacuum. The residual amount of DCM in the microspheres was measured with NMR (Varian Gemini-300) with DMSO-d_6 as a solvent [26,27]. Samples of 50 mg were dissolved in 1 mL of DMSO for one hour and spiked with 5 mg of 1,4-dinitrobenzene (Oekanar®, Fluka) as the internal standard. The amount of the DCM was calculated from the NMR spectra according to the following equation, as adapted from Jones *et al*. [27]:

$$\boldsymbol{DCM_{ppm}} = \frac{\boldsymbol{integral_{(DCM)} x\ No.H_{(standard)} x\ weight_{(standard)} x\ Mw_{(DCM)}}}{\boldsymbol{integral_{(standard)} x\ No.H_{(DCM)} x\ Mw_{(standard)}}}\ \boldsymbol{x\ 1 \cdot 10^6}$$

where, M_w is the molecular weight and No.H is the number of protons of the peak (4H for 1,4-dinitrobenzene and 2H for DCM). The residual amount of DCM in the microspheres should be below the maximum concentration allowed by FDA, *i.e.*, concentration limit of 600 ppm or the permitted daily exposure of 6 mg/day [28,29].

Potential bacterial contamination of the microspheres was determined by inoculation of 5 mg of dry PLHMGA-ms (dispersed in sterile water) on blood agar plates. The plates were incubated at 37°C for 4 days and were checked daily for the presence of bacterial colonies. The endotoxin levels were determined using the Limulus assay (Toxicon Europe, Leuven, Belgium).

2.5. In vitro degradation studies

PLHMGA-ms (10 mg) were suspended in 1.5 mL PBS buffer, pH 7.4 (0.056 M NaCl, 0.033 M Na_2HPO_4, 0.066 M NaH_2PO_4 and 0.05% (w/w) NaN_3) and incubated at 37°C while mildly shaking. A total of six vials was used. At predetermined time-points one vial was removed, centrifuged (4,000 rpm, 5 min)

and the pellet was washed three times with water and freeze-dried overnight. The microspheres were measured for dry weight and the molecular weight of the polymers was analyzed using GPC as described in 2.2.

2.6. In vitro cytotoxicity study

2.6.1. Cell culture

Monodisperse and polydisperse PLHMGA-ms were incubated with three different cell types (human skin fibroblasts (PK-84), human proximal tubular cells (HK-2) and human primary tubular epithelial cells (PTECs)). The PK-84 were cultured in RPMI 1640 medium (Lonza, Breda, The Netherlands), supplemented with 10% v/v fetal calf serum (Perbio Science, Etten-Leur, The Netherlands) and with standard additives. The HK-2 and PTECs were cultured in 1:1 v/v Ham's F12 (L-glutamine) and in Dulbecco's modified Eagle's medium supplemented with 1% v/v glutamine, 1% v/v penicillin, 0.01 mg/L epidermal growth factor, 10 mg/L insulin, 5.5 mg/L transferrin, 6.7 µg/L sodium selenite, 36 µg/L hydrocortisone and 2 mM glutamax. The medium of HK-2 was supplemented with 10% v/v fetal calf serum, whereas the medium of PTECs was supplemented with 1% v/v human pooled serum. All cell cultures were incubated at 37°C with 5% CO_2.

2.6.2. Extraction test

For the preparation of the extracts of microspheres, 5 mg PLHMGA-ms was incubated for 24h at 37°C in 25 mL of complete culture medium. This method allows the extraction of both polar and nonpolar leachables from the microspheres [21]. After 24h-incubation, the samples were centrifuged at 300 g. In a similar way we prepared extracts of latex rubber (thickness 3-4 mm; Hilversum Rubber Factory, Hilversum, The Netherlands) and of polyurethane film (thickness about 1 mm; made from 2363-55D-pellethane® resin; Dow Chemical, Midland, MI, USA) that were used as a positive cytotoxic control (Latex) and as a negative non-cytotoxic control (polyurethane), respectively. PK-84, HK-2 and PTECs were seeded in 24-well plates (cell density of 15,000 cells/cm^2) and after 24 h the medium of the cells was replaced with 500 µL of the extracts of PLHMGA-ms (corresponding to 100 µg microspheres), latex and polyurethane. Cells were incubated for 48 h followed by measurements with CyQuant cell proliferation assay (for quantification of nucleic acid content) and MTS assay (for mitochondrial activity measurements) as described in 2.6.4 and 2.6.5.

2.6.3. Direct contact assay

For direct contact assay, the microspheres were dispersed in complete medium (100 µg in 600 µL) and added to the cell cultures (cell density of 15,000 cells/cm^2). Small pieces of polyurethane film and latex rubber were used as a negative and positive control to show the behavior of the cells in the presence of a biocompatible and cytotoxic material, respectively [30]. Cells were cultured for 72h and the cell morphology was examined every day. The cell viability was analyzed with CyQuant cell proliferation assay and MTS assay as described in 2.6.4 and 2.6.5.

2.6.4. Cell proliferation assay

The CyQuant® cell proliferation assay (Invitrogen, The Netherlands) was performed according to the manufacturer's instructions. In brief, after removing the culture medium (including floating and dead cells) the cells were stored at -80 °C for 48 h. Subsequently, culture plates were defrosted at room temperature and the CyQuant® green dye/cell-lysis buffer was added to each well. The green dye exhibits strong fluorescence enhancement when bound to cellular nucleic acids. After 5 min incubation at room temperature, the fluorescence was quantified using a fluorescence microplate reader (Varioscan, Thermo Fisher Scientific Inc.) with a 480/520-nm filter set.

2.6.5. Mitochondrial activity assay

The mitochondrial activity – MTS assay (CellTiter 96® AQueous One Solution, Promega Benelux Bv, The Netherlands) was performed according to manufacturer's instructions. Briefly, 100 µL of the culture medium containing the samples was mixed with 20 µL of the MTS reagent. The MTS reagent is reduced by metabolically active cells into a colored product. After 2-hour incubation at 37°C and 5% CO_2 atmosphere the absorbance was recorded at 490 nm with a fluorescence microplate reader (Varioscan, Thermo Fisher Scientific Inc.).

2.7. In vivo experiments

2.7.1. Animals

Animal experiments were carried out in 10-12 week old male Fischer 344/NCrHsd rats (Harlan Nederland, The Netherlands; n=3/time-point). Animals were fed laboratory chow and acidified water *ad libitum*, and were housed according to institutional rules with 12:12 h dark/light cycles. The protocol was

approved by the Animal Ethical Committee of the University of Groningen. During the injections, rats were anesthetized under general isoflurane/O_2 inhalation and palliative treatment was used consisting of buprenorphine. At specific time-points rats were sacrificed by cervical neck dislocation.

2.7.2. Subcutaneous injection

Mono- and polydisperse PLHMGA-ms suspensions were prepared by mixing 20 mg of the microspheres with 150 µl of an autoclaved viscous carrier (0.4% carboxymethylcellulose-CMC, 0.02% Tween-20 and 5% mannitol in water). Microparticle suspensions were injected subcutaneously on the back of the rats. Injection sites were explanted at day 7, 14 and 28. Implants were fixed in zinc fixative solution (0.1M Tris-buffer, 3.2 mM calcium acetate, 23 mM zinc acetate, 37 mM zinc chloride, pH 6.5-7; Merck, Darmstadt, Germany) overnight, prior to paraffin embedding. Implants were cut into 4 µm thick sections.

2.7.3. Subcapsular renal injection

For injection under the renal capsule, monodisperse PLHMGA-ms were used. A midline incision was made under the left kidney capsule of a rat and 50 µL of microsphere suspension (10 mg of microspheres in 50 µL of 0.4% CMC, 0.02% Tween-20 and 5% mannitol in water) was injected with a 26G blunt Hamilton needle (Chrom8 International, The Netherlands). The kidneys were explanted at day 3, 7 and 14. Kidneys were flushed *in vivo* with saline solution, excised and paraffin-embedded. Implants were cut into 4 µm thick sections.

2.8. (Immuno)histochemistry

Tissue sections were stained for infiltration of macrophages (ED-1 macrophage marker) and for myofibroblasts (α-SMA staining). Four µm thick sections were deparaffinized and antigen retrieval was performed overnight in a 0.1M Tris-HCl buffer, pH 9.0, at 80°C [31]. The non-specific binding was blocked with 2% bovine serum albumin for 30 min, while the endogenous peroxidase activity was suppressed by incubating the samples in 0.1% H_2O_2 for 10 min. In ED-1 staining, sections were then incubated with mouse-anti-rat ED-1 monoclonal antibody (10 µg/mL) for 1h followed by horseradish peroxidase-conjugated rabbit-anti-mouse polyclonal antibody (13 µg/mL; DAKO, Denmark) for 30 min. For α-SMA staining, after antigen retrieval and blocking of the non-specific binding, tissue sections were incubated in mouse α-SMA monoclonal antibody (0.44 µg/mL) for 1h, followed by incubation in horseradish-conjugated rabbit-anti mouse polyclonal antibody (13 µg/mL; DAKO, Denmark) for 30 min. After the incubation with the secondary antibody all sections were washed three times with PBS and the enzyme

activity was developed with 3-amino-9-ethylcarbazole (AEC; Sigma-Aldrich, The Netherlands). All tissue sections were counterstained with hematoxylin for 5 min at 37°C.

3. Results and discussion

3.1. Characteristics of the PLHMGA copolymer

The synthesized PLHMGA (Figure 1) had an average molecular weight of 22 kDa (relative to the polystyrene standards) with a PDI of 1.7 as measured by GPC. The copolymer composition was 34/66 mol/mol (BMMG/D,L-lactide before hydrogenation) as measured with NMR (feed ratio 35/65). The glass transition temperature of PLHMGA (T_g) was 35.6°C. Due to the use of palladium-based catalyst during the de-protection step, the obtained copolymer might contain residual amounts of this metal. Instrumental neutron activation analysis showed that the palladium content in PLHMGA was 174 ppm, which corresponds to 1.74 µg of palladium in 10 mg of PLHMGA-ms. According to European Medicines Agency, the parenteral permitted daily exposure to palladium is 10 µg/day (for a 50 kg person) while LD50 values for palladium salts range from 3 to 4,900 mg/kg depending on the type of palladium salt and route of administration [32]. Based on these criteria, we do not expect adverse events in the animal studies due to the residual amounts of palladium catalyst.

3.2. *Characteristics of the PLHMGA-ms*

Monodisperse PLHMGA-ms were prepared with a membrane emulsification method. The obtained microspheres had a volume weight mean diameter of 34 µm and were quite monodisperse (distribution: 30-38 µm) (Figure 2A and C). Polydisperse PLHMGA-ms were prepared with a conventional single emulsion method and had a mean particle size of 17 µm (distribution: 5-46 µm) (Figure 2B and D). Scanning electron microscopy (SEM) showed that the microspheres had smooth surface and no visible pores (Figure 2A and B). The residual DCM content measured with NMR was < 400 ppm for both microsphere batches which is below the maximum recommended amount by Food and Drug Administration (600 ppm or 6 mg/day) [28,29]. No bacterial contamination was detected in the prepared microsphere batches. The endotoxin level of the microsphere dispersions was within the approved FDA norm (0.5 EU/mL).

When incubated in PBS buffer at 37°C, both mono- and polydisperse PLHMGA-ms showed 80% weight loss within 35 days, with gradual decrease in the molecular weight (Figure 3). This is in agreement with previously published data of PLHMGA with similar copolymer composition and molecular weight [33]. No

apparent differences were seen in the degradation profile between mono- and polydisperse microspheres, most probably due to the small differences of the average size of the microspheres (34 and 17 µm). According to another study, PLGA microspheres with an average diameter of 3 and 20 µm had similar degradation patterns, whereas nanoparticles of 300 nm in size degraded slower [34].

PLHMGA-ms are known to degrade by hydrolysis into lactic acid and hydroxymethyl glycolic acid [16,18], both endogenous small molecular weight acidic compounds. The latter compound is a derivative of serine, which is converted into glyceric acid and further metabolized *via* the glycolytic pathway [35].

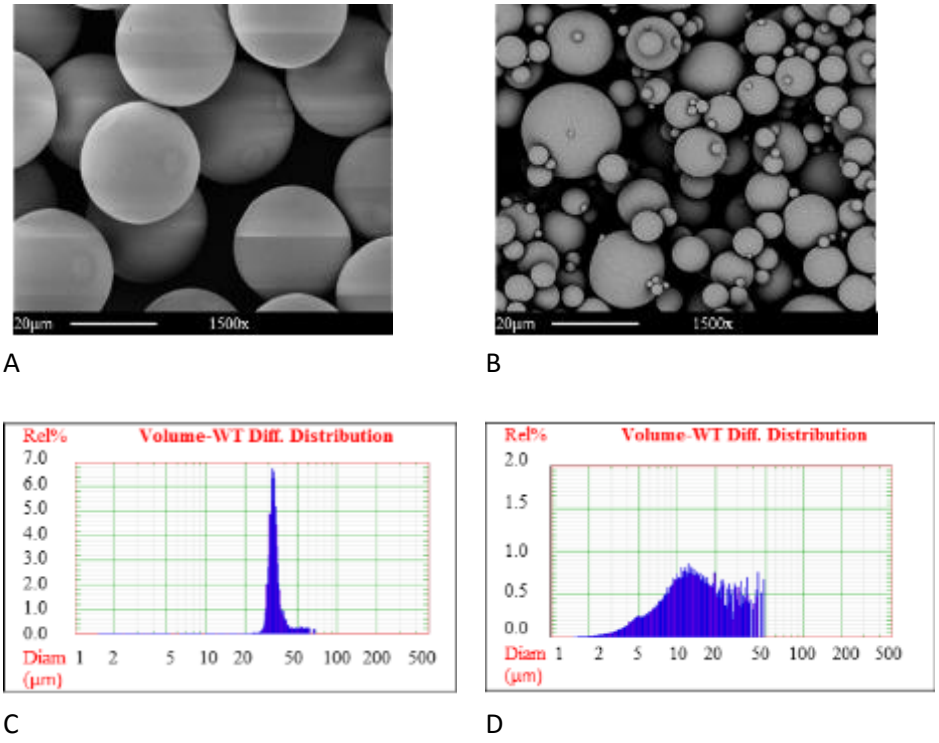

A B

C D

Figure 2. Representative SEM photographs of PLHMGA-ms (A and B; magnification 1500x) and the results of the volume weight particle diameter as measured with AccuSizer (C and D). **A** and **C**: monodisperse PLHMGA-ms prepared with membrane emulsification method and **B** and **D**: polydisperse PLHMGA-ms prepared with a conventional solvent evaporation method.

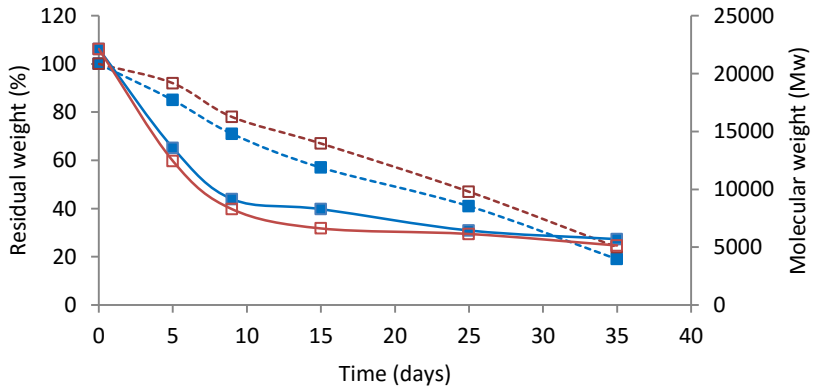

Figure 3. *In vitro* degradation of monodisperse (closed squares) and polydisperse (open squares) PLHMGA-ms. Solid lines represent the residual weight (%), whereas the dashed lines represent the weight average molecular weight (M_w) over time.

3.3. In vitro cytocompatibility of PLHMGA-ms: extraction test and direct contact assay

The *in vitro* cytocompatibility of PLHMGA-ms was tested using three different cultured cell types, *i.e.*, PK-84 (human skin fibroblasts), HK-2 (human proximal tubular cells) and PTECs (primary human proximal tubular epithelial cells). These cell types also reflect the tissues in which the microspheres were evaluated for *in vivo* biocompatibility (PK-84 for the subcutaneous injection and HK-2 and PTECs for the subcapsular renal injection). Figure 4 shows the results from the cytocompatibility study of PLHMGA-ms incubated with PK-84 cells. PLHMGA-ms did not influence the confluency of the cultured cell layer in both direct contact assay and upon incubation with the 24h-extracts of the microspheres. No significant differences were seen between polydisperse and monodisperse PLHMGA-ms in the cell viability assays. Proliferation of the cells was comparable to the control cultures and to polyurethane exposed cells, which served as a control material with good biocompatibility. As a positive (*i.e.*, cytotoxic) control in our assays, we exposed the cells to latex rubber and latex rubber extracts. Extracts of small pieces of latex or direct contact with this material resulted in detachment of exposed cells from the culture plate and extensive cellular lysis was observed within the first 24h (Figure 4E; last panel). Similar cytocompatibility data were also obtained using HK-2 (Figure 5) and PTECs (Figure 6). Thus, PLHMGA-ms showed excellent cytocompatibility with the studied cells. These data encouraged further *in vivo* biocompatibility studies with this copolymer (described in the next sections).

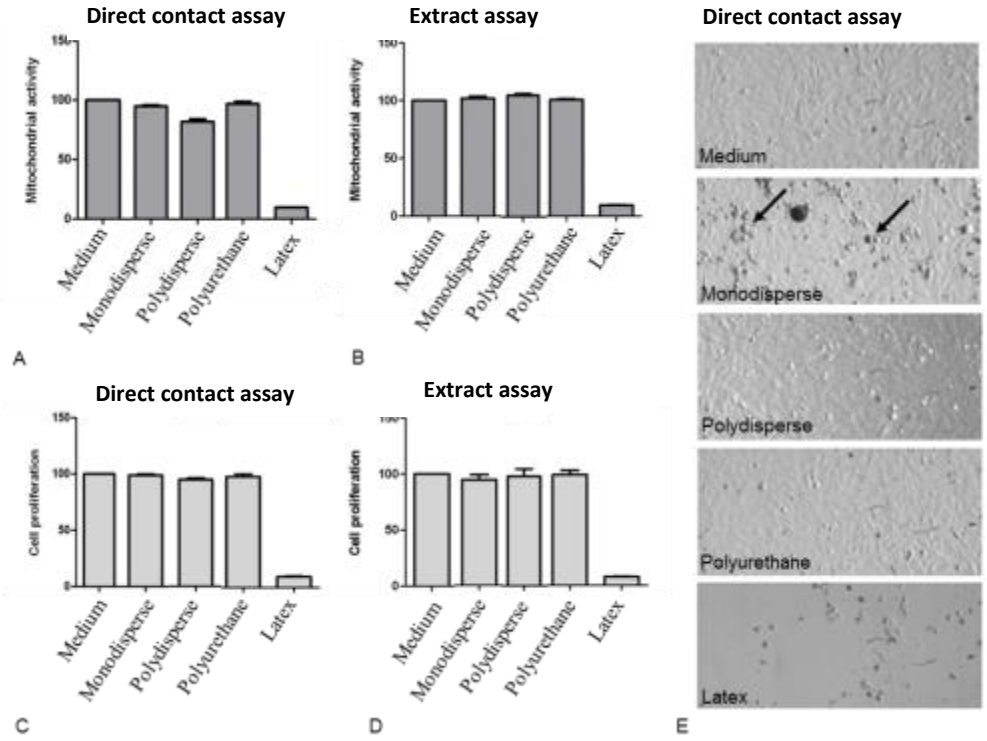

Figure 4. *In vitro* cytocompatibility of PLHMGA-ms (5 mg/600 µL) upon incubation with human skin fibroblasts (PK-84). PK-84 were exposed to mono- and polydisperse PLHMGA-ms in the direct contact assay for 72 h (**A** and **C**) and to their 24-hour extracts for 48 h (**B** and **D**). **E**: cell morphology in direct contact assay (magnifications 100x); arrows indicate the monodisperse PLHMGA-ms. Cell viability was assessed with MTS and cell proliferation assay. Polyurethane and latex were used as a negative and a positive control, respectively.

3.4. In vivo biocompatibility after subcutaneous injection of PLHMGA-ms

The *in vivo* biocompatibility of mono- and polydisperse PLHMGA-ms was assessed after subcutaneous injection of 20 mg microspheres in rats. The tissue samples were explanted at day 7, 14 and 28 and tissue sections were stained with ED-1 and *α*-SMA (Figure 7). PLHMGA-ms were visible in the tissue sections as unstained white round spheres. In tissues injected with monodisperse PLHMGA-ms, a mild inflammatory reaction was observed at day 7 after injection with the recruitment of few inflammatory cells, from which the majority were ED-1 expressing macrophages (Figure 7A) capable of phagocytosis [36].

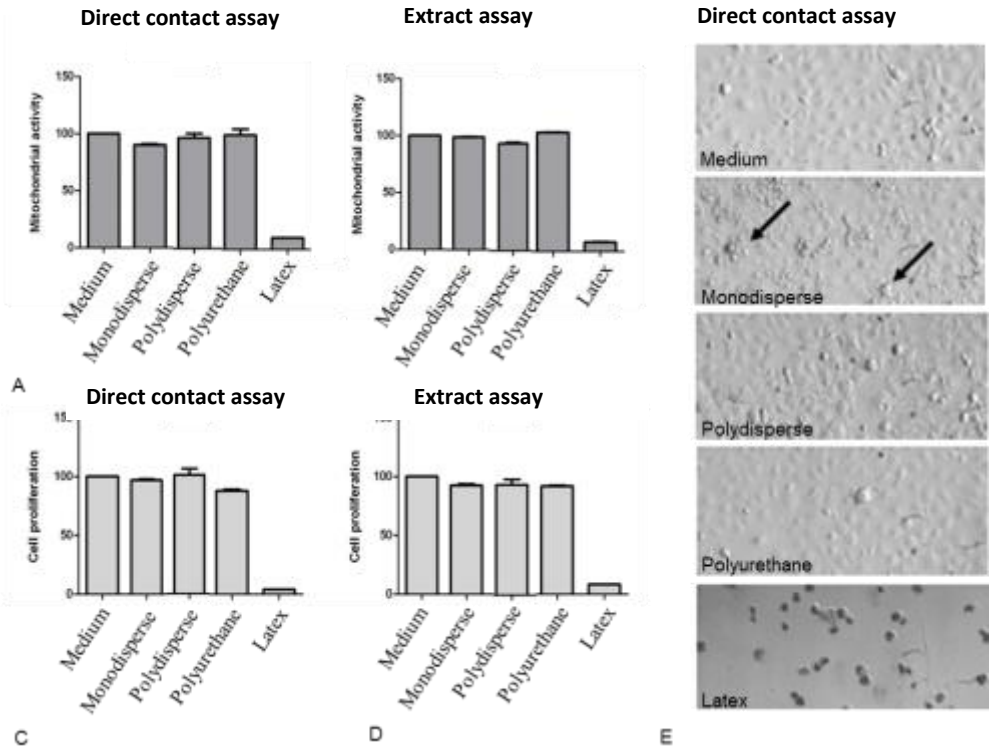

Figure 5. *In vitro* cytocompatibility of PLHMGA-ms (5 mg/600 µL) upon incubation with human proximal tubular cells (HK-2). HK-2 cells were exposed to mono- and polydisperse PLHMGA-ms in the direct contact assay for 72 h (**A** and **C**) and to their 24-hour extracts for 48 h (**B** and **D**). **E**: cell morphology in direct contact assay (magnifications 100x); arrows indicate the monodisperse PLHMGA-ms. Cell viability was assessed with MTS and cell proliferation assay. Polyurethane and latex were used as a negative and a positive control, respectively.

The presence of few foreign body giant cells (FBGCs) was also observed, which are formed by the fusion of macrophages in response to the foreign material [37]. Few myofibroblasts in samples explanted at day 7 were detected with α-SMA staining (Figure 7D). Myofibroblasts are cells with features of smooth muscle cells and are responsible for the wound contraction [38] and are also responsible for synthesizing collagen. Collagen forms the basis of the fibrous capsule, which plays a crucial role in the tissue repair and is considered a normal reaction feature towards the implanted foreign material [37,39]. Staining for α-SMA also allows detection of blood vessels, since vascular smooth muscle cells express this marker [40].

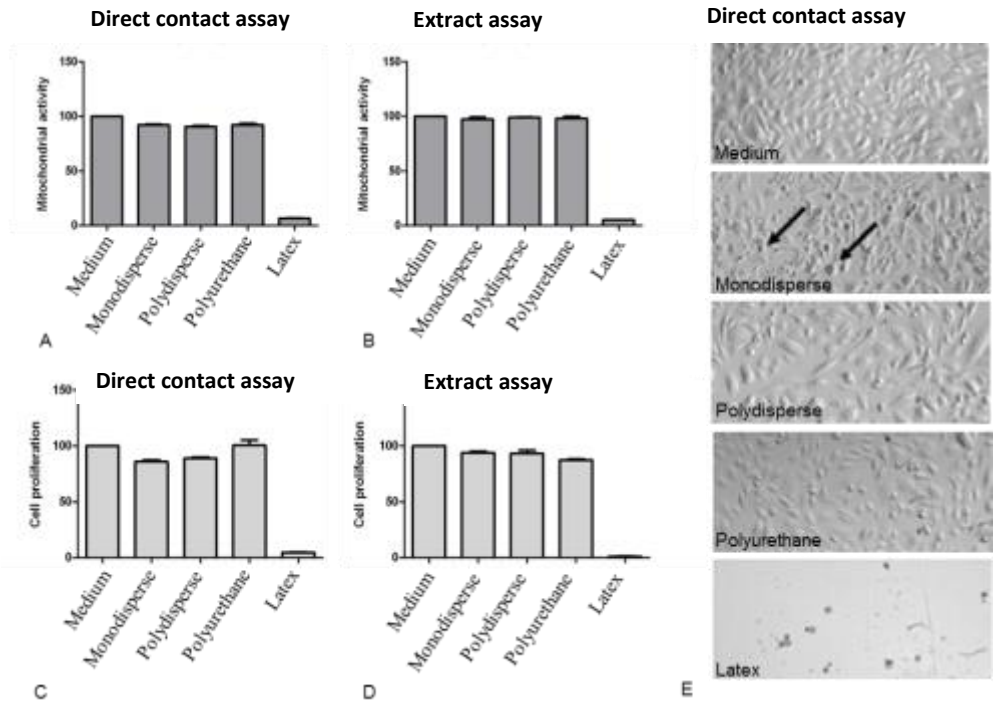

Figure 6. *In vitro* cytocompatibility of PLHMGA-ms (5 mg/600 µL) upon incubation with human primary tubular epithelial cells (PTECs). PTECs were exposed to mono- and polydisperse PLHMGA-ms in the direct contact assay for 72 h (**A** and **C**) and to their 24-hour extracts for 48 h (**B** and **D**). **E**: cell morphology in direct contact assay (magnifications 100x); arrows indicate the monodisperse PLHMGA-ms. Cell viability was assessed with MTS and cell proliferation assay. Polyurethane and latex were used as a negative and a positive control, respectively.

Scattered capillaries and arterioles were observed in sample tissues injected with monodisperse PLHMGA-ms and explanted at day 7. The presence of erythrocytes in the vessel lumina (Figure 7D) suggests functional blood vessels. The inflammatory reaction (macrophages, FBGCs) and myofibroblasts were also seen at day 14, when the microspheres fragmented into smaller residues < 10 µm (Figure 7B and E). At day 28, no particle residues were detected and few infiltrating macrophages were still present (Figure 7C). Myofibroblasts were virtually absent (Figure 7F), marking the end of the fibrotic response towards monodisperse PLHMGA-ms. No fibrous capsule was detected, which indicates a relatively mild foreign body reaction [41].

In a recent study, PLGA monodisperse microspheres with a similar size of 30 µm were investigated for their biocompatibility after subcutaneous injection in rats up to 4 weeks after their administration [42]. As expected from the type of PLGA used in this study, these microspheres hardly showed degradation during the time course of the study and only low numbers of infiltrated inflammatory cells were observed, in agreement with the mild foreign body reaction to PLGA. Polydisperse PLGA microspheres as well as other types of PLGA matrices have been studied extensively for their foreign body reaction and biocompatibility [39,43-45]. Visscher *et al.* [46-48] reported studies of the biocompatibility of 30 µm diameter PLGA (50/50) microspheres after intramuscular injection in rats. The authors observed a mild inflammatory reaction for a period of nine weeks with the presence of lymphocytes, macrophages and FBGCs. Phagocytosis of particles was observed around day 42 after injection, the time-point when particles became smaller than 10 µm in size [44]. Increased infiltration of macrophages was reported at day 56 [47]. The end of the inflammatory response in tissues injected with PLGA microspheres was observed around day 60 after administration [47]. Prolonged inflammatory reaction of PLGA microspheres as compared to the 28 days observed for PLHMGA-ms is caused by the longer (two-month) degradation time of PLGA [39,46,47].

The intensity of the inflammatory reaction towards injected polymeric microspheres is also dependent on particle size distribution. In this study, the effect of particle size distribution on the biocompatibility was tested by subcutaneous injection of polydisperse PLHMGA-ms in rats, prepared by conventional single emulsion method, with size distribution between 5 and 46 µm in diameter (mean: 17 µm). Tissues were explanted at day 7, 14 and 28 and stained with ED-1 and α-SMA (Figure 8). As was the case for monodisperse PLHMGA-ms, prepared by membrane emulsification, substantial numbers of macrophages were observed on 7, 14 and 28 days, as well as FBGCs on day 7 and 14 (Figure 8A-C). In comparison with monodisperse microspheres, increased vascularization was observed in tissue samples at day 14 (Figure 8E). Only a very few myofibroblasts were observed at day 7 and 14 (Figure 8D and E). Interestingly, some large particles were still present at day 28 after injection (Figure 8C and F). Although increased inflammatory responses towards smaller particles have been reported in previous studies [44,46,49-51], in the current study no significant differences were observed in the inflammatory reaction between the tissues injected with monodisperse and polydisperse PLHMGA-ms.

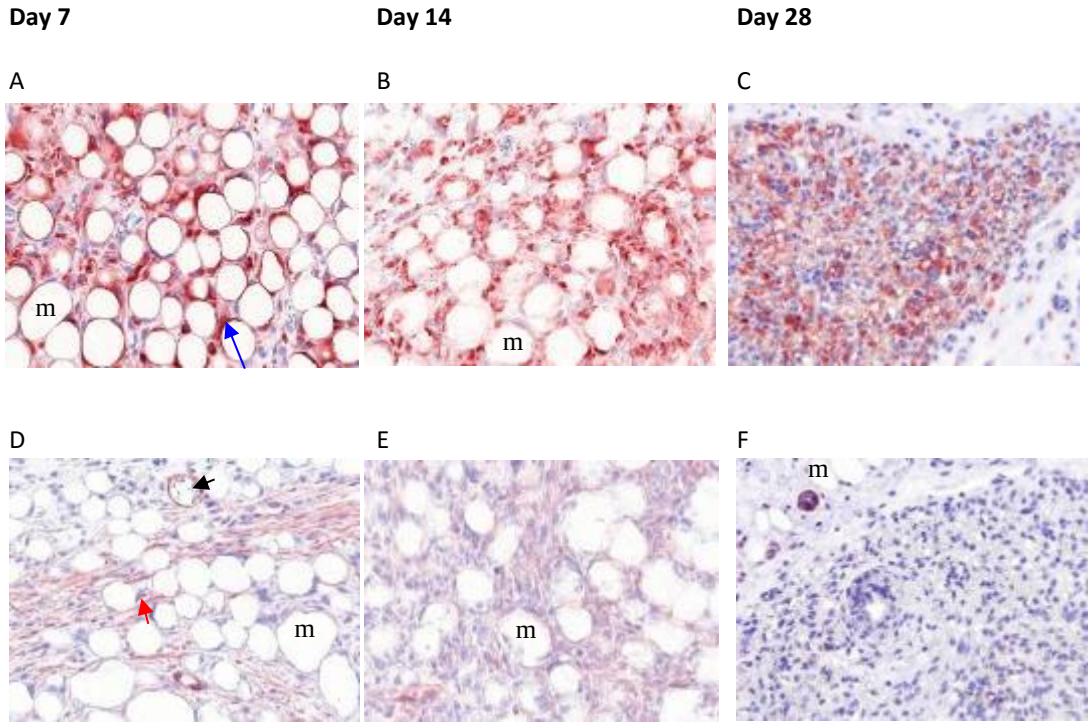

Figure 7. Histological pictures of subcutaneous tissues in which monodisperse PLHMGA-ms were injected. **A-C**: ED-1 staining (macrophages are stained in brown, blue arrow); **D-F**: α-SMA staining (myofibroblasts are stained in pink; red arrow), blood vessels are stained in red (black arrow). Microspheres (m) remain unstained in both stainings and are visible as white spheres at all time-points; (magnification 40x).

3.5. In vivo biocompatibility after subcapsular renal administration of monodisperse PLHMGM-ms

The biocompatibility of monodisperse PLHMGA-ms was also tested after subcapsular renal injection, which is a novel strategy for local drug delivery in the kidney. The injected amount of microspheres (10 mg in 50 µL vehicle) was optimized as the highest concentration of the microspheres that could be delivered under the kidney capsule in view of the high viscosity of such dispersion and the injection *via* a small size needle of only 26G. After the injection, the kidneys were explanted at day 3, 7, and 14. The results of the tissue sections stained with ED-1 and hematoxylin are given in Figure 9.

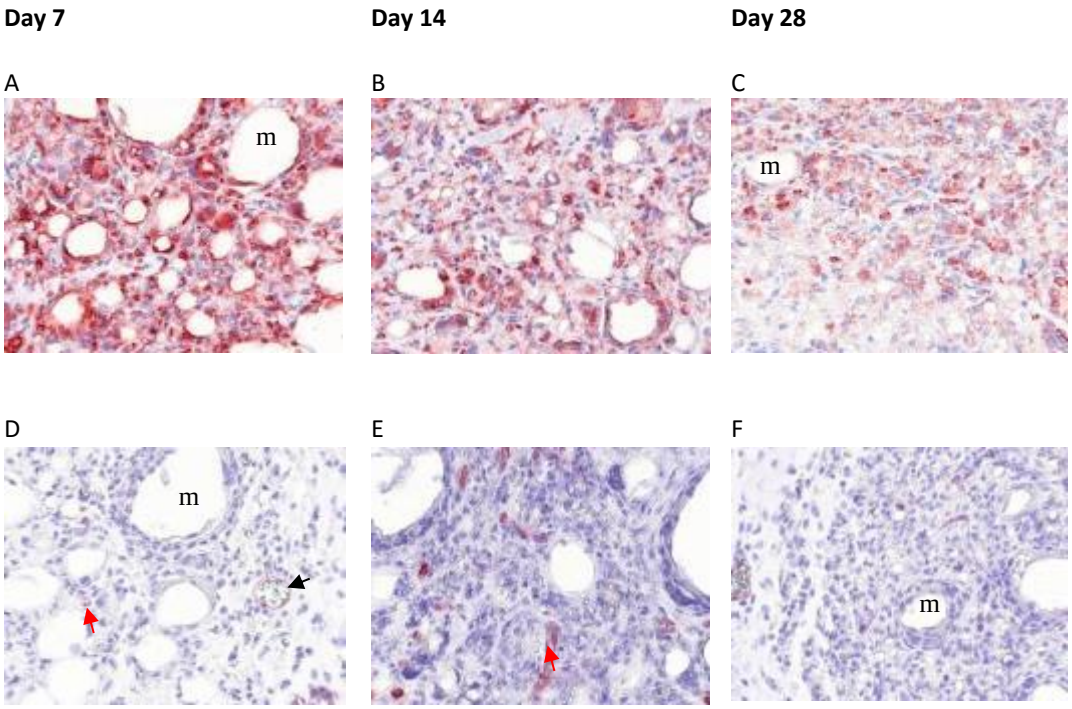

Figure 8. Histological pictures of subcutaneous tissues in which polydisperse PLHMGA-ms were injected. **A-C**: ED-1 staining (macrophages are stained in brown); **D-F**: α-SMA staining (myofibroblasts are stained in pink (red arrow), blood vessels are stained in red (black arrow). Microspheres (m) remain unstained in both stainings and are visible as white spheres; (magnification 40x).

Similar to the subcutaneous injection, microspheres injected under the renal capsule were visible until day 14 as small particulates. Macrophages again appeared as the most abundant inflammatory cells in the injected tissues. Macrophages were mainly visible in the tissue samples explanted at day 3 and 7, with significant reduction at day 14 after injection. The injected microspheres and the inflammation reaction were localized between the cortex and renal capsule with no penetration into the peritubular space (Figure 9). These results show that polymeric microspheres can be injected under the renal capsule without cortical damage or damage to the capsule due to the injection method.

The biocompatibility of a subcapsular depot was previously studied for supramolecular hydrogels in rats [23]. Similar to our results, they showed that subcapsular injected biomaterials primarily resulted in a thickening of the renal capsule with only minimal responses in the renal cortex. From our data we

conclude that monodisperse PLHMGA-ms injected under the kidney capsule have a good biocompatibility and can therefore be used for local delivery of therapeutic molecules in the kidney.

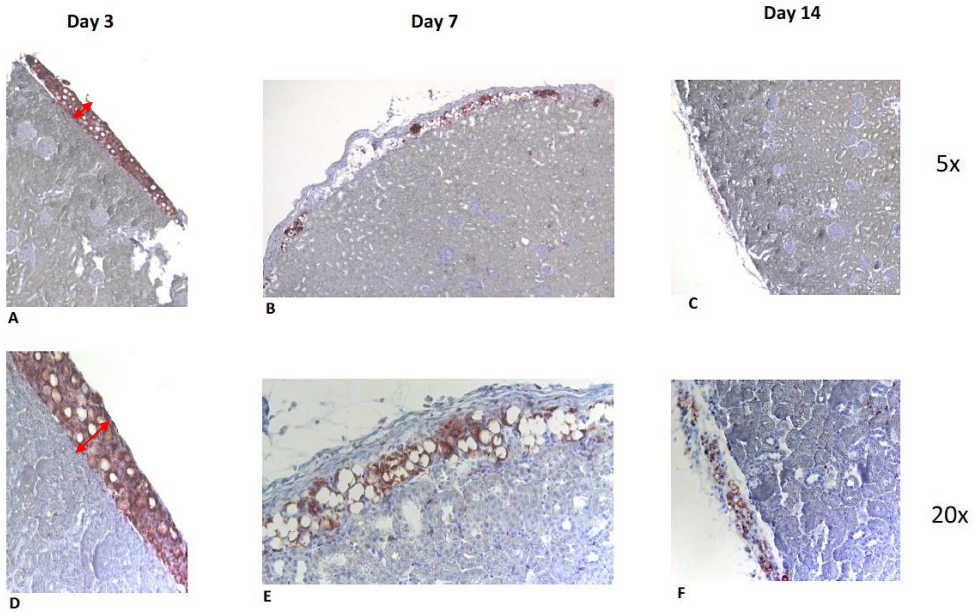

Figure 9. Foreign body reaction elicited by monodisperse PLHMGA-ms injected under the kidney capsule, stained with ED-1 and counterstained with hematoxylin. The area marked with red arrows represents the subcapsular space where the microspheres where injected. This area was analyzed for histological examinations and for possible inflammatory responses. Macrophages are stained with brown, nuclei in blue while microspheres remain unstained and are visible as white spheres. Magnification: 5x (A-C) and 20x (D-F).

3.6. In vitro-in vivo degradation of PLHMGA-ms

In vitro studies in a PBS buffer showed that PLHMGA-ms undergo 80% mass loss during 35 days as described in paragraph 3.2, and at day 28 around 30% of the original mass was present. After subcutaneous and subcapsular renal injection of monodisperse PLHMGA-ms, particles were virtually absent in the tissue sections explanted at day 28 and 14, respectively. This indicates a slightly faster *in vivo* degradation compared to *in vitro*. Similar findings have been reported for PLGA microspheres [52]. It has been demonstrated that PLGA particles inside macrophages degrade faster than particles in buffer likely due to

the relatively low pH and/or the presence of esterases in the phagosomes [53,54], which may also have contributed to faster in vivo degradation of PLHMGA microspheres in the present study.

Conclusion

Monodisperse and polydisperse PLHMGA-ms showed good cytocompatibility after incubation with PK-84, HK-2 and PTECs cells and are biocompatible *in vivo* after subcutaneous administration. Therefore both mono- and polydisperse PLHMGA-ms are promising drug delivery systems for subcutaneous injection. In addition, monodisperse PLHMGA-ms injected under the kidney capsule induced only a localized inflammatory reaction at the site of the depot, showing the feasibility of this type of microspheres for local drug delivery to the kidney.

Acknowledgments

This research forms part of the Project P3.02 DESIRE of the research program of the BioMedical Materials institute, co-funded by the Dutch Ministry of Economic Affairs.

Abbreviations

α-SMA	Monoclonal mouse anti-human Actin
BMMG	3*S*-(benzyloxymethyl)-6*S*-methyl-1,4-dioxane-2,5-dione
DCM	Dichloromethane
ED-1	Mouse anti rat CD68 monoclonal antibody
FBGCs	Foreign body giant cells
HK-2	Human proximal tubular cells
MTS	3-(4,5-dimethylthiazol-2-yl)-5-(3-carboxymethoxyphenyl)-2-(4-sulfophenyl)-2H-tetrazolium
PBS	Phosphate buffered saline
PK-84	Human skin fibroblasts
PLGA	Poly(D,L-lactic-*co*-glycolic acid)
PLBMGA	Poly(D,L-lactic-*ran*-benzyloxymethyl glycolic acid)
PLHMGA	Poly(D,L-lactic-*co*-hydroxymethyl glycolic acid)
PLHMGA-ms	Poly(D,L-lactic-*co*-hydroxymethyl glycolic acid) microspheres
PTECs	Human primary tubular epithelial cells
PVA	Polyvinyl alcohol
SEM	Scanning electron microscope
T_g	Glass transition temperature

References:

1. Kim SJ, Park JG, Kim JH, Heo JS, Choi JW, Jang YS, Yoon J, Lee SJ, Kwon IK. Development of a biodegradable sirolimus-eluting stent coated by ultrasonic atomizing spray. *J Nanosci Nanotechnol,* 11:5689-5697, 2011.
2. Shmueli RB, Ohnaka M, Miki A, Pandey NB, Lima e Silva R, Koskimaki JE, Kim J, Popel AS, Campochiaro PA, Green JJ. Long-term suppression of ocular neovascularization by intraocular injection of biodegradable polymeric particles containing a serpin-derived peptide. *Biomaterials,* 34:7544-7551, 2013.
3. Xuan J, Lin Y, Huang J, Yuan F, Li X, Lu Y, Zhang H, Liu J, Sun Z, Zou H, Chen Y, Gao J, Zhong Y. Exenatide-loaded PLGA microspheres with improved glycemic control: in vitro bioactivity and in vivo pharmacokinetic profiles after subcutaneous administration to SD rats. *Peptides,* 46:172-179, 2013.
4. Menon JU, Ravikumar P, Pise A, Gyawali D, Hsia CC, Nguyen KT. Polymeric nanoparticles for pulmonary protein and DNA delivery. *Acta Biomater,* 2014.
5. Reguera-Nuñez E, Roca C, Hardy E, de la Fuente M, Csaba N, Garcia-Fuentes M. Implantable controlled release devices for BMP-7 delivery and suppression of glioblastoma initiating cells. *Biomaterials,* 35:2859-2867, 2014.
6. Wink JD, Gerety PA, Sherif RD, Lim Y, Clarke NA, Rajapakse CS, Nah HD, Taylor JA. Sustained delivery of rhBMP-2 via PLGA microspheres: cranial bone regeneration without heterotopic ossification or craniosynostosis. *Plast Reconstr Surg,* 2014.
7. Joshi VB, Geary SM, Salem AK. Biodegradable particles as vaccine antigen delivery systems for stimulating cellular immune responses. *Hum Vaccin Immunother,* 9:2584-2590, 2013.
8. Huang SS, Li IH, Hong PD, Yeh MK. Development of Yersinia pestis F1 antigen-loaded microspheres vaccine against plague. *Int J Nanomedicine,* 9:813-822, 2014.
9. Spenlehauer G, Vert M, Benoit JP, Boddaert A. In vitro and In vivo degradation of poly(D,L lactide/glycolide) type microspheres made by solvent evaporation method. *Biomaterials,* 10:557-563, 1989.
10. Vert M, Mauduit J, Li S. Biodegradation of PLA/GA polymers: Increasing complexity. *Biomaterials,* 15:1209-1213, 1994.
11. Estey T, Kang J, Schwendeman SP, Carpenter JF. BSA degradation under acidic conditions: A model for protein instability during release from PLGA delivery systems. *J Pharm Sci,* 95:1626-1639, 2006.
12. Park TG, Lu W, Crotts G. Importance of in vitro experimental conditions on protein release kinetics, stability and polymer degradation in protein encapsulated poly (d,l-lactic acid-co-glycolic acid) microspheres. *J Control Release,* 33:211-222, 1995.
13. Patten PA, Schellekens H. The immunogenicity of biopharmaceuticals. Lessons learned and consequences for protein drug development. *Dev Biol (Basel),* 112:81-97, 2003.
14. Hermeling S, Crommelin DJ, Schellekens H, Jiskoot W. Structure-immunogenicity relationships of therapeutic proteins. *Pharm Res,* 21:897-903, 2004.
15. Leemhuis M, Van Nostrum CF, Kruijtzer JAW, Zhong ZY, Ten Breteler MR, Dijkstra PJ, Feijen J, Hennink WE. Functionalized poly(a-hydroxy acid)s via ring-opening

polymerization: Toward hydrophilic polyesters with pendant hydroxyl groups. *Macromolecules,* 39:3500-3508, 2006.
16. Leemhuis M, Kruijtzer JA, Nostrum CF, Hennink WE. In vitro hydrolytic degradation of hydroxyl-functionalized poly(alpha-hydroxy acid)s. *Biomacromolecules,* 8:2943-2949, 2007.
17. Ghassemi AH, Van Steenbergen MJ, Talsma H, Van Nostrum CF, Crommelin DJA, Hennink WE. Hydrophilic polyester microspheres: Effect of molecular weight and copolymer composition on release of BSA. *Pharm Res,* 27:2008-2017, 2010.
18. Samadi N, Van Nostrum CF, Vermonden T, Amidi M, Hennink WE. Mechanistic studies on the degradation and protein release characteristics of poly(lactic-co-glycolic-co-hydroxymethylglycolic acid) nanospheres. *Biomacromolecules,* 14:1044-1053, 2013.
19. Ghassemi AH, van Steenbergen MJ, Barendregt A, Talsma H, Kok RJ, van Nostrum CF, Crommelin DJ, Hennink WE. Controlled release of octreotide and assessment of peptide acylation from poly(D,L-lactide-co-hydroxymethyl glycolide) compared to PLGA microspheres. *Pharm Res,* 29:110-120, 2012.
20. Liu Y, Ghassemi AH, Hennink WE, Schwendeman SP. The microclimate pH in poly(D,L-lactide-co-hydroxymethyl glycolide) microspheres during biodegradation. *Biomaterials,* 33:7584-7593, 2012.
21. ISO Guidelines. Biological Evaluation of Medical Devices Part 1: Evaluation and Testing, International Standard ISO-10993. April 23, 2013.
22. Kazazi-Hyseni F, Landin M, Lathuile A, Veldhuis GJ, Rahimian S, Hennink WE, Kok RJ, van Nostrum CF. Computer Modeling Assisted Design of Monodisperse PLGA Microspheres with Controlled Porosity Affords Zero Order Release of an Encapsulated Macromolecule for 3 Months. *Pharm Res,* 31:2844-2856, 2014.
23. Dankers PYW, van Luyn MJA, Huizinga-van der Vlag A, van Gemert GML, Petersen AH, Meijer EW, Janssen HM, Bosman AW, Popa ER. Development and in-vivo characterization of supramolecular hydrogels for intrarenal drug delivery. *Biomaterials,* 33:5144-5155, 2012.
24. Blaauw M. Comparison of the catalogues of the k_0^- and the k_{Zn} single comparator methods for standardization in INAA. *J Radioanal Nucl Chem Art,* 191:387-401, 1995.
25. Nakashima T, Shimizu M, Kukizaki M. Particle control of emulsion by membrane emulsification and its applications. *Adv Drug Deliv Rev,* 45:47-56, 2000.
26. Avdovich HW, Lebelle MJ, Savard C, Wilson WL. Nuclear magnetic resonance identification and estimation of solvent residues in cocaine. *Forensic Sci Int,* 49:225-235, 1991.
27. Jones IC, Sharman GJ, Pidgeon J. 1H and 13C NMR data to aid the identification and quantification of residual solvents by NMR spectroscopy. *Magn Reson Chem,* 43:497-509, 2005.
28. Grodowska K, Parczewski A. Organic solvents in the pharmaceutical industry. *Acta Pol Pharm,* 67:3-12, 2010.
29. FDA Guidance Documents. International Conference on Harmonization (ICH) - Guidance for Industry: Q3C Impurities: Residual Solvents. December, 1997.
30. De Groot CJ, van Luyn MJA, van Dijk-Wolthuis WNE, Cadée JA, Plantinga JA, Otter WD, Hennink WE. In vitro biocompatibility of biodegradable dextran-based hydrogels tested with human fibroblasts. *Biomaterials,* 22:1197-1203, 2001.

31. Koopal SA, Iglesias Coma M, Tiebosch ATMG, Suurmeijer AJH. Low-temperature heating overnight in Tris-HCl buffer pH 9 is a good alternative for antigen retrieval in formalin-fixed paraffin-embedded tissue. *Appl Immunohistochem,* 6:228-233, 1998.
32. EMEA. Guideline on the specification limits for residues of metal catalysts. European Medicines Agency. London. 2007.
33. Ghassemi AH, van Steenbergen MJ, Talsma H, van Nostrum CF, Jiskoot W, Crommelin DJA, Hennink WE. Preparation and characterization of protein loaded microspheres based on a hydroxylated aliphatic polyester, poly(lactic-co-hydroxymethyl glycolic acid). *J Control Release,* 138:57-63, 2009.
34. Samadi N, Abbadessa A, Di Stefano A, van Nostrum CF, Vermonden T, Rahimian S, Teunissen EA, van Steenbergen MJ, Amidi M, Hennink WE. The effect of lauryl capping group on protein release and degradation of poly(d,l-lactic-co-glycolic acid) particles. *J Control Release,* 172:436-443, 2013.
35. Rabson R, Tolbert NE, Kearney PC. Formotion of serine and glyceric acid by the glycolate pathway. *Arch Biochem Biophys,* 98:154-163, 1962.
36. Dijkstra CD, Dopp EA, Joling P, Kraal G. The heterogeneity of mononuclear phagocytes in lymphoid organs: Distinct macrophage subpopulations in the rat recognized by monoclonal antibodies ED1, ED2 and ED3. *Immunology,* 54:589-599, 1985.
37. Anderson JM. Biological responses to materials. *Annu Rev Mater Sci,* 31:81-110, 2001.
38. Desmoulière A, Darby IA, Gabbiani G. Normal and Pathologic Soft Tissue Remodeling: Role of the Myofibroblast, with Special Emphasis on Liver and Kidney Fibrosis. *Lab Invest,* 83:1689-1707, 2003.
39. Anderson JM, Shive MS. Biodegradation and biocompatibility of PLA and PLGA microspheres. *Adv Drug Deliv Rev,* 28:5-24, 1997.
40. Skalli O, Ropraz P, Trzeciak A, Benzonana G, Gillessen D, Gabbiani G. A monoclonal antibody against a-smooth muscle actin: A new probe for smooth muscle differentiation. *J Cell Biol,* 103:2787-2796, 1986.
41. Shishatskaya EI, Voinova ON, Goreva AV, Mogilnaya OA, Volova TG. Biocompatibility of polyhydroxybutyrate microspheres: In vitro and in vivo evaluation. *J Mater Sci Mater Med,* 19:2493-2502, 2008.
42. Zandstra J, Hiemstra C, Petersen AH, Zuidema J, van Beuge MM, Rodriguez S, Lathuile AAR, Veldhuis GJ, Steendam R, Bank RA, Popa ER. Microsphere size influences the foreign body reaction. *Eur Cell Mater,* 28:335-347, 2014.
43. Athanasiou KA, Niederauer GG, Agrawal CM. Sterilization, toxicity, biocompatibility and clinical applications of polylactic acid/polyglycolic acid copolymers. *Biomaterials,* 17:93-102, 1996.
44. Cadée JA, Brouwer LA, Den Otter W, Hennink WE, Van Luyn MJA. A comparative biocompatibility study of microspheres based on crosslinked dextran or poly(lactic-co-glycolic)acid after subcutaneous injection in rats. *J Biomed Mater Res,* 56:600-609, 2001.
45. Kohane DS, Lipp M, Kinney RC, Anthony DC, Louis DN, Lotan N, Langer R. Biocompatibility of lipid-protein-sugar particles containing bupivacaine in the epineurium. *J Biomed Mater Res,* 59:450-459, 2002.

46. Visscher GE, Pearson JE, Fong JW, Argentieri GJ, Robison RL, Maulding HV. Effect of particle size on the in vitro and in vivo degradation rates of poly(DL-lactide-co-glycolide) microcapsules. *J Biomed Mater Res,* 22:733-746, 1988.
47. Visscher GE, Robison RL, Maulding HV, Fong JW, Pearson JE, Argentieri GJ. Biodegradation of and tissue reaction to 50:50 poly(DL-lactide-co-glycolide) microcapsules. *J Biomed Mater Res,* 19:349-365, 1985.
48. Visscher GE, Robison MA, Argentieri GJ. Tissue response to biodegradable injectable microcapsules. *J Biomater Appl,* 2:118-131, 1987.
49. Tabata Y, Ikada Y. Effect of the size and surface charge of polymer microspheres on their phagocytosis by macrophage. *Biomaterials,* 9:356-362, 1988.
50. Thomasin C, Corradin G, Men Y, Merkle HP, Gander B. Tetanus toxoid and synthetic malaria antigen containing poly(lactide)/poly(lactide-co-glycolide) microspheres: importance of polymer degradation and antigen release for immune response. *J Control Release,* 41:131-145, 1996.
51. Champion JA, Walker A, Mitragotri S. Role of particle size in phagocytosis of polymeric microspheres. *Pharm Res,* 25:1815-1821, 2008.
52. Jiang W, Gupta RK, Deshpande MC, Schwendeman SP. Biodegradable poly(lactic-co-glycolic acid) microparticles for injectable delivery of vaccine antigens. *Adv Drug Deliv Rev,* 57:391-410, 2005.
53. Van Apeldoorn AA, Van Manen H-, Bezemer JM, De Bruijn JD, Van Blitterswijk CA, Otto C. Raman imaging of PLGA microsphere degradation inside macrophages. *J Am Chem Soc,* 126:13226-13227, 2004.
54. Walter E, Dreher D, Kok M, Thiele L, Kiama SG, Gehr P, Merkle HP. Hydrophilic poly(DL-lactide-co-glycolide) microspheres for the delivery of DNA to human-derived macrophages and dendritic cells. *J Control Release,* 76:149-168, 2001.

Chapter 4

Release and pharmacokinetics of near-infrared labeled albumin from monodisperse poly(D,L-lactic-*co*-hydroxymethyl glycolic acid) microspheres after subcapsular renal injection

Filis Kazazi Hyseni[1]
Stefan H van Vuuren[2]
Dione M van der Giezen[2]
Ebel Pieters[1]
Farshad Ramazani[1]
Sergio Rodriguez[3]
Gert J Veldhuis[3]
Roel Goldschmeding[2]
Cornelus F van Nostrum[1]
Wim E Hennink[1]
Robbert Jan Kok[1]

[1.] Department of Pharmaceutics, Utrecht Institute for Pharmaceutical Sciences, Utrecht University, Utrecht, The Netherlands
[2.] Department of Pathology, University Medical Center Utrecht, Utrecht, The Netherlands
[3.] Nanomi B.V., Oldenzaal, The Netherlands

Acta Biomaterialia, 22:141-154, Aug 2015

Abstract

Subcapsular renal injection is a novel administration method for local delivery of therapeutics for the treatment of kidney related diseases. The aim of this study was to investigate the feasibility of polymeric microspheres for sustained release of protein therapeutics in the kidney and study the subsequent redistribution of the released protein. For this purpose, monodisperse poly(D,L-lactic-*co*-hydroxymethyl glycolic acid) (PLHMGA) microspheres (40 μm in diameter) loaded with near-infrared dye-labeled bovine serum albumin (NIR-BSA) were prepared by a membrane emulsification method. Rats were injected with either free NIR-BSA or with NIR-BSA loaded microspheres (NIR-BSA-ms) and the pharmacokinetics of the released NIR-BSA was studied for three weeks by *ex vivo* imaging of organs and blood. Quantitative release data were obtained from kidney homogenates and possible metabolism of the protein was investigated by SDS-PAGE analysis of the samples. The *ex vivo* images showed a rapid decrease of the NIR signal within 24 h in kidneys injected with free NIR-BSA, while, importantly, the signal of the labelled protein was still visible at day 21 in kidneys injected with NIR-BSA-ms. SDS-PAGE analysis of the kidney homogenates showed that intact NIR-BSA was released from the microspheres. The locally released NIR-BSA drained to the systemic circulation and subsequently accumulated in the liver, where it was degraded and excreted renally. The *in vivo* release of NIR-BSA was calculated after extracting the protein from the remaining microspheres in kidney homogenates. The *in vivo* release rate was faster (89 ±4% of the loading in two weeks) compared to the *in vitro* release of NIR-BSA (38 ±1% in two weeks). In conclusion, PLHMGA microspheres injected under the kidney capsule provide a local depot from which a formulated protein is released over a prolonged time-period.

1. Introduction

Acute kidney injury and chronic renal failure are conditions that are associated with high mortality rates [1-3]. These conditions often progress to end-stage renal failure and are characterized by the inability of the kidneys to adequately filter waste products from the blood [2]. One of the main causes for the progression towards renal failure is a local inflammatory process that occurs in the kidneys [2,4-6]. In this respect, several protein drugs are recognized as potential therapeutics for the treatment of renal diseases [7-10]. However, considering the pharmacokinetic characteristics of many proteins, including short half-life and instability, protein drugs require frequent administrations via injections [11]. The development of novel drug delivery systems, such as protein loaded polymeric microspheres, possibly overcomes the above mentioned shortcomings by encapsulation of the therapeutic and enabling its local and sustained release [12-14]. In addition, the local administration of a depot that affords continuous release of a therapeutic protein in the kidney may enable increased renal effectiveness combined with a reduction of extrarenal adverse effects. Subcapsular renal injection is a relatively new strategy for drug delivery to the kidney, where the drug eluting depot is injected with a small size needle under the kidney capsule. This technique has been recently studied for stem cells [15] and for drug eluting depots, i.e. hydrogels [16,17] and polymeric microspheres [18,19]. Dankers et al. [16] showed good biocompatibility of supramolecular hydrogels, suitable for short-time boost release of proteins, and demonstrated that a therapeutic protein (bone morphogenic protein 7) released from such a depot reduced local fibrotic responses in kidneys from healthy rats. Falke et al. [19] demonstrated that a depot of rapamycin-loaded microspheres inhibited fibrotic responses in rats with the unilateral ureter obstruction model. However, to our knowledge, there are no studies that report on the *in vivo* release profile and subsequent fate of the therapeutic compounds from such a subcapsular depot. Therefore, the purpose of the present study was to assess the feasibility of protein delivery from polymeric microspheres that have been injected subcapsularly, as well as the subsequent fate after intrarenal delivery.

The applied microspheres in this study were based on poly(D,L-lactic-*co*-hydroxymethyl glycolic acid) (PLHMGA), an aliphatic polyester with improved properties for protein delivery [20-23]. Recently, it was demonstrated that monodisperse PLHMGA microspheres have good biocompatibility after subcutaneous and subcapsular renal administration in rats [18]. Such monodisperse microspheres can be prepared by membrane emulsification method, in which uniform-sized droplets are formed after a primary w/o emulsion (containing protein and polymer solutions, respectively) is pressed through a membrane with uniformly sized pores [24,25]. In the present study, PLHMGA

microspheres were loaded with near-infrared (NIR) dye labeled albumin (NIR-BSA). The advantage of labeling proteins with NIR dyes is that the NIR wavelength (700-900 nm) ensures sensitive detection of the labeled protein, as living tissues have relatively low absorbance and scattering in this range [26]. One of the major challenges, however, is to discriminate between NIR signal of NIR-BSA that is still loaded in the polymeric microspheres from the NIR-BSA released from the microspheres. The latter can be either intact or metabolically processed by the kidney. Therefore, at different time points after injection, animals were sacrificed and the levels of released NIR-BSA were quantified in kidney homogenates. This approach provides valuable data about the release of the model protein from the microspheres injected under the renal capsule as well as pharmacokinetic data that can be used to predict the further pharmacokinetic fate of proteins once released in the kidney parenchyma.

2. Materials and Methods

2.1. Materials

O-Benzyl-L-serine was purchased from Senn Chemicals AG (Dielsdorf, Switzerland). DL-Lactide was purchased from Purac (The Netherlands). Tin(II) 2-ethylhexanoate ($SnOct_2$), poly(vinyl alcohol) (PVA; M_w = 13,000-23,000), dimethylsulfoxide (DMSO) and bovine serum albumin (BSA; A4503) with molecular weight of 66,776 Da, were obtained from Sigma-Aldrich (Germany). 1,4-Butanediol, 99+% was obtained from Acros Organics (Belgium). IRDye® 800CW – NHS ester (MW=1,166 Da) from LI-COR Biosciences was supplied by Westburg BV (Leusden, The Netherlands). Carboxymethyl cellulose (CMC, with viscosity of 2,000 mPa·s of a 1% solution in water) was obtained from Bufa B.V. (255611, The Netherlands). Halt™ Protease and phosphatase inhibitor cocktail, EDTA-free (78445) was obtained from Thermo Scientific (IL, USA). RIPA buffer (50 mM Tris-HCl, pH 7.5, 150 mM sodium chloride, 1% Triton X-100, 1% sodium deoxycholate, 0.1% SDS, 2 mM EDTA) was provided by Teknova (CA, USA). Sodium phosphate dibasic (Na_2HPO_4) and sodium azide (NaN_3) were purchased from Fluka (The Netherlands). Dichloromethane (DCM), chloroform, tetrahydrofuran and methanol were purchased from Biosolve BV (The Netherlands). Sodium dihydrogen phosphate (NaH_2PO_4) and sodium chloride (NaCl) were supplied from Merck (Germany).

2.2. Synthesis and characterization of PLHMGA

Poly(D,L-lactic-*co*-hydroxymethyl glycolic acid) (PLHMGA) was synthesized as previously described by Leemhuis et al. [27]. In this study, a molar ratio of 35% BMMG (3*S*-(benzyloxymethyl)-6*S*-methyl-1,4-dioxane-2,5-dione) and 65% D,L-

lactide (mol/mol) was used, with butanediol as an initiator (1:300 mol/mol monomer) and tin (II) 2-ethylhexanoate as a catalyst (1:600 mol/mol monomer). Molecular weight of PLHMGA was determined by GPC (Waters Alliance System) using a Waters 2695 separating module and a Waters 2414 refractive index detector, operating with tetrahydrofuran at a flow rate of 1 mL/min, and calibrated with polystyrene standards (PS-2, Mw = 580 – 377,400 D, EasiCal, Varian). Two PL-gel 5 µm Mixed-D columns fitted with a guard column were used. The copolymer composition was determined with NMR (Gemini-300 MHz) analysis, using chloroform-d, 99.8 atom% (Sigma-Aldrich) as solvent. The thermal properties of the copolymer were measured with differential scanning calorimetry (DSC - Q 2000, TA Instruments). For DSC measurements, approximately 5 mg of the copolymer was placed in aluminum pan (T zero pan/lid set, TA Instruments) and the sample was scanned with a modulated heating method in three cycles [20]. The sample was heated until 120°C (5°C/min) and then cooled down to -50°C, followed by a heating until 120°C (5°C/min). The temperature modulation was ±1°C/min.

2.3. Conjugation of NIR dye to BSA

The NIR dye, IRDye® 800CW –NHS ester, was conjugated to BSA following the manufacturer's protocol for labelling high molecular weight proteins (LI-COR, Inc. Biosciences). In brief, BSA dissolved in water (10 mg/ml) was brought to pH 8.5 with 1M potassium phosphate (pH 9) and mixed with a solution of the dye (4 mg/ml DMSO) in a 1:3 molar ratio. The albumin/dye solution was incubated for 2 h at room temperature while gently stirred and protected from light. The labeled protein was purified by size exclusion chromatography with Zeba™ desalting Spin Columns (Thermo Scientific), yielding a buffer salt-free protein solution that was freeze-dried (Alpha 1-2, Martin Christ, Germany). The lyophilized protein was kept in -20°C until further use. The purity of NIR-BSA was analyzed with GPC (Waters Alliance System) using a Waters 2695 separating module and a Waters photodiode array, with PBS as an eluent and at a flow rate of 1 mL/min. The column used was Biosep-3000 (Phenomenex, Germany). The dye-to-protein ratio of the conjugate was determined according to the manufacturer's protocol (LI-COR, Inc. Biosciences) by measuring the absorbance of NIR-BSA at 280 and 780 nm with a UV spectrophotometer (UV-2450 Shimadzu, Japan). The conjugate was diluted in a mixture of PBS and methanol (1:1) and the following formula was used for calculating the dye/protein (D/P in mol/mol) ratio,

$$D/P = \left[\frac{A_{780}}{\varepsilon_{dye}}\right] \div \left[\frac{A_{280} - (0.03 \times A_{780})}{\varepsilon_{protein}}\right]$$

where 0.03 is a correction factor for the absorbance of the IRDye® 800CW at 280 nm (equal to 3.0% of its absorbance at 780 nm) while ε_{dye} (270,000 M^{-1} cm^{-1}; LI-COR Biosciences) and $\varepsilon_{protein}$ (43,824 M^{-1} cm^{-1} [28]) are molar extinction coefficients for the dye and BSA, respectively.

2.4. Preparation and characterization of NIR-BSA loaded PLHMGA microspheres

PLHMGA microspheres were prepared with a cross-flow membrane emulsification process, where the dispersed phase (w_1/o) was pumped into the continuous phase (w_2) which was flowing along the membrane (hydrophilic Iris-20, microsieve™ membrane technology, Nanomi B.V., The Netherlands) [24,29]. The dispersed phase (w_1/o) was prepared by adding 0.8 mL of a solution containing BSA and NIR-BSA in water (1:1; 50 mg protein/ml) to 20% w/w PLHMGA in DCM solution (1.1 g PLHMGA / 3.24 mL DCM). The dispersed phase was homogenized using an Ultra-Turrax T8 (IKA Works, USA) with dispersing element S10N-10G, at a speed of 20,000 rpm for 30 seconds. Next, the dispersed phase was passed through the Iris-20 membrane at a constant rate of 10 mL/h using a syringe pump (Nexus 6000, Chemyx, USA) into 60 mL of the continuous phase (PVA 4% in water, w/v). The continuous phase was pumped with a rate of 4.6 mL/min across the membrane. At the end of the process (24 min), the formed emulsion was stirred for 3 h to evaporate DCM. The hardened microspheres were collected by centrifugation at 3,000 rpm for 2 min (Hermle Z233MK-2 centrifuge), washed three times with water, frozen with liquid nitrogen and freeze-dried (Alpha 1-2, Martin Christ, Germany). Blank PLHMGA microspheres were prepared with the same procedure, except that the internal water phase (W_1) contained no protein. All the particles were prepared aseptically in a flow cabinet using autoclaved equipment and sterile water.

The volume-weight mean diameter of the obtained microspheres was measured with an optical particle sizer (Accusizer 780, Santa Barbara, California, USA). At least 5,000 microspheres were analyzed. The BSA loading content of the microspheres was determined by dissolving 10 mg of microspheres in 1 mL of DMSO for one hour followed by the addition of 5 mL of 0.05 M NaOH and 0.5% SDS solution [20,30]. The BSA concentration of the formed solution was measured with BCA protein assay (Interchim, USA) according to the manufacturer's protocol. The loading efficiency was calculated as the amount of BSA entrapped in the microspheres divided by the BSA amount added during the preparation of microspheres, times 100%. The loading of NIR-BSA was not measured with an infrared imager as the NIR signal was lost after the addition of NaOH to the solution (results not shown). Bjornson et al. [31] also reported that the half-life of another near-infrared dye, indocyanin green, in alkaline solution was only 2h as a result of the formation of basic colorless compounds when this dye was exposed to alkaline solutions.

2.5. In vitro degradation and release study of PLHMGA microspheres

Around 10 mg of NIR-BSA encapsulated PLHMGA microspheres (NIR-BSA-ms) was suspended in 1.5 mL of 100 mM phosphate buffer (pH 7.4) containing 56 mM NaCl, 33 mM NaH_2PO_4, 66 mM Na_2HPO_4 and 0.05% (w/v) NaN_3 (to prevent bacterial growth). The vials, protected from light, were incubated at 37°C while gently shaking. At different time-points, vials (n=1) were removed and centrifuged (4,000 rpm for 5 minutes; Hermle Z233MK-2 centrifuge). The microspheres were washed three times with water, lyophilized and analyzed for residual dry weight and PLHMGA molecular weight, as described in paragraph 2.2. The release of NIR-BSA was studied in triplicate. At different time-points, a single sample of NIR-BSA microspheres was analyzed for polymer degradation, while triplicate samples were analyzed for NIR-BSA release. To study polymer degradation, the sample was centrifuged (4,000 rpm for 5 minutes; Hermle Z233MK-2 centrifuge), after which the pellet was washed three times with water, lyophilized and analyzed for residual dry weight and PLHMGA molecular weight, as described in paragraph 2.2. For analysis of NIR-BSA at indicated time-points, three vials were centrifuged and the supernatant was removed, replaced by fresh release buffer and the vials were placed back in the incubator. The amount of released protein was measured with BCA protein assay, whereas the release of NIR-BSA was also quantified with Odyssey near-infrared scanner (LI-COR, Inc. Biosciences) employing a 800 nm detector. Calibration was done with NIR-BSA dissolved in the release buffer with concentration ranging from 0.008 – 17 µg/mL for the Odyssey imager, whereas for the BCA protein assay BSA was used in concentrations ranging from 10 – 100 µg/mL.

2.6. Animal experiments

The protocol for the animal experiment was approved by the Animal Ethical Committee of the University of Utrecht (Number 2012.II.09.133). The animal experiment was carried out using female Fischer 344 rats (Harlan Nederland, The Netherlands) with an average weight of 170 g. Animals had free access to acidified water and standard laboratory chow, and were housed according to institutional rules with 12:12 h dark/light cycles. Rats were anesthetized by inhalation of isoflurane (4% induction, 1.5 - 3% for maintenance of anesthesia) and were given carprofen (5 mg/kg s.c.) analgesia at 12 h and 24 h after the surgical intervention. The left kidney was exposed by a retroperitoneal incision and gently lifted to allow the injection of the samples under the renal capsule. To this end, two adjacent pockets were created under the renal capsule with a 26G blunt Hamilton needle (Chrom8 International, the Netherlands) and 25

µL of the sample was injected in each pocket with the same needle (50 µL per kidney). The injection spot in the renal capsule was sealed with fibrin glue (Tissucol® DUO 500, Baxter AG, Austria) to prevent reflux of the injected fluid upon withdrawal of the needle from the subcapsular pocket.

Animals were divided into three groups. The rats of the first group (n=15, 3 animals per time-point) were injected with 50 µL of a dispersion of NIR-BSA-ms in vehicle (10 mg microspheres / 50 µL, equivalent to 160 µg NIR-BSA; composition of vehicle see below). Rats of the second group (n=5, 1 animal per time-point) were injected similarly with 50 µL of a dispersion of placebo microspheres, while rats of the third group (n=15, 3 animals per time-point) were injected with a solution of 160 µg NIR-BSA in 50 µL vehicle. Vehicle for the injections was a solution of 0.6% carboxymethyl cellulose containing 0.02% Tween-20 and 5% mannitol, which was autoclaved before dispersion of the microspheres or dissolution of NIR-BSA. Animals from the first and the second group (i.e. rats injected with microspheres) were sacrificed at day 0 (directly after injection) and at day 3, 7, 14 and 21 post injection. Rats injected with NIR-BSA were sacrificed at 0, 2, 4, 6 and 24 h post injection. Animals were anesthetized and a blood sample from the aorta was collected in EDTA tubes. Heart, lungs, spleen, kidneys, liver and bladder were excised, snap frozen with liquid nitrogen and kept in -20°C until further measurements. From the rats of the first group (i.e. NIR-BSA-ms group) blood samples were also harvested, via the tail vein, in between the sacrificing time-points (0, 2, 4, 6, 24 h and at every other day until 21 days).

2.7. NIR imaging of kidneys and other organs

The strength of the NIR signal in the collected organs was imaged by scanning of the excised organs with an Odyssey scanner at the 800 nm filter. Prior to imaging, the kidneys and other organs were defrosted and rinsed with saline. Kidneys were cleaned from the surrounding fat tissue. A region of interest encompassing the whole organ was scanned and reported as relative fluorescence values calculated by the manufacturer's software. The background signal was corrected by scanning the representative organs of animals injected with blank microspheres.

2.8. Analysis of NIR fluorescence in blood

Blood samples were serially diluted (1:2 dilution steps) in 96-well plates with RIPA buffer (supplemented with protease and phosphatase inhibitor cocktail). The serial dilutions were made to determine the range where the fluorescence intensity varies in a linear manner with the concentration, to avoid saturation of the fluorescent signal [32]. NIR fluorescence was determined by scanning with an Odyssey scanner. Only values in the linear range were used to calculate the

relative fluorescence in blood. Calibration curves were made by spiking blood from control rats with NIR-BSA (range 0.008 – 17 µg/mL).

Blood samples were also subjected to SDS-PAGE electrophoresis followed by NIR scanning of the gels, in order to discriminate NIR fluorescent degradation products from intact NIR-BSA (NuPAGE® Novex® 4-12% Bis-Tris gels, non-reducing conditions). As a control, NIR-BSA (10 µg/mL) and NIR dye (0.5 µg/mL) were used. After separation, the gels were visualized with Odyssey imager. The detection limit of NIR-BSA with this method was 0.6 µg/mL.

2.9. Analysis of NIR fluorescence in tissue homogenates

Organs were mixed with RIPA buffer supplemented with protease and phosphatase inhibitors (1 mL of buffer / g of tissue) in tissue homogenizing tubes containing zirconium oxide beads (Tissue homogenizing CK28 – 2 or 7 mL, Bertin technologies, France) and homogenized at a speed of 4,000 rpm for 5 seconds (Precellys24 tissue homogenizer, Bertin technologies, France). All tissue homogenates were also analyzed by SDS-PAGE as described in 2.8. Homogenates of the left kidneys injected with free NIR-BSA were further analyzed for quantitative measurements of the NIR fluorescence after serial dilutions, as described in 2.8. Homogenates of the left kidneys injected with NIR-BSA-ms were extracted as shown in Figure 1A, in order to differentiate between released NIR-BSA and NIR-BSA still entrapped in the microspheres. In brief, the left kidney homogenates in RIPA buffer were centrifuged (13,000 rpm for 20 min; Hermle Z233MK-2 centrifuge) and the supernatant containing the released NIR-BSA (supernatant I) was harvested. The pellet with kidney tissue and the injected microspheres were treated with 1 mL of DCM while gently shaking for 3 h to fully dissolve the microspheres, and centrifuged. NIR imaging of the sample confirmed that the protein from the microsphere pellet was now in the layer floating on top of the DCM layer. This upper layer (supernatant II) was carefully transferred into another vial. The remaining traces of DCM were evaporated under nitrogen gas and the samples were homogenized with 1 mL of PBS. Both supernatants were serially diluted in 96-well plates and measured with Odyssey imager. For calibration, NIR-BSA in RIPA buffer was used for supernatant I and NIR-BSA in PBS for supernatant II. The method was optimized by spiking control kidney homogenates with a known amount of NIR-BSA loaded microspheres (Figure 1B).

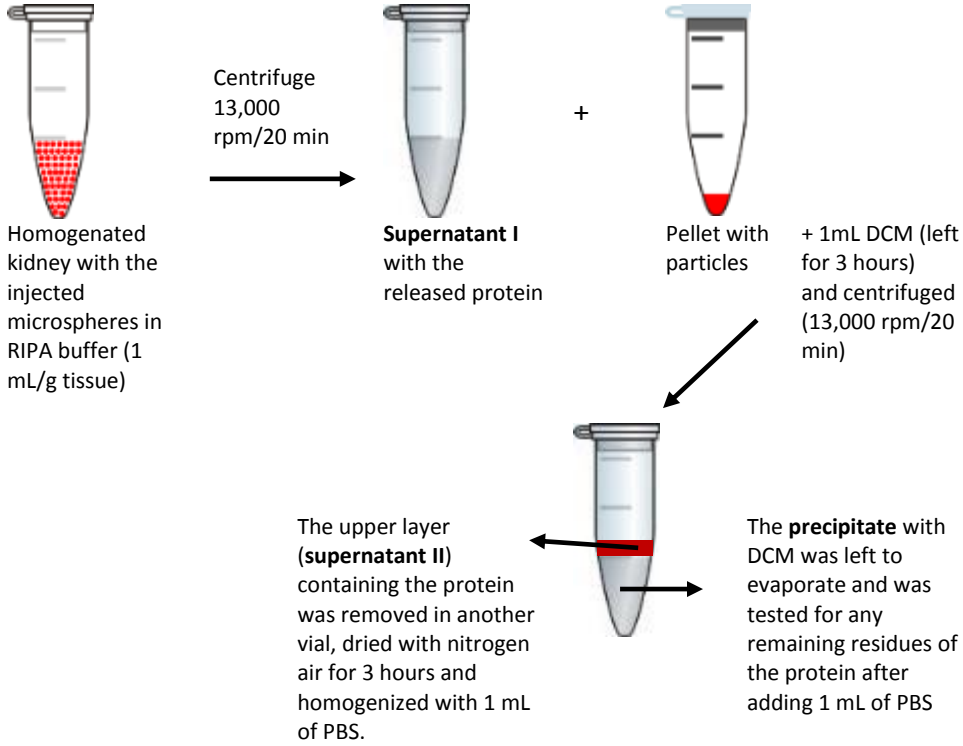

A.

Kidney homogenate spiked with:	Amount of NIR-BSA (mg/mL)	Supernatant I (%)	Supernatant II (%)	Precipitate (%)	Recovery (%)
Free NIR-BSA	1.0	100 ±1	2.0 ±0.1	0.24 ±0.01	102 ±1
NIR-BSA-ms	0.3	12 ±1	62 ±5	0.36 ±0.05	74 ±4

B.

Figure 1. A. The extraction method of NIR-BSA from homogenates of left kidneys injected with NIR-BSA microspheres to determine the released protein from the microspheres (supernatant I) and protein loaded in the microspheres (supernatant II). **B.** Results of the optimization of the extraction procedure. For optimization, kidney homogenates were spiked with either empty microspheres and known amount of free NIR-BSA (n=2) or with NIR-BSA loaded microspheres (n=3).

2.10. Calculations and Statistical Analysis

The *in vivo* cumulative release of NIR-BSA from kidneys injected with NIR-BSA-ms was calculated as 100 - percentage of NIR-BSA recovered from the injected microspheres. The *in vitro-in vivo* level A correlation curve was plotted as the percentage of the released NIR-BSA *in vitro* (measured with the BCA assay) versus the percentage of NIR-BSA released *in vivo,* as shown elsewhere [33,34]. NIR-BSA concentrations measured in the injected left kidneys (supernatant I) were used to calculate the renal area under the curve (AUC) by the trapezoidal rule. All data are represented as means ± standard deviations.

3. Results and Discussion

3.1. Labeling of BSA and preparation of PLHMGA microspheres

Near infrared (NIR) dye (IRdye® 800CW-NHS) was conjugated to BSA (MW 66 kDa) with an average of 1.3 molecules of NIR dye per molecule of BSA (Figure 2A, B). GPC and SDS-PAGE analysis of purified NIR-BSA demonstrated that free dye could not be detected in the product and no aggregates of BSA were visible (Figure 2C-E). PLHMGA with weight average molecular weight (M_w) of 27 kD, polydispersity of 1.8 and glass transition temperature of 35°C, was used to prepare NIR-BSA loaded microspheres (NIR-BSA-ms) by cross-flow membrane emulsification process, which yielded monodisperse microspheres with a smooth surface and no visible pores (Figure 3A and B). NIR-BSA-ms had a volume weight mean diameter of 40 ±5 µm, while blank microspheres had a mean diameter of 37 ±4 µm (Figure 3C and D). The BSA loading was 31 mg/g polymer (theoretical albumin loading was 36 mg/g) and the loading efficiency was 87%. Figure 4 (A and B) shows the results of the *in vitro* degradation of the microspheres at 37°C. PLHMGA microspheres loaded with NIR-BSA showed a continuous weight loss and a decrease in weight average molecular weight (M_w) during the course of the 35-day incubation period, suggesting degradation via bulk erosion [35,36]. The observed erosion rate is similar to the degradation of empty PLHMGA microspheres with same size and polymer composition [18]. The *in vitro* cumulative protein release from microspheres, determined both with the NIR imager and the BCA protein assay, was comparable for the two methods (Figure 4C). During the course of the incubation of 35 days, after a burst release of 8 ±1% (within 3h of incubation), around 60 ±3% of the encapsulated protein was released from the PLHMGA microspheres, in agreement with the results of a previous study [20]. A slightly lower total recovery of NIR-BSA was determined by NIR analysis compared to the cumulative recovery by BCA protein analysis (Figure 4C). A

plausible explanation for this might be the instability of the dye at 37°C, which was also observed when NIR-BSA was incubated in buffer for a period of one month.

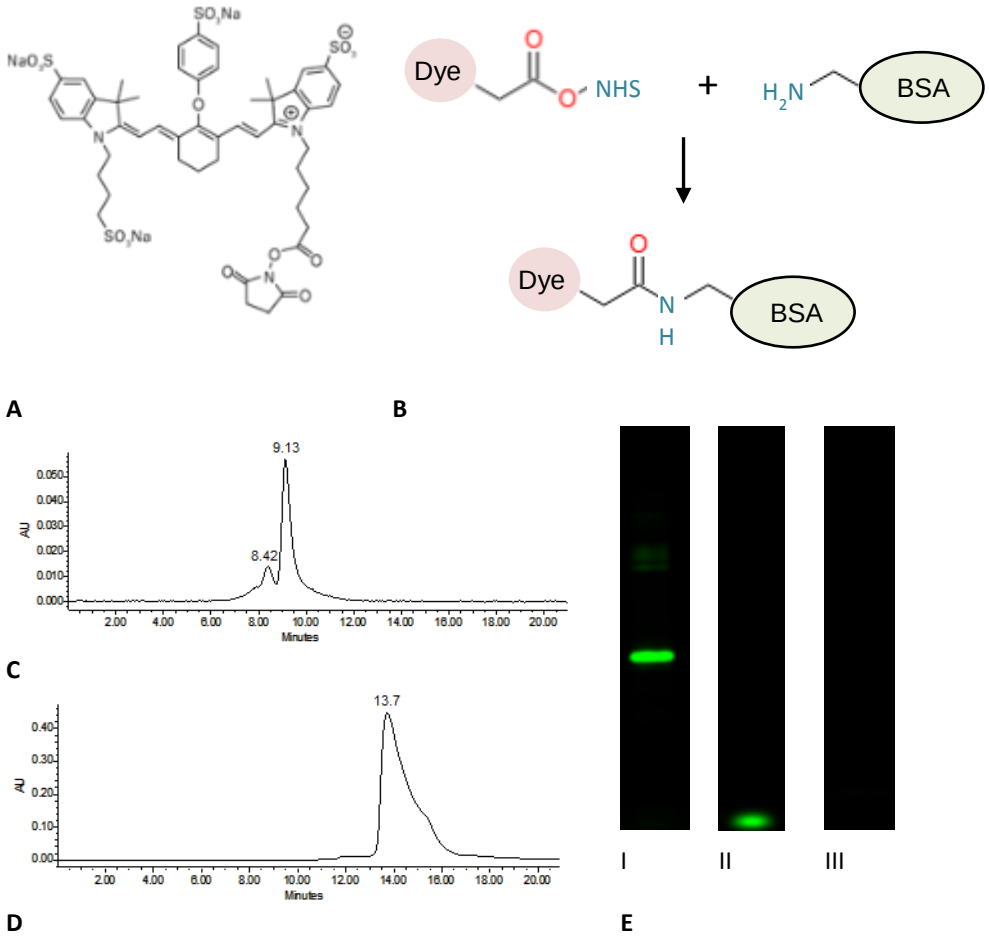

Figure 2. Labeling of bovine serum albumin (BSA) with NIR dye and analysis of the purity of the labeled NIR-BSA. **A.** Structure of the NIR dye (IRDye® 800CW NHS ester); **B.** Reaction between the NIR dye and BSA; **C.** GPC chromatogram of NIR-BSA detected at 780 nm; **D.** GPC chromatogram of the NIR dye detected at 780 nm; **E.** SDS-PAGE gels imaged with Odyssey near-infrared imager (**I.** NIR-BSA; **II.** NIR dye and **III.** Unlabeled BSA).

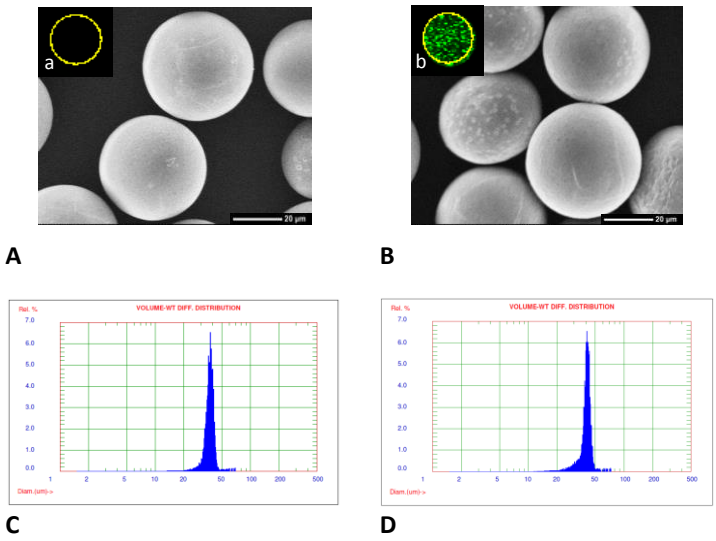

Figure 3. Characteristics of PLHMGA microspheres. **A, a and C**: blank PLHMGA microspheres; **B, b and D**: NIR-BSA loaded PLHMGA microspheres. **A and B:** Representative SEM photographs (magnification ~1000x); **a and b:** Visualization of microspheres with Odyssey near-infrared imager (the yellow line is the circumference of a single well of a 96-well plate) and **C and D:** volume weight particle diameter distribution as measured with AccuSizer.

3.2. Ex vivo imaging of subcapsularly injected depots

Since normal tissues do not absorb NIR light extensively, NIR optical imaging is emerging as an alternative to radiotracer-based scanning techniques for studying the pharmacokinetics of (bio)macromolecules and drug delivery systems [37-40]. In animal studies, NIR *in vivo* imaging is now regularly applied for monitoring the tumor accumulation of nanoparticles or other types of nanocarriers, especially in subcutaneously implanted tumor xenografts [41,42]. Major limitations of *in vivo* imaging are, however, the proper visualization of fluorescence accumulation in organs in the peritoneal cavity due to scattering of the emitted light [43] and thus quantification of the obtained signals [32]. It has been shown that better imaging results, from magnetic resonance imaging, can be obtained when the kidney is repositioned to a more superficial location in the

abdomen [44]. Such an invasive surgical procedure will, however, also affect the normal perfusion and physiological function of the kidney. Other studies also report quantification of the signal in whole body imaging with non-invasive tomographic imaging [42,45]. However, these techniques are relying on mathematical algorithms to compensate for scattering of the signal [42,45]. Moreover, in this study, we also aimed to differentiate between the NIR signal from released NIR-BSA and the protein still loaded in the microspheres. Therefore, we proceeded with *ex vivo* imaging of the organs and analysis of the NIR signal in kidney homogenates as described below.

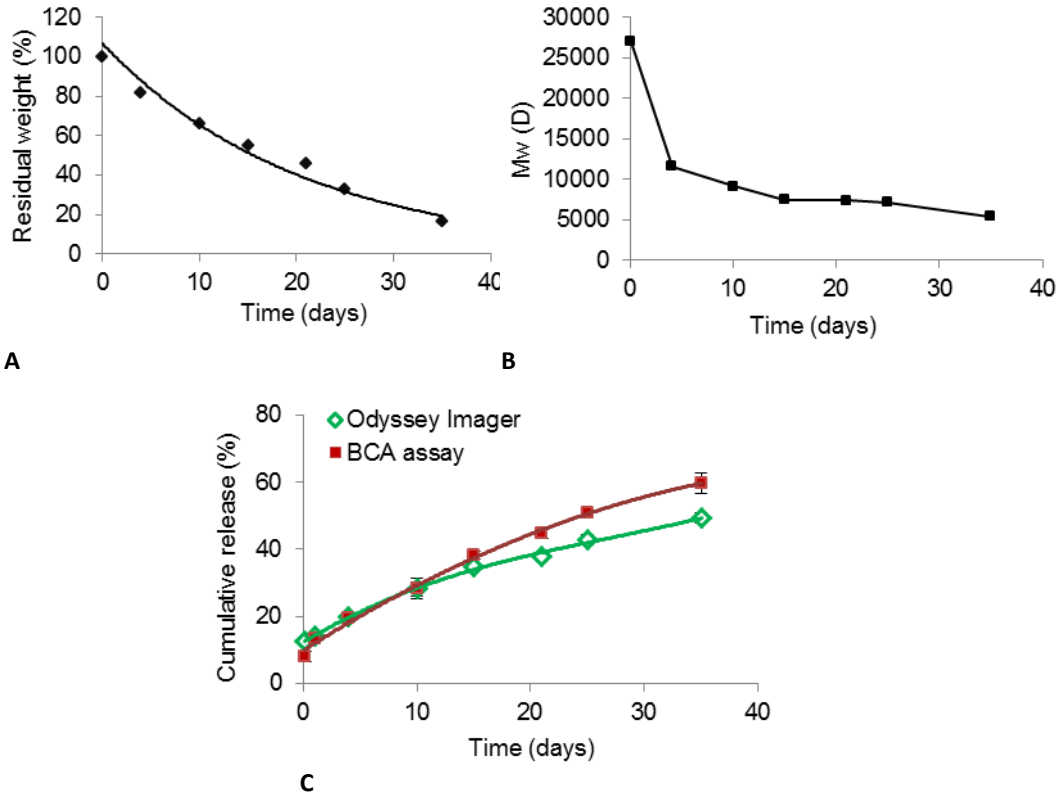

Figure 4. *In vitro* degradation of NIR-BSA loaded PLHMGA microspheres and the cumulative release profile of protein over time: **A.** Residual weight of the microspheres (%) (n=1), **B.** PLHMGA weight average molecular weight (M_w) (n=1) and **C.** Cumulative release of NIR-BSA and BSA from PLHMGA microspheres in PBS measured with Odyssey infrared imager (NIR-BSA release) and with BCA assay (total BSA release) (n=3).

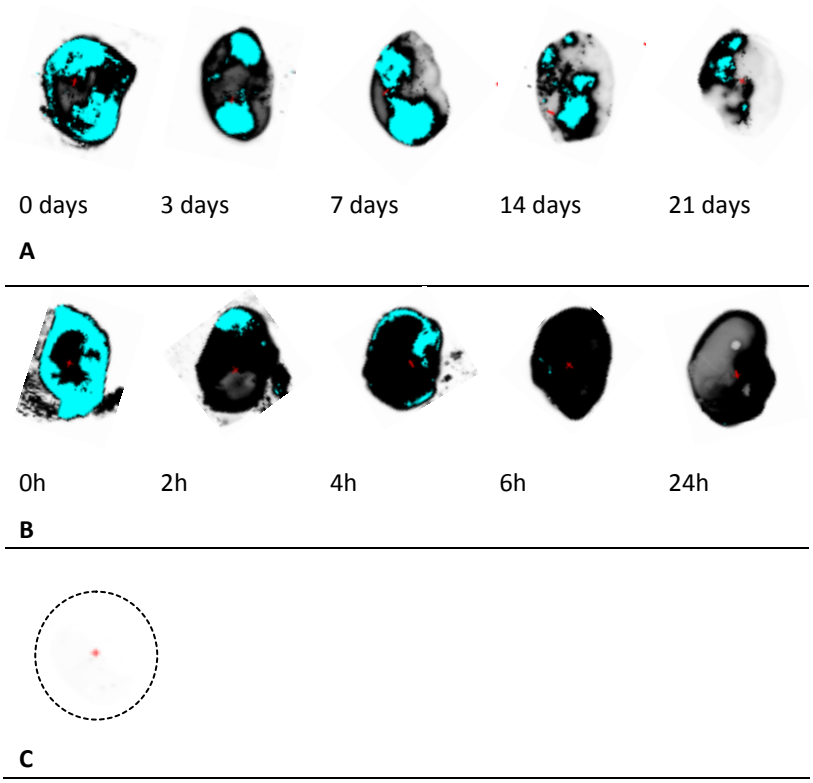

Figure 5. NIR-imaging of the injected kidneys visualized *ex vivo* with Odyssey infrared imager. **A.** Images of kidneys injected with NIR-BSA microspheres explanted at time points up to 3 weeks post injection. **B.** Images of kidneys injected with free NIR-BSA explanted at time points up to 24 h post injection. **C.** Blank kidney from the control group showing no fluorescence signal. Colors from grey to black represent the signal of the NIR dye from low to high signal, respectively. Cyan color indicates overexposure of the fluorescent signal.

The kidneys injected with NIR-BSA and with NIR-BSA-ms were imaged *ex vivo* after termination of the animals. In Figure 5A it is shown that kidneys injected with NIR-BSA-ms contained two adjacent pockets filled with the implanted microspheres, which can be explained by the applied injection procedure as described in 2.6. The NIR signal in the kidneys of the animals of this group decayed reaching around 20% intensity of the signal at the end of the experiment. These data suggest that PLHMGA microspheres injected under the kidney capsule degrade over time while continuously releasing the encapsulated NIR-BSA protein. Figure 5B shows the images of kidneys injected with NIR-BSA, i.e. the labeled

protein dissolved in the viscous vehicle. As can be observed, the injected protein was distributed throughout the kidney showing a widespread fluorescence as a result of fluid convection under the renal capsule. The fluorescent signal decreased gradually afterwards, resulting in relative low fluorescence intensity levels at 24 h post injection. The relative fluorescence at this time-point was, however, higher than the background signal of blank kidney, as can be observed in Figure 5C. These data support that the protein released from the microspheres is able to distribute further over the kidney and, in principle, can also reach more distant areas in this organ. Furthermore, the disappearance of locally injected NIR-BSA within hours after its injection also underscores the need for a depot system that can effectuate prolonged levels of the released protein in the kidney.

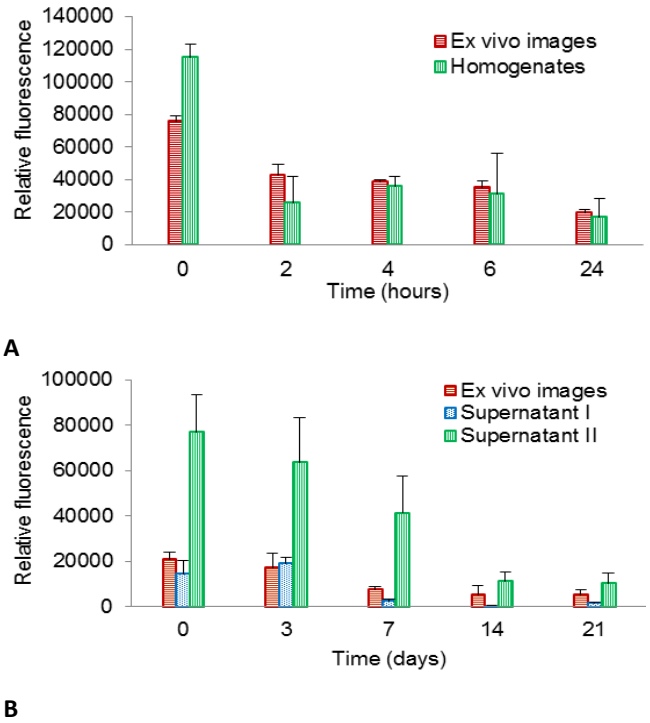

Figure 6. Relative fluorescence of the left kidneys (n=3) injected with **A.** NIR-BSA and **B.** NIR-BSA microspheres. Homogenates of the kidneys injected with NIR-BSA microspheres were treated according to the procedure described in Figure 1A, where supernatant I refers to the released NIR-BSA and supernatant II refers to NIR-BSA recovered from the implanted microspheres.

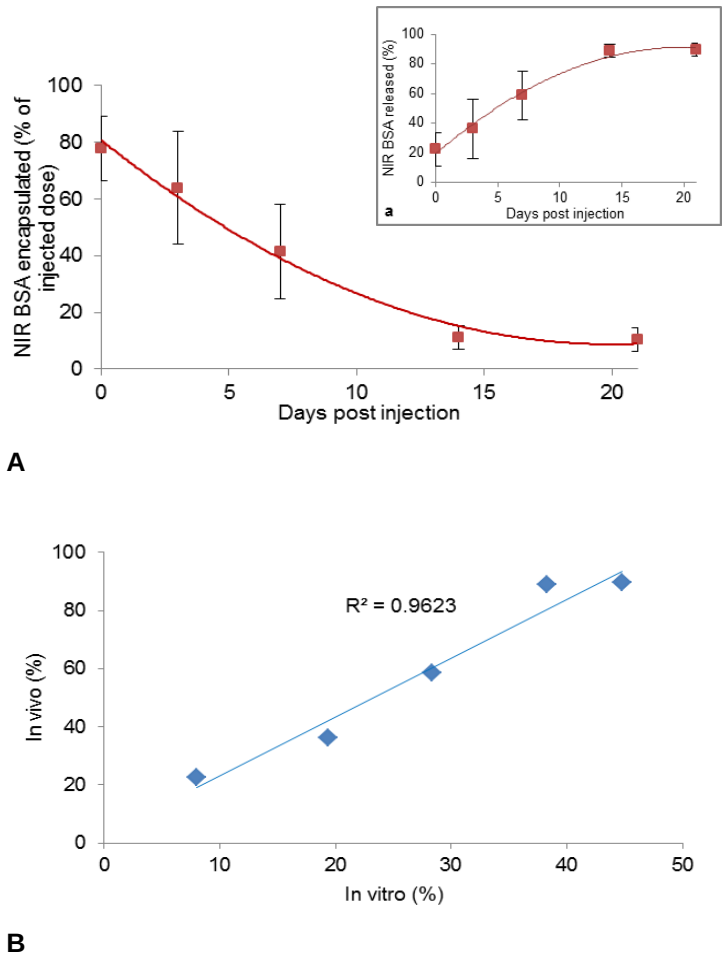

Figure 7. Analysis of NIR-BSA release from a subcapsular microsphere depot over time. **A.** NIR-BSA extracted from microspheres was measured as outlined in Figure 1 (supernatant II), and expressed as percentage of the injected dose of NIR-BSA; insert **a:** *in vivo* cumulative release of NIR-BSA. **B.** *In vitro-in vivo* correlation plot of NIR-BSA release. The fitted linear curve showed an R^2 of 0.96.

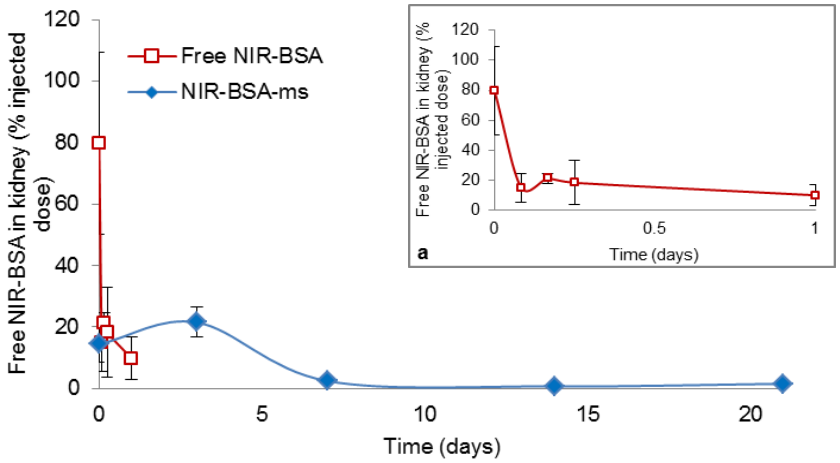

Figure 8. Free/released NIR-BSA measured in the kidney homogenates (n=3) injected subcapsularly with NIR-BSA (also shown in **a**) or with NIR-BSA microspheres. NIR-BSA levels were determined as shown in Figure 1A (supernatant I) and expressed as the percentage of the injected dose of NIR-BSA.

3.3. Quantification of NIR-BSA in kidney homogenates

To quantify the levels of NIR-BSA, the injected kidneys were homogenized and analyzed with an Odyssey infrared imager, after serial dilution of the homogenates. The serial dilutions are necessary to obtain samples that are in the linear range of the fluorescence detection to avoid underestimation of the signal as a result of saturation [32]. Homogenates of the kidneys injected with NIR-BSA-ms were further treated with the method shown and described in Figure 1A, where the released protein was separated from the protein still encapsulated in the microspheres. In the homogenized kidney tissues spiked with NIR-BSA-ms (Figure 1B), this extraction method showed a total NIR-BSA recovery of 62 ±5% from the extracted pellet (supernatant II) and an additional 12 ±1% of NIR-BSA released directly in supernatant of the homogenized tissue (supernatant I). The initial release after tissue homogenization is in good agreement with the results of the *in vitro* burst release of NIR-BSA-ms (Figure 4C). These results show that the quantification of NIR-BSA levels within tissue and its further subdivision in encapsulated and released protein is only semi-quantitative, as it was not further corrected or normilized for the recovery of the extraction method.

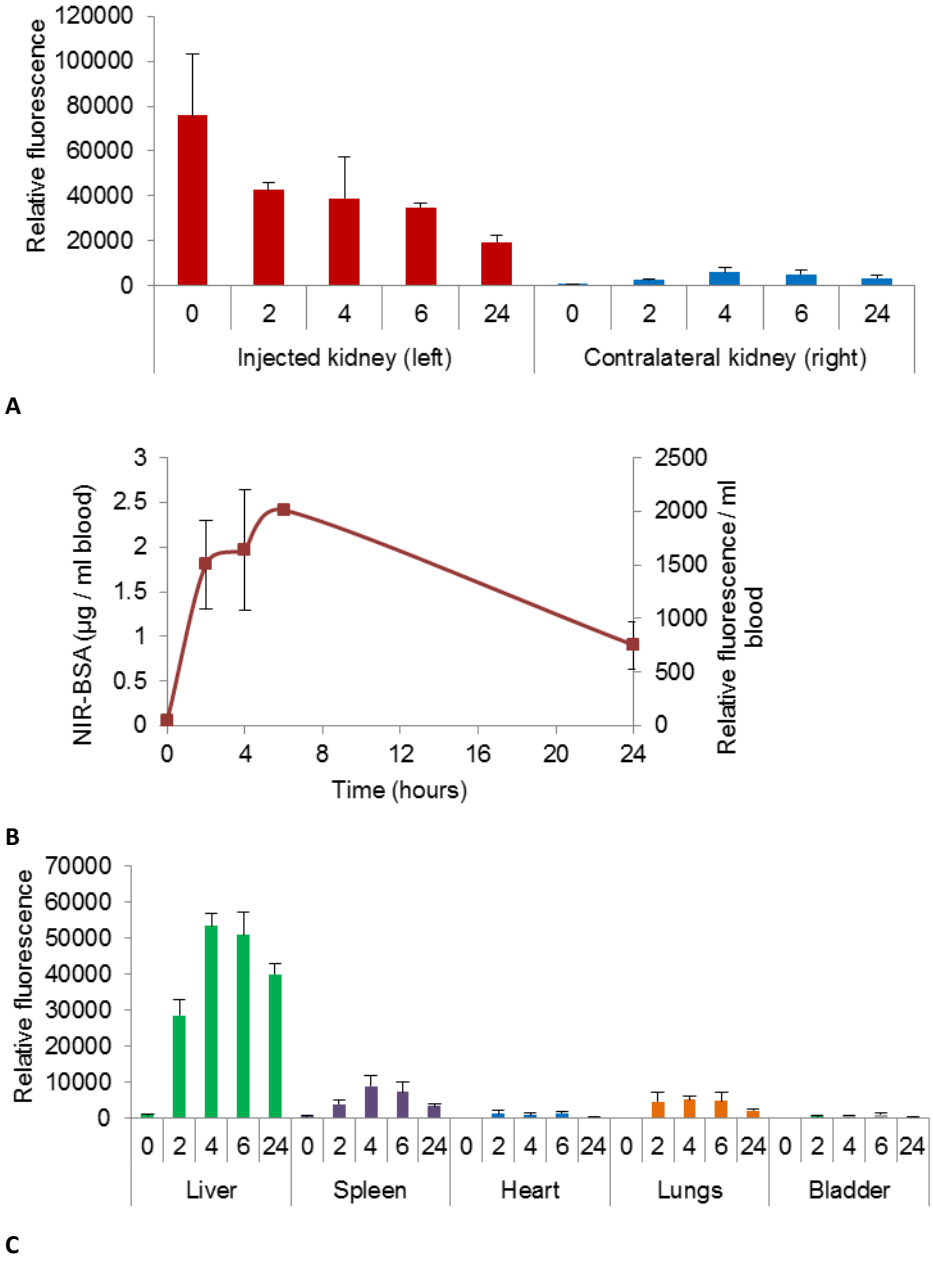

Figure 9. Biodistribution of NIR-fluorescent compounds in animals injected with NIR-BSA (n=3). Organs were explanted and blood samples were collected at time 0, 2, 4, 6 and 24 h and were imaged with Odyssey infrared imager. **A.** Injected left kidney and the contralateral kidney, **B.** Blood samples and **C.** Other organs (liver, spleen, heart, lungs and bladder which also contained urine).

Nevertheless, as shown in Figure 6, NIR fluorescence quantification was more accurate in homogenized tissues compared to image analysis of the *ex vivo* scanned kidneys. For rats injected with NIR-BSA (Figure 6A) a large difference was observed at the first time-point, immediately after injection. This can be explained by oversaturation and quenching of the NIR signal in the *ex vivo* imaging analysis, which was overcome by diluting the homogenate samples. Moreover, in kidneys injected with NIR-BSA-ms (Figure 6B), extraction of the encapsulated protein from the microspheres resulted in a larger dequenching effect at all time-points.

The encapsulated NIR-BSA recovered from the kidneys showed a gradual decline from 80 ±11% directly after injection to around 10 ±4% at day 21 post injection (Figure 7A). The insert in Figure 7a reflects the *in vivo* release of NIR-BSA from the microspheres and was calculated as 100 - percentage of the encapsulated NIR-BSA. It is more appropriate to calculate the *in vivo* release in such an indirect way than to derive it from the tissue levels of released NIR-BSA (supernatant I), since the released protein is subject to further redistribution and metabolism. As shown in Figure 4C, with *in vitro* incubation of NIR-BSA-ms in phosphate buffer at 37°C, 60% of the protein was released at day 35, as calculated with the BCA assay. In Figure 7B, an *in vitro-in vivo* analysis was performed by plotting the percentage of the released NIR-BSA *in vitro* versus the percentage of NIR-BSA released *in vivo*. When comparing both *in vitro* and *in vivo* release, it is evident that protein release was faster *in vivo* with 89 ±4% release within two weeks while 38 ±1% was released *in vitro* in two weeks. In a previous study, we have shown that empty PLHMGA microspheres degraded *in vitro* within 35 days, which is in good agreement with the current *in vitro* degradation of NIR-BSA loaded microspheres [18].

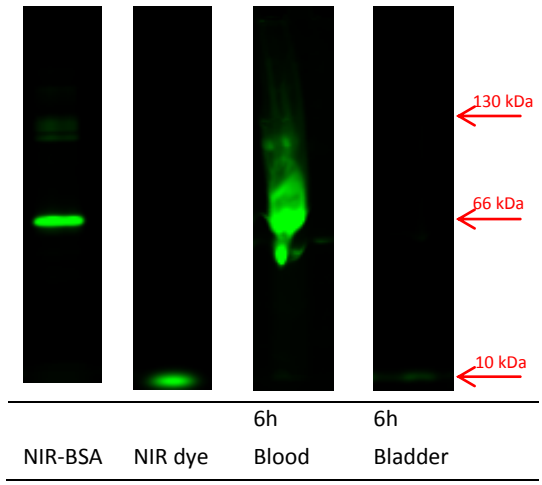

Figure 10a. SDS-PAGE analysis of reference compounds NIR-BSA, NIR dye, blood and bladder homogenate of animals injected with NIR-BSA. Rats were sacrificed at 0, 2, 4, 6 and 24 h after injection. The blood sample and bladder homogenate are shown at time point 6 hours after injection, when the detected fluorescent signal was the highest in these samples. No signal was detected at other time-points.

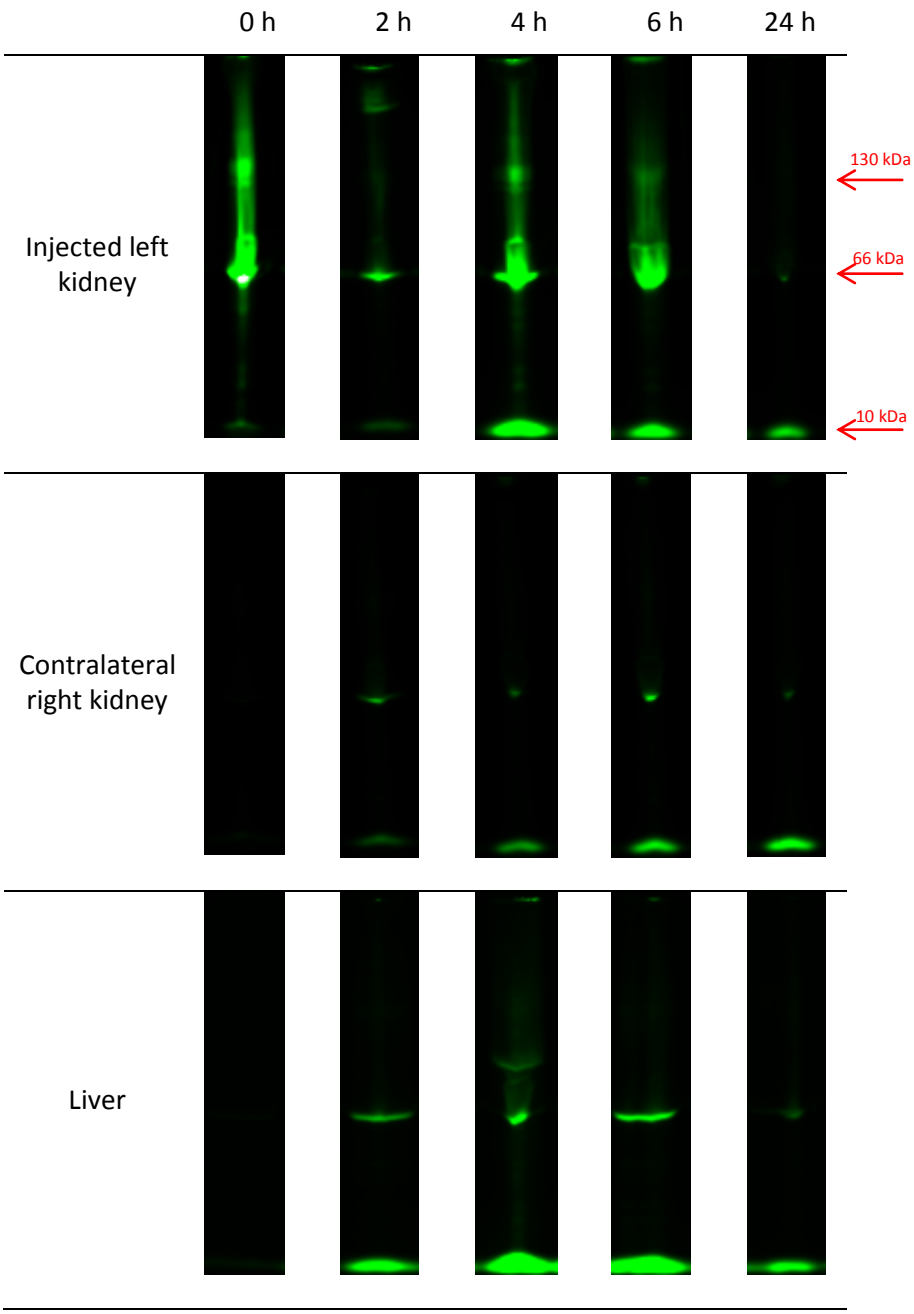

Figure 10b. SDS-PAGE of organ homogenates from animals injected with NIR-BSA. The animals were sacrificed at 0, 2, 4, 6 and 24 h after injection.

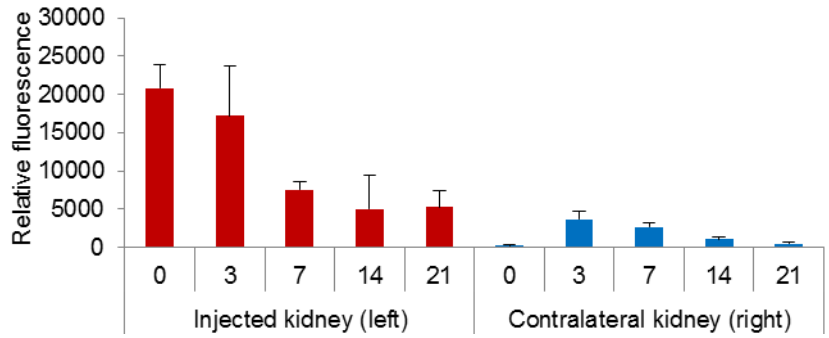

A

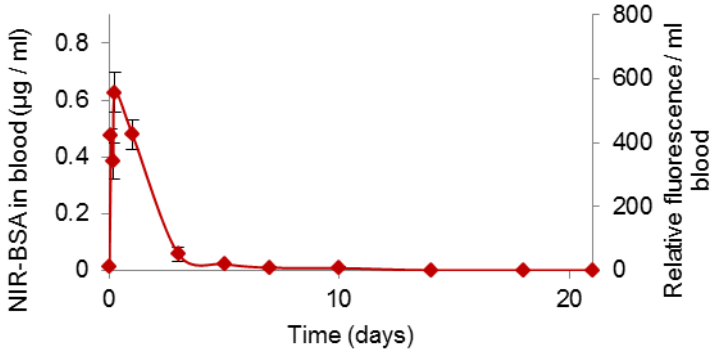

B

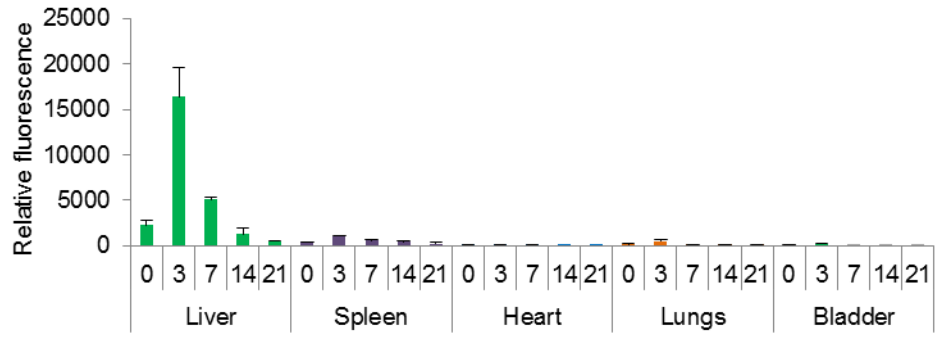

C

Figure 11. Biodistribution of NIR-fluorescent compounds in animals injected with NIR-BSA microspheres (n=3). Organs were explanted at day 0, 3, 7, 14 and 21 and were imaged with Odyssey infrared imager. Blood samples were collected also in between time-points. **A.** Injected left kidney and contralateral right kidney, **B.** Blood samples (signal detected until day 10 after injection) and **C.** Other organs (liver, spleen, heart, lungs and bladder which also contained urine).

The *in vivo* degradation of PLHMGA microspheres was also in good agreement albeit different detection methods were used. In this previous study microspheres were not labeled and their presence in the tissue was mainly scored by visual recognition of their localisation under the renal capsule, whereas the current study enabled NIR fluorescence detection of the microspheres at the early time points, and recovery of released and still encapsulated protein from the kidney homogenates. Therefore, while in both studies the intact microspheres were mostly gone in days 7-14 post injection due to erosion, the near-infrared signal was stil detectable during the later stages of the experiment. Small microfragments of the eroded microspheres will not be pellitized as completely as intact microspheres in the extraction protocol as shown in Figure 1, which will lead to an overestimation of the *in vivo* payload release rate in the present study. Nevertheless, a faster *in vivo* release of the payload from the injected microspheres compared to *in vitro* release was earlier reported by other authors, likely because *in vivo* hydrolytic enzymes contribute to the degradation of the particles [46-49].

Figure 8 shows the renal levels of free NIR-BSA in the injected kidney homogenates calculated as the percentage of the injected dose. Of note, the effectuated levels of free NIR-BSA in the kidney result from the overall balance between the release rate and the local clearance of NIR-BSA in the kidney tissue. In the kidneys injected with NIR-BSA, the relative NIR-fluorescence decreased rapidly from 80 to 15% within the first 2 h after administration and around 10% of the dose was detected in this group at 24 hours post injection.

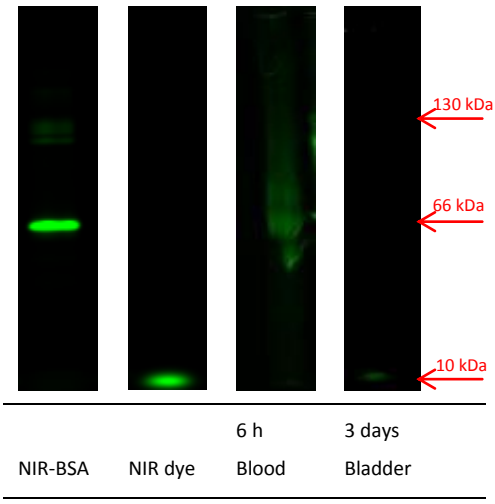

Figure 12a. SDS-PAGE of reference compounds NIR-BSA, NIR dye, blood and bladder homogenate of animals injected with NIR-BSA microspheres. The animals were sacrificed at day 0, 3, 7, 14 and 21. Blood samples were collected additionally in between time-points. The blood sample and bladder homogenate are shown at time-point 6 h and 3 days, respectively, the time-points with maximum detected concentration. There is a faint band present in the blood sample at 66 kDa and in the bladder homogenate at 10 kDa. No signal was detected in blood and bladder samples at other time-points.

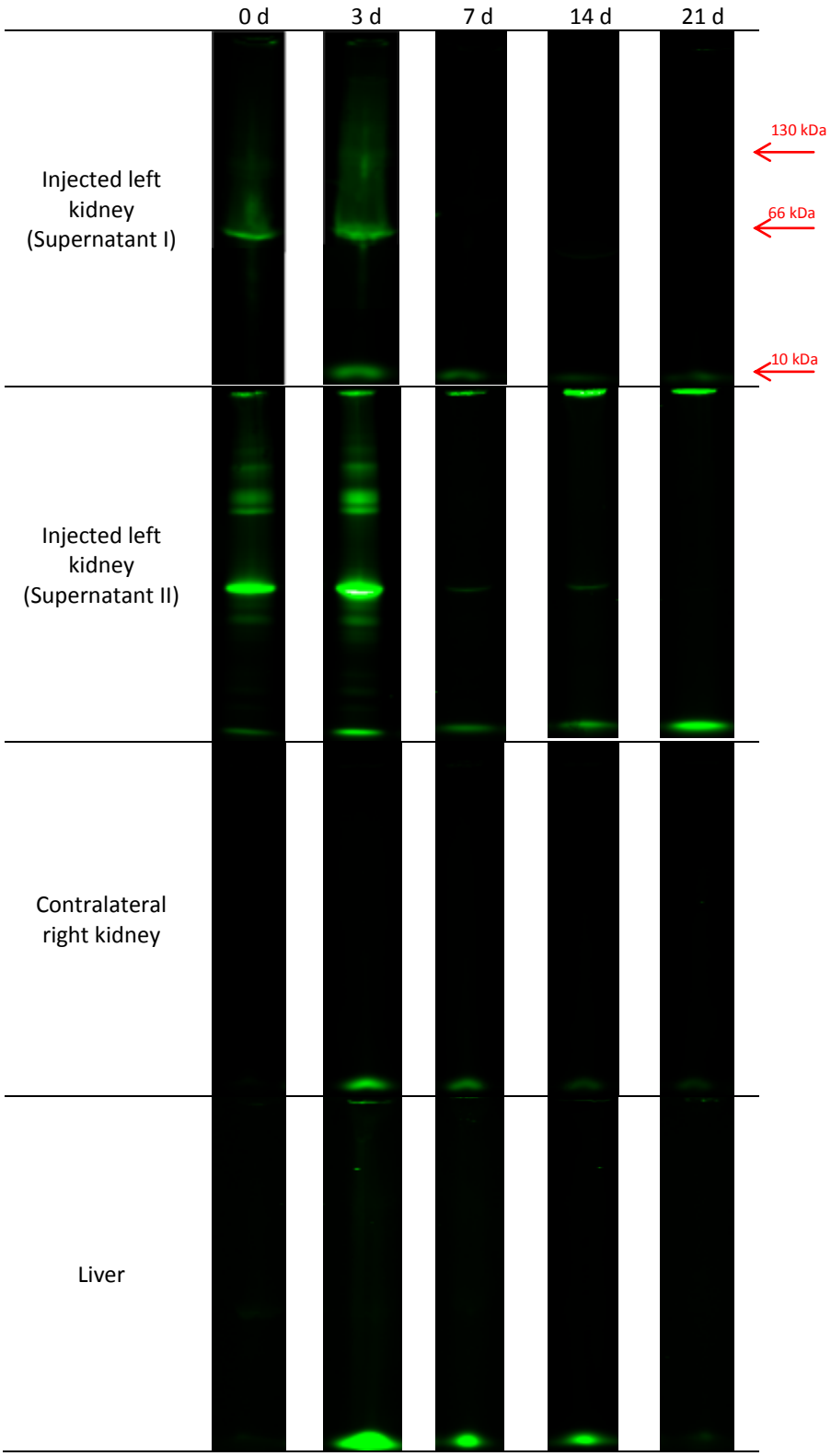
0 d
3 d
7 d
14 d
21 d
Injected left kidney (Supernatant I)
Injected left kidney (Supernatant II)
Contralateral right kidney
Liver
130 kDa
66 kDa
10 kDa

Figure 12b. SDS-PAGE analysis of the organ homogenates from animals injected with NIR-BSA microspheres. The animals were sacrificed at day 0, 3, 7, 14 and 21 after injection. The homogenates of the injected left kidneys were treated as shown in Figure 1, where supernatant I represents the released protein from NIR-BSA microspheres and supernatant II is the signal measured from NIR-BSA after dissolving the microspheres. The low molecular weight compounds seen in the supernatant II are probably the degradation products of the NIR-BSA during liver metabolism, which are taken up by the kidneys, as also seen in the contralateral kidney, whereas the high molecular weight compounds that remain on the injection spot in the gel are probably caused by the extraction method.

In the kidneys injected with NIR-BSA-ms, an initial burst release of 14 ±6% was seen, which is in agreement with the *in vitro* release data and the validation of the tissue extraction method as discussed above. The highest kidney levels of NIR-BSA were measured at day 3 post injection with 21 ±5% of the injected dose. During the sustained release phase after injection of the depot, NIR-BSA tissue levels are mostly dependent on amount of protein released from the microspheres and the clearance of the NIR-BSA from the kidney tissue. Since no change is expected in the elimination mechanism of NIR-BSA during the course of the experiment, the observed peak level of NIR-BSA at day 3 indicates that this time-point corresponds to the highest release rate of the protein per time, which was equal to the protein being eliminated via the kidneys. Thereafter, a continuous fluorescent signal was seen in these kidneys until day 21 post injection. The AUC of the free NIR-BSA in the kidneys, as calculated from Figure 8, was six times higher for animals injected with NIR-BSA-ms (2,440 %·h; supernatant I; 0-7 days), compared to the AUC in the group injected with NIR-BSA (420 %·h; 0-24 h). This shows that the administration of NIR-BSA-ms resulted in prolonged tissue levels of NIR-BSA in the kidney compared to the injection of unencapsulated NIR-BSA.

3.4. Redistribution of NIR-BSA and metabolism

The organ distribution of NIR-BSA was assessed from the NIR-scanning of the explanted organs. Total organ relative NIR-signals of animals injected with NIR-BSA are shown in Figure 9. The increased levels of NIR-BSA in the blood 2 hours onwards demonstrate that the subcapsular injected protein redistributed from the injection site into the circulation, where it subsequently accumulated mainly in the liver. The fluorescence signal showed high peak levels between 4 and 6 hours post injection in all major organs, including the contralateral kidney (Figure 9), which suggests that the degradation products are excreted from the circulation and

undergo renal elimination. This is in agreement with other studies as well [41,45,50,51].

To determine whether the fluorescence was due to the intact NIR-BSA or to degradation products of NIR-BSA, homogenates and blood samples were subjected to SDS-PAGE separation after which the gels were scanned with the Odyssey NIR scanner (Figure 10a and 10b). Intact NIR-BSA was detectable as a fluorescent band at 66 kDa, while protein degradation products were detected at the bottom of the gel (10 kDa). Blood (at 6h) contained intact NIR-BSA, while NIR-fluorescence in the bladder originated from low-MW compounds (10 kDa), most likely NIR-BSA degradation products. Further discrimination was observed in tissues between the presence of intact NIR-BSA (the injected kidney at early time points) and NIR-BSA degradation products (in liver and other organs from 2 h and onwards). We postulate that intact NIR-BSA accumulates from the circulation in the liver while the enzymatically cleaved protein fragments are subsequently eliminated by the kidneys in urine. Previous studies with either the NIR dye or proteins labeled with this dye support the observed metabolic route of NIR-BSA [32,45,50,51]. Liver is known as the major organ for metabolizing albumin [52], where native albumin is taken up by the hepatocytes and degraded via lysosomes [53], whereas denaturated or chemically modified albumins are taken up by the liver macrophages (Kupffer cells) and are finally degraded in the lysosomes [54]. The degradation products are then known to be cleared by the kidneys [45].

In the group of animals injected with NIR-BSA-ms, organs were explanted at day 0, 3, 7, 14 and 21. Additional blood samples were drawn during the first 24 hours and every second day, as described in section 2.6. Similar to the group injected with NIR-BSA, a redistribution of the NIR-fluorescent signal was observed to the blood and the liver, although at a completely different time scale and intensities (Figure 11). The above reported release of NIR-BSA in the kidney (Figure 8), which peaked at day 3 post injection, coincided with the peak levels detected in liver and contralateral kidney (Figure 11). Analysis of blood (Figure 11B), however, showed an earlier peak with maximum NIR-fluorescence at 6h, which coincides with the redistribution of NIR-BSA injected under the renal capsule (Figure 9B). This makes it amenable that this early peak reflects initial burst-release of NIR-BSA from the injected microspheres. After day 7 post injection of NIR-BSA-ms, the levels of NIR-fluorescence in organs dropped to relatively low but still detectable values. At day 21 post injection NIR-fluorescence was still detectable in liver and contralateral kidney indicating that the depot was still releasing its cargo until the end of the experimental period (Figure 11).

SDS-PAGE analysis of organ homogenates and blood samples from animals injected with NIR-BSA-ms are shown in Figure 12a and 12b. Intact NIR-BSA protein was mainly detected in the blood sample and in the injected kidney. SDS-PAGE analysis of the extracted microspheres (Supernatant II) showed presence of

monomeric NIR-BSA until day 14 post injection in the injected kidney, while liver, contralateral kidney and bladder homogenates mainly showed the presence of NIR-BSA degradation products of around 10 kDa. These low-molecular weight products represent the liver metabolites from NIR-BSA that undergo elimination through the kidneys. The presence of NIR-fluorescent degradation products in liver reflect that at least up to day 14, the microsphere depot has released its loaded cargo into the kidney from which it eventually redistributed to the circulation, while at day 21 hardly any NIR-BSA or NIR-BSA degradation products are detectable anymore in tissues.

Conclusion

In the present study, we demonstrate that protein loaded PLHMGA microspheres injected under the kidney capsule can serve as a depot of proteins, providing a continuous release at the site of administration over a period of three weeks. Additionally, the fluorescent signal remained the highest in the injected kidney at all time-points, while systemic levels remained very low. This approach therefore has the potential to reduce side effects of therapeutic proteins by increasing their presence at the site of injection and decreasing it elsewhere in the body. The use of the NIR dye in this study allows detection of low concentrations of the protein in tissue samples. We have also shown that the fluorescence signal detected in *ex vivo* images was not representative of true protein amounts as compared to measurements in tissue homogenates and thus requiring additional treatment of the samples. Cumulatively, this study shows an attractive delivery system of proteins into the kidney characterized by a longer release period and mainly local accumulation.

Acknowledgments

This research forms part of the Project P3.02 DESIRE of the research program of the BioMedical Materials institute, co-funded by the Dutch Ministry of Economic Affairs.

References:

1. Star RA. Treatment of acute renal failure. *Kidney Int,* 54:1817-1831, 1998.
2. Silverstein DM. Inflammation in chronic kidney disease: Role in the progression of renal and cardiovascular disease. *Pediatr Nephrol,* 24:1445-1452, 2009.
3. Kimmel PL, Phillips TM, Simmens SJ, Peterson RA, Weihs KL, Alleyne S, Cruz I, Yanovski JA, Veis JH. Immunologic function and survival in hemodialysis patients. *Kidney Int,* 54:236-244, 1998.
4. Klahr S, Schreiner G, Ichikawa I. The progression of renal disease. *N Engl J Med,* 318:1657-1666, 1988.
5. Peppa M, Uribarri J, Cai W, Lu M, Vlassara H. Glycoxidation and Inflammation in Renal Failure Patients. *Am J Kidney Dis,* 43:690-695, 2004.
6. Declèves AE, Sharma K. Novel targets of antifibrotic and anti-inflammatory treatment in CKD. *Nat Rev Nephrol,* 2014.
7. Arcasoy MO. The non-haematopoietic biological effects of erythropoietin. *Br J Haematol,* 141:14-31, 2008.
8. Asadullah K, Sterry W, Volk HD. Interleukin-10 therapy - Review of a new approach. *Pharmacol Rev,* 55:241-269, 2003.
9. Yao Y, Zhang J, Tan DQ, Chen XY, Ye DF, Peng JP, Li JT, Zheng YQ, Fang L, Li YK, Fan MX. Interferon-γ improves renal interstitial fibrosis and decreases intrarenal vascular resistance of hydronephrosis in an animal model. *Urology,* 77:761.e8-761.e13, 2011.
10. Zeisberg M. Bone morphogenic protein-7 and the kidney: Current concepts and open questions. *Nephrol Dial Transplant,* 21:568-573, 2006.
11. Tomlinson IM. Next-generation protein drugs. *Nat Biotechnol,* 22:521-522, 2004.
12. Pisal DS, Kosloski MP, Balu-Iyer SV. Delivery of therapeutic proteins. *J Pharm Sci,* 99:2557-2575, 2010.
13. Tran VT, Benoit JP, Venier Julienne MC. Why and how to prepare biodegradable, monodispersed, polymeric microparticles in the filed of pharmacy? *Int J Pharm,* 407:1-11, 2011.
14. Mitragotri S, Burke PA, Langer R. Overcoming the challenges in administering biopharmaceuticals: formulation and delivery strategies. *Nat Rev Drug Discov,* 2014.
15. Curtis LM, Chen S, Chen B, Agarwal A, Klug CA, Sanders PW. Contribution of intrarenal cells to cellular repair after acute kidney injury: Subcapsular implantation technique. *Am J Physiol Renal Physiol,* 295:F310-F314, 2008.
16. Dankers PYW, van Luyn MJA, Huizinga-van der Vlag A, van Gemert GML, Petersen AH, Meijer EW, Janssen HM, Bosman AW, Popa ER. Development and in-vivo characterization of supramolecular hydrogels for intrarenal drug delivery. *Biomaterials,* 33:5144-5155, 2012.
17. Dankers PYW, Hermans TM, Baughman TW, Kamikawa Y, Kieltyka RE, Bastings MMC, Janssen HM, Sommerdijk NAJM, Larsen A, Van Luyn MJA, Bosman AW, Popa ER, Fytas G, Meijer EW. Hierarchical formation of supramolecular transient networks in water: A modular injectable delivery system. *Adv Mater,* 24:2703-2709, 2012.
18. Kazazi-Hyseni F, Zandstra J, Popa E, Goldschmeding R, Lathuile A, Veldhuis G, Van Nostrum C, Hennink W, Kok R. Biocompatibility of poly(d,l-lactic-co-hydroxymethyl

glycolic acid) microspheres after subcutaneous and subcapsular renal injection. *Int J Pharm,* 482:99-109, 2014.
19. Falke LL, Van Vuuren SH, Kazazi-Hyseni F, Ramazani F, Nguyen TQ, Veldhuis GJ, Maarseveen EM, Zandstra J, Zuidema J, Duque LF, Steendam R, Popa ER, Kok RJ, Goldschmeding R. Local therapeutic efficacy with reduced systemic side effects by rapamycin-loaded subcapsular microspheres. *Biomaterials,* 42:151-160, 2014.
20. Ghassemi AH, Van Steenbergen MJ, Talsma H, Van Nostrum CF, Crommelin DJA, Hennink WE. Hydrophilic polyester microspheres: Effect of molecular weight and copolymer composition on release of BSA. *Pharm Res,* 27:2008-2017, 2010.
21. Ghassemi AH, van Steenbergen MJ, Talsma H, van Nostrum CF, Jiskoot W, Crommelin DJA, Hennink WE. Preparation and characterization of protein loaded microspheres based on a hydroxylated aliphatic polyester, poly(lactic-co-hydroxymethyl glycolic acid). *J Control Release,* 138:57-63, 2009.
22. Liu Y, Ghassemi AH, Hennink WE, Schwendeman SP. The microclimate pH in poly(D,L-lactide-co-hydroxymethyl glycolide) microspheres during biodegradation. *Biomaterials,* 33:7584-7593, 2012.
23. Seyednejad H, Ghassemi AH, van Nostrum CF, Vermonden T, Hennink WE. Functional aliphatic polyesters for biomedical and pharmaceutical applications. *J Control Release,* 152:168-176, 2011.
24. Kazazi-Hyseni F, Landin M, Lathuile A, Veldhuis GJ, Rahimian S, Hennink WE, Kok RJ, van Nostrum CF. Computer Modeling Assisted Design of Monodisperse PLGA Microspheres with Controlled Porosity Affords Zero Order Release of an Encapsulated Macromolecule for 3 Months. *Pharm Res,* 31:2844-2856, 2014.
25. Nakashima T, Shimizu M, Kukizaki M. Membrane emulsification by microporous glass. *Key Eng Mat,* 61-62:513-516, 1991.
26. Frangioni JV. In vivo near-infrared fluorescence imaging. *Curr Opin Chem Biol,* 7:626-634, 2003.
27. Leemhuis M, Van Nostrum CF, Kruijtzer JAW, Zhong ZY, Ten Breteler MR, Dijkstra PJ, Feijen J, Hennink WE. Functionalized poly(a-hydroxy acid)s via ring-opening polymerization: Toward hydrophilic polyesters with pendant hydroxyl groups. *Macromolecules,* 39:3500-3508, 2006.
28. Peters T, Putman F, editors. The plasma proteins. : Academic Press, 1975.
29. Nakashima T, Shimizu M, Kukizaki M. Particle control of emulsion by membrane emulsification and its applications. *Adv Drug Deliv Rev,* 45:47-56, 2000.
30. Sah H. A new strategy to determine the actual protein content of poly(lactide-co-glycolide) microspheres. *J Pharm Sci,* 86:1315-1318, 1997.
31. Bjornsson OG, Murphy R, Chadwick VS, Bjornsson S. Physicochemical studies on indocyanine green: Molar lineic absorbance, pH tolerance, activation energy and rate of decay in various solvents. *J Clin Chem Clin Biochem,* 21:453-458, 1983.
32. Oliveira S, Cohen R, van Walsum MS, van Dongen GAMS, Elias SG, van Diest PJ, Mali W, van Paul MP, Henegouwen B. A novel method to quantify IRDye800CW fluorescent antibody probes ex vivo in tissue distribution studies. *EJNMMI Research,* 2:1-9, 2012.

33. D'Aurizio E, Sozio P, Cerasa LS, Vacca M, Brunetti L, Orlando G, Chiavaroli A, Kok RJ, Hennink WE, Di Stefano A. Biodegradable microspheres loaded with an anti-Parkinson prodrug: An in vivo pharmacokinetic study. *Mol Pharm,* 8:2408-2415, 2011.
34. Schliecker G, Schmidt C, Fuchs S, Ehinger A, Sandow J, Kissel T. In vitro and in vivo correlation of buserelin release from biodegradable implants using statistical moment analysis. *J Control Release,* 94:25-37, 2004.
35. Ghassemi AH, van Steenbergen MJ, Talsma H, van Nostrum CF, Jiskoot W, Crommelin DJA, Hennink WE. Preparation and characterization of protein loaded microspheres based on a hydroxylated aliphatic polyester, poly(lactic-co-hydroxymethyl glycolic acid). *J Control Release,* 138:57-63, 2009.
36. Samadi N, Van Nostrum CF, Vermonden T, Amidi M, Hennink WE. Mechanistic studies on the degradation and protein release characteristics of poly(lactic-co-glycolic-co-hydroxymethylglycolic acid) nanospheres. *Biomacromolecules,* 14:1044-1053, 2013.
37. Heuveling DA, Visser GW, de Groot M, de Boer JF, Baclayon M, Roos WH, Wuite GJ, Leemans CR, de Bree R, van Dongen GA. Nanocolloidal albumin-IRDye 800CW: a near-infrared fluorescent tracer with optimal retention in the sentinel lymph node. *Eur J Nucl Med Mol Imaging,* 39:1161-1168, 2012.
38. Leblond F, Davis SC, Valdes PA, Pogue BW. Pre-clinical whole-body fluorescence imaging: Review of instruments, methods and applications. *J Photochem Photobiol B,* 98:77-94, 2010.
39. Durand E, Chaumet-Riffaud P, Grenier N. Functional renal imaging: new trends in radiology and nuclear medicine. *Semin Nucl Med,* 41:61-72, 2011.
40. Gross S, Piwnica-Worms D. Molecular imaging strategies for drug discovery and development. *Curr Opin Chem Biol,* 10:334-342, 2006.
41. Oliveira S, Van Dongen GAMS, Stigter-Van Walsum M, Roovers RC, Stam JC, Mali W, Van Diest PJ, Van Bergen En Henegouwen PMP. Rapid visualization of human tumor xenografts through optical imaging with a near-infrared fluorescent anti-epidermal growth factor receptor nanobody. *Mol Imaging,* 11:33-46, 2012.
42. Kunjachan S, Gremse F, Theek B, Koczera P, Pola R, Pechar M, Etrych T, Ulbrich K, Storm G, Kiessling F, Lammers T. Noninvasive optical imaging of nanomedicine biodistribution. *ACS Nano,* 7:252-262, 2013.
43. Hou Y, Liu Y, Chen Z, Gu N, Wang J. Manufacture of IRDye800CW-coupled Fe3O4 nanoparticles and their applications in cell labeling and in vivo imaging. *J Nanobiotechnology,* 8 2010.
44. Eker OF, Quesson B, Rome C, Arsaut J, Deminière C, Moonen CT, Grenier N, Couillaud F. Combination of cell delivery and thermoinducible transcription for in vivo spatiotemporal control of gene expression: A feasibility study. *Radiology,* 258:496-504, 2011.
45. Vasquez KO, Casavant C, Peterson JD. Quantitative whole body biodistribution of fluorescent-labeled agents by non-invasive tomographic imaging. *PLoS ONE,* 6 2011.
46. Wöhl-Bruhn S, Badar M, Bertz A, Tiersch B, Koetz J, Menzel H, Mueller PP, Bunjes H. Comparison of in vitro and in vivo protein release from hydrogel systems. *J Control Release,* 162:127-133, 2012.
47. van Apeldoorn AA, Van Manen H-, Bezemer JM, De Bruijn JD, Van Blitterswijk CA, Otto C. Raman imaging of PLGA microsphere degradation inside macrophages. *J Am Chem Soc,* 126:13226-13227, 2004.

48. Walter E, Dreher D, Kok M, Thiele L, Kiama SG, Gehr P, Merkle HP. Hydrophilic poly(DL-lactide-co-glycolide) microspheres for the delivery of DNA to human-derived macrophages and dendritic cells. *J Control Release,* 76:149-168, 2001.
49. Jiang G, Woo BH, Kang F, Singh J, DeLuca PP. Assessment of protein release kinetics, stability and protein polymer interaction of lysozyme encapsulated poly(D,L-lactide-co-glycolide) microspheres. *J Control Release,* 79:137-145, 2002.
50. Marshall MV, Draney D, Sevick-Muraca EM, Olive DM. Single-dose intravenous toxicity study of IRDye 800CW in sprague-dawley Rats. *Mol Imaging Biol,* 12:583-594, 2010.
51. Tanaka E, Ohnishi S, Laurence RG, Choi HS, Humblet V, Frangioni JV. Real-Time Intraoperative Ureteral Guidance Using Invisible Near-Infrared Fluorescence. *J Urol,* 178:2197-2202, 2007.
52. Rothschild MA, Oratz M, Schreiber SS. Regulation of albumin metabolism. *Annu Rev Med,* 26:91-104, 1975.
53. Ohshita T, Hiroi Y. Degradation of serum albumin by rat liver and kidney lysosomes. *J Nutr Sci Vitaminol (Tokyo),* 44:641-653, 1998.
54. Nilsson M, Berg T. Uptake and degradation of formaldehyde-treated 125I-labelled human serum albumin in rat liver cells in vivo and in vitro. *Biochim Biophys Acta,* 497:171-182, 1977.

Chapter 5

A comparison of different encapsulation methods for the formulation of recombinant erythropoietin in polymeric microspheres

Filis Kazazi Hyseni[1]
Jurjen J Westeneng[1]
Liem A Halim[1]
Niels Grasmeijer[2]
Wouter LJ Hinrichs[2]
Henderik W Frijlink[2]
Marco van de Weert[3]
Christine N Hiemstra[4]
Rob Steendam[4]
Sima Rahimian[1]
Vera Brinks[1]
Cornelus F van Nostrum[1]
Wim E Hennink[1]
Robbert Jan Kok[1]

[1.] Department of Pharmaceutics, Utrecht Institute for Pharmaceutical Sciences, Utrecht University, Utrecht, The Netherlands
[2.] Department of Pharmaceutical Technology and Biopharmacy, University of Groningen, AV Groningen, The Netherlands
[3.] Section for Biologics, Department of Pharmacy, Faculty of Health and Medical Sciences, University of Copenhagen, Copenhagen, Denmark
[4.] InnoCore Pharmaceuticals, Groningen, The Netherlands

Abstract

The encapsulation of therapeutic proteins encounters several challenges. One of the major issues is the relative high instability of the proteins during formulation conditions due to their fragile structure. The current study evaluates different techniques for the encapsulation of a model therapeutic protein, recombinant erythropoietin (EPO), in polymeric microspheres. Two different types of protein-friendly copolymers were used for the preparation of microspheres, poly(D,L-lactic-*co*-hydroxymethyl glycolic acid) (PLHMGA) and SynBiosys multi-block copolymers (50CP10C20-LL40 and 30CP15C20-LL40) composed of poly(ε-caprolactone-PEG- ε-caprolactone) blocks and poly(L-lactide) blocks. First, a dry powder of EPO was prepared by spray drying an aqueous solution of inulin (0.5% w/v) and Tween-80 (EPO/inulin/Tween-80 weight ratio of 1/100/3.8). Next, the EPO/inulin/Tween-80 powder was formulated with PLHMGA using three different double-emulsion/extraction encapsulation methods, w/o/w, s/o/w and s/o/o. Concurrently, SynBiosys microspheres were prepared by the s/o/o method. The structural integrity of EPO was studied in the spray dried powder and after the formulation processes using anti-EPO Western blotting. The release of EPO from the microspheres when incubated in a buffer of pH 7.4 at 37°C was studied by anti-EPO ELISA and Western blotting. Spray drying EPO/inulin/Tween-80 resulted in particles with a size of around 1 µm and the structure of EPO remained intact with no formation of dimers or trimers. The obtained EPO-loaded PLHMGA microspheres had a mean diameter of 15 ±1, 12 ±1 and 31 ±21 µm for w/o/w, s/o/w and s/o/o methods, respectively, and a high loading efficiency of 87, 89 and 96%, respectively. SynBiosys microspheres had a mean diameter of 44 ±1 and 27 ±3 µm for 50CP10C20-LL40 and 30CP15C20-LL40, respectively, and a loading efficiency close to 100%. Western blot images showed that EPO was mostly in its monomeric form after encapsulation in the polymeric microspheres, with only 2-7% of dimersformed during the formulation processes using the three different preparation methods. All formulations released EPO as a burst (0.7 – 30% of the loading) during the first 24 h of incubation. After the burst release, only negligible amounts of EPO release could be detected. Further attempts to detect released EPO failed due to limitations in the analytical methods to detect EPO in the microsphere pellets or supernatant of the in vitro release assay. In conclusion, particles loaded with monomeric EPO were prepared by spray drying a solution of this protein with inulin and Tween-80. Encapsulation of EPO/inulin/Tween-80 particles in PLHMGA and SynBiosys microspheres resulted in relatively stable EPO structure with low amounts of dimers formed. However, the in vitro release study showed that EPO was released only during the first 24 h of incubation and no further release was detectable by ELISA.

1. Introduction

Polymeric microspheres have a number of potential applications in the field of drug delivery, especially in sustained release formulations of proteins and peptides [1-3] as well as low molecular weight drugs [4-6]. Protein therapeutics especially benefit from polymeric delivery systems in reducing their frequent administration and thus patient compliance. Extensive research is ongoing in the area of sustained depots for proteins [7]. Apart from other polymeric systems such as hydrogels [8,9], polymeric microspheres are also considered for this purpose, e.g. to achieve local release or sustained plasma levels of the released compound [10]. However, the use of polymeric microspheres for the delivery of therapeutic proteins is challenging as a result of the susceptibility of the protein structure for changes due to stress factors to which the proteins are exposed during the different steps of microsphere preparation methods [11]. So far most studies involve model proteins, like lysozyme or albumin, for encapsulation into polymeric microspheres [12,13]. These proteins are readily available and display a relatively high stability. A wide variety of techniques and approaches has been reported to improve protein encapsulation and, more importantly, the stability of the formulated protein. Water-free encapsulation processes and incorporation of different additives and stabilizers are among many other approaches to achieve non-aggregated and stable formulation of proteins [11,14].

For the encapsulation of hydrophilic molecules into polymeric microspheres a water-in-oil-in-water (w/o/w) process is commonly employed, where an aqueous solution of this hydrophilic molecule is emulsified into an organic solution of the polymer [15,16]. This primary w/o emulsion is then added to a second water phase containing a stabilizer, such as polyvinylalcohol (PVA). Subsequently, the solvent is removed by extraction or evaporation and the microspheres are collected by filtration or centrifugation. However, when proteins are encapsulated with this technology, the protein stability remains an issue. In the w/o/w method, the protein may partly aggregate already during the preparation of the first w/o emulsion, where proteins because of their surface active properties tend to adsorb at the water/organic solvent interface causing protein unfolding, inactivation and irreversible aggregation [17-20]. As a result, microspheres prepared with w/o/w method are generally characterized by an incomplete release of the encapsulated protein. For this reason, alternative methods have emerged which avoid the use of water in their inner phase of the particles (solid-in-oil-in-water (s/o/w) emulsification) or that are even completely water-free (solid-in-oil-in-oil (s/o/o) emulsification). In these methods, protein powders are suspended in an organic solvent in which a polymer is dissolved. This suspension is then emulsified in an aqueous/non-aqueous outer phase that is non-solvent for the polymer, to prepare polymeric droplets that can further solidify upon evaporation of the solvent into microparticles [3]. The advantage of the water-free

methods is that the protein is in its solid state during the preparation of microspheres. Proteins in this dehydrated state have less conformational mobility and are therefore less likely to unfold during processing [19,21,22]. In addition, minimal solubility of proteins in the oil phases ensures higher loadings and encapsulation efficiencies [19]. However, these methods also have their drawbacks. Aggregation of proteins has been reported to occur during preparation of particles using the s/o/w method as a result of exposure of the dry protein to the oil/water interface [23]. On the other hand, the s/o/o method can be associated with a high burst release, which is a result of the distribution of the encapsulated protein particles inside the microspheres [21,24] and the surface porosity of microspheres [25].

In the present study, we questioned whether results obtained with stable model proteins can be translated to formulate therapeutic proteins, which often are encapsulated at lower doses (micrograms rather than milligrams) and which are mostly more sensitive to degradation than the model proteins used in many studies. Therefore, in the present study the encapsulation of a therapeutic protein, recombinant erythropoietin (EPO), was used. EPO is known to be sensitive to stress factors that are experienced during encapsulation in polymeric particles [26-29]. The main therapeutic application of EPO is for the treatment of anemia in patients with kidney failure and for patients with cancer [30]. However, recent studies also refer to a local effect of EPO in the kidney, characterized with the possibility to decrease immunological responses in acute and chronic kidney failure [31-33]. Therefore, EPO-loaded polymeric microspheres can be of potential interest to achieve these local effects of EPO in the kidney.

In this study, different encapsulation methods (w/o/w, s/o/w and s/o/o) were investigated to obtain EPO-loaded microparticles. Prior to encapsulation, the first step was to load EPO in sugar glass particles with a spray-dried method using a polysaccharide, inulin, as stabilizer. Sugar glasses strongly reduce diffusion and molecular mobility of a loaded protein preventing its aggregation and degradation [34,35]. Inulin has excellent properties as a protectant for protein molecules, owing to its high glass transition temperature (130°C [36]), hydrophilicity and good hydrogen bonding capacity [37,38]. Tween-80 was added as a surfactant to further protect the protein structure against aggregation during spray drying [39]. EPO was encapsulated using the relatively protein-friendly polymers, such as poly(D,L-lactic-*co*-hydroxymethyl glycolic acid) (PLHMGA) and SynBiosys polymers composed of poly(ε-caprolactone-PEG-*ε*-caprolactone) blocks and poly(L-lactide) blocks. PLHMGA, because of its more hydrophilic nature than e.g. PLGA, ensures rapid release of the acidic degradation products into the external medium, thus preventing the degradation of the loaded protein during *in vitro* release studies [40]. SynBiosys polymers are block copolymers consisting of relatively short polylactide blocks intercalated with polyethyleneglycol/caprolactone blocks. This ensures a polymeric network which controls the release of protein by swelling and

erosion [41]. Earlier studies have shown the benefits of PLHMGA and SynBiosys polymers for the encapsulation of peptides and proteins [41-45]. The spray dried EPO powder was encapsulated with w/o/w, s/o/w and s/o/o methods and the prepared microspheres were subjected to *in vitro* release studies. The concentration of the released EPO was measured with ELISA, whereas the integrity of protein structure during the various processing steps and after release was studied with Western blot.

2. Materials and Methods

2.1. Materials

O-Benzyl-L-serine was purchased from Senn Chemicals AG (Switzerland). Tin (II) 2-ethylhexanoate ($SnOct_2$), poly(vinyl alcohol) (PVA; M_w= 13,000-23,000 g/mol), palladium 10 w% (dry basis) on activated carbon, dimethylsulfoxide (DMSO), Tween-80 and silicone oil (viscosity of 350 cSt (25°C); density of 0.968 g/mL) were obtained from Sigma-Aldrich (Germany). D,L-lactide was obtained from Purac (The Netherlands). ε-Caprolactone, 1,4-butanediol, n-heptane (99+%, pure) and acetonitrile (HPLC gradient grade 99 w%) were obtained from Acros Organics (Belgium). 1,4-Butanediisocyanate was purchased from Bayer (Germany). Prefilled syringes of NeoRecormon containing 30,000 IU/mL were a gift of Roche. Sodium phosphate dibasic (Na_2HPO_4) and sodium azide (NaN_3) were purchased from Fluka (The Netherlands). Dichloromethane (DCM) and tetrahydrofuran were purchased from Biosolve BV (The Netherlands). Sodium dihydrogen phosphate (NaH_2PO_4) and sodium chloride (NaCl) were supplied by Merck (Germany). Inulin 4 kDa, with a degree of polymerization of 11 and a glass transition temperature of 130°C [36], was obtained from Sensus (Roosendaal, The Netherlands). All experiments were performed with Millipore water.

2.2. Synthesis and characterization of PLHMGA

Poly(D,L-lactic-*co*-hydroxymethyl glycolic acid) (PLHMGA) was synthesized as previously described [46]. In brief, BMMG (3*S*-(benzyloxymethyl)-6*S*-methyl-1,4-dioxane-2,5-dione) was synthesized from *O*-benzyl-L-serine. In the second step BMMG (35 mol%) and D,L-lactide (65 mol%) were copolymerized in the melt at 130°C using butanediol and tin (II) 2-ethylhexanoate as initiator and catalyst, respectively, to yield poly(D,L-lactic-*ran*-benzyloxymethyl glycolic acid) (PLBMGA). Next, the resulting PLBMGA was dissolved in chloroform, precipitated in cold methanol and dried *in vacuo*. In the third step, the protecting benzyl groups of PLBMGA were removed by hydrogenation of the polymer dissolved in tetrahydrofuran for 16 hours at room temperature, using 10% w/w palladium on activated carbon (Pd/C) as a catalyst. The catalyst was removed by filtration

through 0.2 µm nylon filters (Alltech Associates) and the formed copolymer, PLHMGA, was dried *in vacuo.*

The molecular weight of the polymer was determined by GPC (Waters Alliance System) with a Waters 2695 separating module and a Waters 2414 refractive index detector, using tetrahydrofuran as solvent at a flow rate of 1 mL/min; polystyrene standards (PS-2, Mw = 580 – 377,400 Da, EasiCal, Varian) were used for calibration. Two PL-gel 5 µm Mixed-D columns fitted with a guard column (Polymer Labs, Mw range 0.2 – 400 kDa) were used. The composition of the copolymer was determined by NMR (Gemini-300 MHz) in chloroform-*d*, 99.8 atom% (Sigma-Aldrich) as a solvent [46]. The thermal properties of the copolymer were measured with differential scanning calorimetry (DSC - Q 2000, TA Instruments). Approximately 5 mg of copolymer was transferred into an aluminum pan (T zero pan/lid set, TA Instruments) and the sample was scanned with a modulated heating method in three cycles [42]. The sample was heated until 120°C (5°C/min) and then cooled down to – 50°C, followed by a heating until 120°C (5°C/min). The temperature modulation was ±1°C/min. The glass transition temperature (T_g) was determined from the second heating scan.

2.3. Synthesis and characterization of SynBiosys copolymers

Two different biodegradable multi-block copolymers, SynBiosys 30CP15C20-LL40 and SynBiosys 50CP10C20-LL40, were used for the preparation of microspheres. The first copolymer was composed of 30 w% poly(ε-caprolactone)-PEG_{1500}-poly(ε-caprolactone) (PCL-PEG_{1500}-PCL) with a molecular weight of 2,000 g/mol and 70 w% of poly(L-lactide) (PLLA) with a molecular weight of 4,000 g/mol. The second copolymer consisted of 50 w% PCL-PEG_{1000}-PCL (M_W=2,000 g/mol) and 50 w% of PLLA (M_W=4,000 g/mol). These two types of copolymers were synthesized according to the procedure described previously [47]. In short, first the prepolymers, PCL-PEG_{1500}-PCL, PCL-PEG_{1000}-PCL and PLLA, were synthesized by standard stannous octoate catalyzed ring-opening polymerization. Next, the prepolymers were chain-extended with 1,4-butanediisocyanate to obtain SynBiosys 30CP15C20-LL40 and SynBiosys 50CP10C20-LL40 multiblock copolymers.

The molecular weights of the multiblock copolymers were determined using size exclusion chromatography coupled to refractive index detector (SEC-HPLC, Waters, Breeze, USA) [41,44]. Samples (0.01 g) were dissolved in 1 mL of DMF. PEG standards with molecular weights of 1–218 kg/mol were used for calibration and were prepared likewise. Samples and PEG standards were injected (50 µL) onto the SEC column (Thermo Fisher, Column 1: Plgel 5 µm 500 Å, column 2: Plgel 5 µm 500 Å, column 3: Plgel 5 µm 104 Å, eluent: DMF with 0.1 M LiBr, flow: 1 mL/min). The intrinsic viscosity of the polymers dissolved in chloroform was measured at three different polymer concentrations at a temperature of 25°C using an Ubbelohde viscometer (DIN, type 0C Schott Geräte supplied with a Schott

AVS-450 Viscometer equipped with a water bath). The composition of the copolymers was determined by NMR (VXR Unity Plus, Varian, USA- 300 MHz) in chloroform-*d*, 99.8 atom% (Sigma-Aldrich) as a solvent. The thermal properties of the copolymers were measured with differential scanning calorimetry, as described in 2.2.

2.4. Preparation of EPO/inulin sugar glass particles

In order to remove the excipients that would interfere with spray drying, NeoRecormon formulation (30 000 IU, corresponding to 0.25 mg in 0.6 mL of recombinant human EPO) was desalted using a PD-10 column (Sephadex^{TM} G-25 Medium, GE Healthcare) according to the spin protocol as given by the manufacturer. The desalted EPO solution was subsequently mixed with an aqueous solution of inulin (5 mg/mL in water; final volume of 10 mL) to obtain a final EPO/inulin ratio of 1/100 (w/w). Tween-80 was added as stabilizer to the spray drying solution in molar ratios ranging from 0/1 to 100/1 mol/mol of Tween-80/EPO. Solutions of only inulin (used as a control) and EPO and inulin with or without Tween-80 were spray dried using a Nano Spray-drier B-90 (Büchi Labortechnik AG, Flawil, Switzerland). The inlet temperature and the liquid flow rate were set at 80°C and 1 mL/min, respectively. The atomizing air flow rate was fixed at 150 L/min. The resulting outlet temperature was 35°C. The formed particles were collected through a high-efficiency cyclone in a glass container from where they were transferred into a glass vial and sealed with a rubber stopper and aluminum cap to prevent absorption of water. Particles were stored at 4°C until further use.

2.5. Encapsulation of EPO/inulin/Tween-80 particles in PLHMGA microspheres using w/o/w method

To obtain microspheres in which EPO had undergone the same stresses up to its actual encapsulation, spray dried EPO/inulin/Tween-80 particles were prepared using the w/o/w method. Forty four mg of the spray dried EPO/inulin/Tween80 (with Tween-80/EPO molar ratio of 100/1) particles (corresponding to 420 µg EPO) was dissolved in 0.2 mL of water. The resulting EPO solution was then homogenized with a PLHMGA solution in DCM (20% w/w; 250 mg polymer in 0.76 mL of DCM) at 20,000 rpm (Ultra-Turrax T8, IKA Works, USA) for 30 seconds. Next, the obtained primary emulsion was homogenized with the second water phase of 1.5 mL of 1% PVA for 30 seconds. The w/o/w emulsion was then added dropwise into 7.3 mL of 0.5% PVA and 1% NaCl and left to stir for 3 hours for extraction and evaporation of DCM. The particles were collected by centrifugation (4,000 rpm for 5 min), followed by three times washing steps by

resuspending them in water and centrifuging. After the washing steps, the microspheres were freeze-dried overnight (Alpha 1-2, Martin Christ, Germany).

2.6. Encapsulation of EPO/inulin/Tween-80 particles in PLHMGA microspheres using s/o/w method

Forty four mg of EPO/inulin/Tween-80 (with Tween/EPO molar ratio of 100/1) particles was dispersed in the organic phase consisting of 250 mg PLHMGA (15% w/w EPO/inulin/Tween-80 particles/PLHMGA) dissolved in 0.76 mL of DCM (20% w/w) and homogenized at 20,000 rpm for 30 seconds. The s/o microsuspension was then homogenized in 1.5 mL of 1% PVA in water. The resulting s/o/w emulsion was added dropwise into 7.3 mL of an aqueous solution of 0.5 % PVA and 1% NaCl and left to stir for 3 h to evaporate DCM. Particles were washed and collected as described above for microspheres prepared with the w/o/w method. The prepared microspheres were freeze-dried overnight.

2.7. Encapsulation of EPO/inulin/Tween-80 particles in PLHMGA and SynBiosys microspheres using s/o/o method

Forty four mg of EPO/inulin/Tween-80 (with Tween/EPO molar ratio of 100/1) particles was dispersed in 250 mg PLHMGA (15% w/w; 1:5.6 ratio of EPO/inulin particles to PLHMGA) dissolved in 0.76 mL of DCM (20% w/w) and homogenized at 20,000 rpm for 30 seconds. The s/o microsuspension was then homogenized in 1.5 g of silicone oil (1.5:1.0 w/w silicone oil:DCM) which is a non-solvent for PLHMGA, resulting in coacervation of the polymer. The s/o/o suspension was added dropwise to 50 g of heptane (50:1 w/w heptane:DCM) and stirred for three hours (250 rpm) to extract DCM and silicone oil. The hardened microspheres were washed three times with heptane to remove residual DCM and silicone oil, and were collected by centrifugation at 4,000 rpm for 5 minutes. The remaining heptane was removed by overnight drying of the microspheres *in vacuo*.

EPO loaded SynBiosys (30CP15C20-LL40 and 50CP10C20-LL40) microspheres were prepared by s/o/o method in a similar way as described for PLHMGA s/o/o microspheres. EPO/inulin/Tween-80 (111 mg; with Tween/EPO molar ratio of 100/1) particles (10% w/w; 1:10 ratio of EPO particles to SynBiosys copolymer) were dispersed in DCM in which SynBiosys copolymer was dissolved (4% w/w; 1 g copolymer in 18.2 mL of DCM), followed by homogenization at 14,000 rpm for 60 sec. The formed s/o suspension was homogenized in 36 g of silicone oil (1.5:1.0 w/w silicone oil:DCM). The resulting s/o/o suspension was added dropwise into 1,215 g of heptane (50:1 w/w heptane:DCM) and left to stir for three hours followed by washing steps with heptane as described above and overnight drying *in vacuo*.

2.8. Characterization of the EPO loaded microspheres

The size of the microspheres was measured with an optical particle sizer (Accusizer 780, California, USA). At least 5,000 microspheres were analyzed and the volume-weight mean particle diameter is reported. The morphology of the microspheres was analyzed with scanning electron microscope (SEM, Phenom, FEI Company, The Netherlands). Lyophilized microspheres were transferred onto 12-mm diameter aluminum specimen stubs (Agar Scientific Ltd., England) using double-sided adhesive tape. Prior to analysis, the microspheres were coated with platinum using an ion coater under vacuum. For the loading efficiency of PLHMGA microspheres, 10 mg of microspheres was dissolved in 1 mL of DMSO for one hour at room temperature while gently shaking, as described by Bittner *et al*. [26]. DMSO showed full recovery of EPO when spiked to empty PLHMGA microspheres compared to other solvents (data not shown). The concentration and integrity of EPO was determined by measuring the intensity of the protein bands with Western blot (described in 2.11.). The loading efficiency of SynBiosys microspheres was measured according to a protocol provided by Innocore Pharmaceuticals. In brief, 10 mg of microspheres was dissolved in 0.6 mL of acetonitrile for 15 minutes, followed by centrifugation at 14,000 rpm for 10 min to spin down the protein. The supernatant containing the dissolved polymer was removed and the obtained protein pellet was redispersed in 0.6 mL of acetonitrile. Following another centrifugation step, the final precipitate with the protein was dissolved in 1 mL of PBS and the concentration and integrity of EPO was measured with Western blot.

2.9. In vitro release of EPO from PLHMGA and SynBiosys microspheres

Aliquots of 10 mg of EPO loaded PLHMGA microspheres (corresponding to approximately 17 µg of EPO) were suspended in 1.5 mL of 100 mM phosphate buffered saline (pH 7.4) containing 56 mM NaCl, 35 mM Na_2HPO_4, 65 mM NaH_2PO_4 and 0.05% (w/v) NaN_3 (added to prevent bacterial growth). The *in vitro* release study was performed in triplicate. Microspheres were incubated at 37°C while gently shaking. At different time-points up to 40 days, vials were removed and centrifuged (4,000 rpm for 5 minutes) and 1 mL of the supernatant was removed and 1 mL fresh buffer was added. In another set of microspheres, the release was studied without refreshing the buffer. At each time point one vial was removed, centrifuged and the supernatant was collected. Pellets were dissolved in DMSO, as described in 2.8, and were used for the detection of possible EPO aggregates during the release study. To study the release in different *in vitro* settings, aliquots of 20 mg of SynBiosys microspheres (corresponding to approximately 21 µg of EPO) were dispersed in 1 mL of the release buffer (pH 7.4) and incubated in oven at 37°C while gently shaking. The composition of the release buffer was as follows: 75 mM NaCl, 35 mM NaH_2PO_4, 65 mM Na_2HPO_4, glycine 66 mM and 0.05% NaN_3.

The protein incubated at 37°C in this buffer had a good stability (Supplemental data). At different time-points vials were centrifuged (4,000 rpm for 5 min) and the supernatant was completely replaced with fresh buffer. The release of EPO from SynBiosys microspheres was also analyzed in samples where the buffer was not refreshed. The concentration of the released EPO in the different release samples was measured with ELISA and possible aggregates were detected with Western blot analysis. Integrity of the EPO structure was measured after dissolving the pellets of the remaining microspheres during the *in vitro* study in acetonitrile. The samples were analyzed as described in paragraphs 2.10 and 2.11.

2.10. Quantification of EPO by ELISA

For quantification of EPO by ELISA, a Quantikine® IVD® Human Erythropoietin ELISA kit (R&D Systems, Abingdon, UK) was used according to the protocol provided by the manufacturer. In short, microplate wells pre-coated with mouse anti-human EPO antibody were incubated with standards (concentration ranging from 0 to 200 mIU/mL) and release samples for 1 h on a shaker (500 rpm). The excess sample or standard was removed with washing steps and the wells were then incubated with rabbit anti-human EPO polyclonal antibody conjugated to horseradish peroxidase for 1 h on a shaker (500 rpm). Wells were washed again to remove the excess conjugate and the bound enzyme conjugate was detected by adding a substrate solution (equal volumes of 0.01 N buffered hydrogen peroxide and 0.35 g/L tetramethylbenzidine) that is converted into a blue colored complex by the horseradish peroxidase enzyme. The reaction was stopped by the addition of sulfuric acid solution (the blue color is turned into yellow). The absorbance of this final complex was determined in a microplate reader at 450 nm (FLUOstar OPTIMA, BMG Labtech GMBH, Germany). All data were corrected for background by using a reference wavelength of 600 nm and EPO concentrations were calculated using a calibration curve (2.5-200 mIU/mL corresponding to 0.02-1.64 ng/mL).

2.11. Quantification and characterization of EPO by SDS-PAGE and Western Blot

Anti-EPO immunostaining on Western blot was used, as described by Halim *et al.* [48], to quantify the amount of loaded EPO in the microspheres and to detect the formation of EPO dimers and aggregates during the various steps of the encapsulation processes. An amount of 8 µL of the reconstituted samples (EPO standard, spray dried samples, microspheres dissolved in DMSO or acetonitrile and the *in vitro* release samples) was mixed with 3 µL of non-reducing SDS-PAGE buffer (containing 1M Tris-HCl pH 6.8, 50% glycerol, 10% SDS and 1% bromophenol blue (Bio-Rad, USA)). Samples were loaded on a NuPAGE® Novex® 4-12% Bis-Tris Gel (Life Technologies, USA). The desalted EPO sample was used as a control and for

the calibration curve in concentrations of 16, 8 and 4 µg/mL, whereas prestained protein ladder (PAGERuler, ThermoFisher Scientific, USA) was used as a molecular weight standard. Separation was performed in 1x MOPS SDS running buffer (NuPAGE® Life Technologies, USA) at a voltage of 70 V for 30 minutes followed by 150 V for 60 minutes. After separation, samples were transferred to an iBlot® Transfer Stack (nitrocellulose membrane, 0.2 µm) using the iBlot® Blotting System (Invitrogen, Life Technologies, USA) following the manufacturer's instructions. The membrane was incubated in blocking buffer containing 5% non-fat dry milk (ELK, Campina Melkunie, The Netherlands) in 1xTBS-$T_{0.05}$ (50 mM Tris-HCl, 150 mM sodium chloride and 0.05% (w/v) Tween-20, pH 7.4) for 60 minutes at room temperature with constant orbital shaking. After the washing steps with 1xTBS-$T_{0.05}$ EPO was detected with a primary antibody directed against human EPO (custom made rabbit polyclonal anti-EPO, 10 µg/mL, Biogenes, Germany) in 5% bovine serum albumin (A4503, Sigma-Aldrich, Germany) by overnight incubation at 4°C. The blot was washed four times for 5 minutes with 1xTBS-$T_{0.05}$ and then incubated with anti-rabbit IgG (goat polyclonal, horse-radish peroxidase labeled, 1:2,000, Jackson ImmunoResearch, USA) for 60 minutes at room temperature. After four times wash with 1xTBS-$T_{0.05}$, the blot was exposed to SuperSignal® West Femto Maximum Sensitivity Substrate (1:2 in phosphate buffered saline, ThermoFisher Scientific, USA) for 10 seconds at room temperature. Bands were visualized with a Gel Doc Imaging system equipped with a XRS camera and Quantity One analyses software (Bio-Rad, USA). The intensities of the different bands were quantified with ImageJ software (National Institutes of Health, USA).

3. Results and Discussion

3.1. Characteristics of PLHMGA and SynBiosys copolymers

The synthesized copolymers that were used for the preparation of EPO loaded microspheres had the following characteristics. PLHMGA had a weight average molecular weight of 25 kDa (M_w; relative to polystyrene standards) with a PDI of 2 as measured by GPC. The copolymer composition was 34/66 mol/mol (BMMG/D,L-lactide) as determined with NMR and the glass transition temperature (T_g) was 34°C. SynBiosys 30CP15C20-LL40 multiblock copolymer had an M_w of 35 kDa (relative to PEG standards) with a PDI of 1.6 as measured by GPC. The intrinsic viscosity was 0.6 dL/g and the T_g was -41°C. The copolymer composition as measured with NMR was 65 mol/mol for lactate/PEG ratio and 4 mol/mol for caprolactone/PEG. SynBiosys 50CP10C20-LL40 multiblock copolymer had an M_w of 50 kDa, PDI of 1.6, intrinsic viscosity of 0.8 dL/g and a T_g of -49°C. The copolymer composition was 27 mol/mol for lactate/PEG and 8 mol/mol for caprolactone/PEG.

3.2. Preparation of EPO-inulin sugar glass particles

The sugar glass particles were prepared by spray drying using the settings chosen by a model described by Grasmeijer et al. [36]. An outlet temperature of 35°C was selected at which EPO likely does not aggregate [49,50]. The chosen parameters resulted in EPO-inulin powder with particles of around 1 µm, as measured with SEM (Figure 1A-C) and with a yield between 70-80%. Control particles of inulin only had a smooth surface (Figure 1A), while the addition of EPO resulted in particles with a wrinkled appearance (Figure 1B). In addition, Western blot images showed the presence of dimers and trimers of EPO in the EPO/inulin spray dried formulation, accounting for 30% and 10% relative intensity of the immunostained EPO bands (Figure 1D-II). It was shown that surface morphology of the spray dried particles depends on the relationship between particle surface tension, feed viscosity and sugar crystallization, which are changed upon addition of a protein into the sugar solution [51-53]. Using electron spectroscopy for chemical analysis measurements, the presence of protein was detected on the surface of the spray dried particles, which likely results in protein aggregation [39,54]. This enrichment of protein on the particle surface points to protein adsorption at the water/air interface of the droplets [55]. It has been suggested that structural changes of the protein at the water/air interface occur as a result of protein unfolding exposing the reactive groups, mainly sulfhydryl groups, which are buried in the interior of the protein structure [56]. High concentrations of proteins at interfaces promote conditions favorable for these groups to react forming covalent disulfide bonds. A recent review summarizes observations of protein denaturation at water/air interfaces and their subsequent reactions [57].

EPO (32 kDa glycoprotein hormone) has two disulfide bonds (Cys^{7}-Cys^{161} and Cys^{29}-Cys^{33}) and four polysaccharide chains (3 *N*-glycans and a single *O*-glycan) [58]. In the monomeric EPO molecule no free thiol groups are present. Under denaturating conditions covalent dimerization and aggregation of EPO occurs as a result of intermolecular disulfide interchange initiated by a reduction of the Cys^{7}-Cys^{161} disulfide bond [50]. This type of aggregation is believed to occur as a result of β-elimination of an intact disulfide bridge catalyzed by a hydroxide ion, which results in the formation of free thiols, similar to insulin [59]. The free thiol groups will then reoxidize across two EPO molecules giving dimers. Random intermolecular reoxidation of Cys^{7} and Cys^{161} result in higher molecular weight forms [50]. Factors that influence the reaction of dimerization of EPO in solution are mainly elevated temperature, pH, concentration of protein and buffer composition, while in the solid state it is mainly moisture [60-62].

Adler et al [39] studied whether the addition of a surfactant reduces protein adsorption at the water/air interface in a mixture of trehalose, BSA and Tween-80 during spray drying. Tween-80 preferentially adsorbs at the water/air interface compared to the protein, reducing unfolding and subsequent aggregation

of the protein. Therefore, in order to reduce the formation of dimers and trimers of EPO during spray drying, addition of Tween-80 surfactant to the EPO/inulin solution was studied. Addition of Tween-80 at a 60/1 and 100/1 (mol/mol, Tween-80/EPO) indeed prevented the formation of EPO dimers and trimers (Figure 1D and Table I). Therefore, EPO/inulin/Tween-80 spray dried particles prepared with 100/1 molar ratio of Tween-80 to EPO were used for further encapsulation in PLHMGA and SynBiosys microspheres. The concentration of EPO in these particles was 9.5 µg per mg of spray dried particles as measured with Western blot assay.

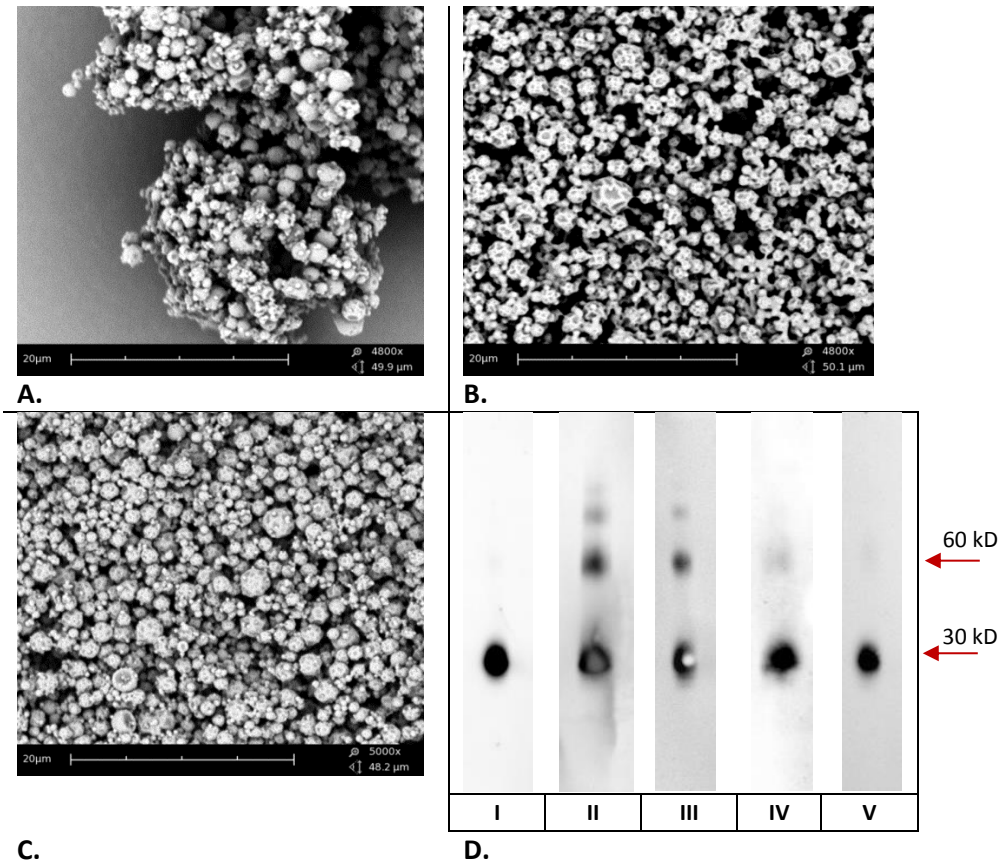

Figure 1. Characteristics of EPO/inulin sugar glass particles. **A-C**. Representative SEM pictures of spray dried particles: **A.** inulin only; **B.** EPO/inulin and **C.** EPO/inulin/Tween-80 (100/1 molar ratio of Tween-80/EPO) and **D**. Western blot images of EPO after spray drying: **I.** EPO standard, **II.** EPO/inulin only particles; and particles with different molar ratios of Tween-80: **III.** 10/1; **IV.** 60/1, **V.** 100/1 (mol/mol Tween-80/EPO).

Table I. Characteristics of EPO/inulin/Tween-80 sugar glass particles prepared with spray drying (inulin concentration= 5 mg/mL; flow= 1mL/min; inlet temp = 80°C; outlet temp = 35°C). Different amounts of Tween-80 were added in order to stabilize EPO during spray drying with inulin. Possible conformational changes of EPO were visualized with Western blot and measured with ImageJ software.

Sugar glass particles	EPO/inulin/ Tween-80 (mg)	Tween-80/ EPO (mol/mol)	Yield (%)	EPO (% ratio between monomer/dimer/trimer)
I.	1/100/0	0/1	71	60/30/10
II.	1/100/0.4	10/1	78	70/25/5
III.	1/100/2.3	60/1	72	92/8/0
IV.	1/100/3.8	100/1	80	100/0/0

3.3. Characteristics of microspheres prepared with w/o/w, s/o/w and s/o/o methods

The characteristics of the EPO-loaded PLHMGA microspheres are given in Figure 2 and Table II. The conventional w/o/w method provided microspheres with a smooth surface and no visible pores. The mean particle diameter was 15 ±1 μm (average of three independently prepared batches; size distribution 8-22 μm). Microspheres prepared using the s/o/w method had a mean diameter of 12 ±1 μm (average of three independently prepared batches; size distribution 6-17 μm). Hence, the encapsulation of solid inulin-based particles with an average size of 1 μm did not affect the second emulsification and solidification processes of the PLHMGA polymeric microspheres. The yield of microspheres for both methods was 60-70%. Larger microspheres were formed with s/o/o method with a mean particle diameter of 31 ±21 μm and a wide size distribution (between 6 and 90 μm). SEM images showed the presence of irregularly shaped PLHMGA microspheres obtained with the s/o/o method (Figure 2) and additionally the yield was also low (35 ±5%; n=3). It has been shown previously that the size and the polydispersity of the microspheres prepared with the s/o/o method depend on the polymer characteristics and can be tailored by the volume ratio between the organic solvent (in which the polymer is dissolved) and the silicone oil [25,63].

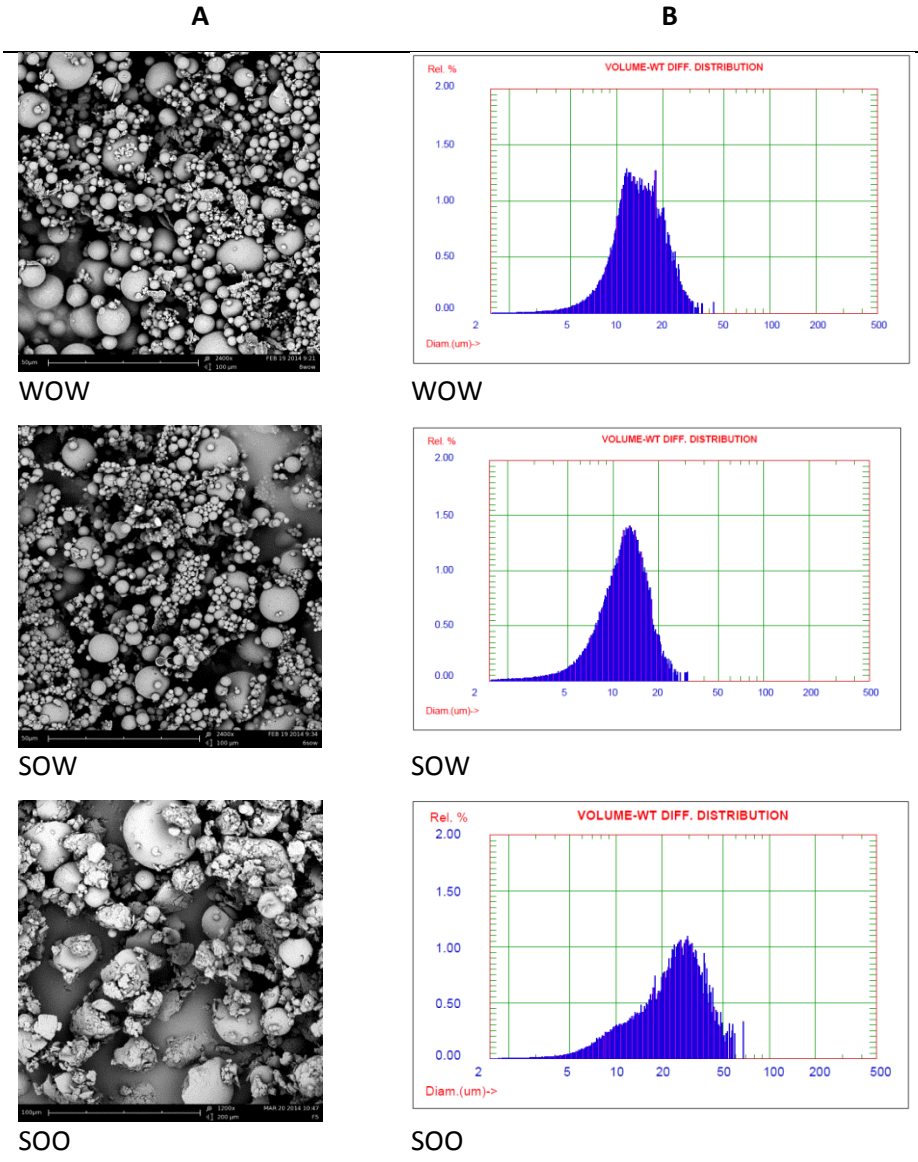

Figure 2. Representative SEM images **(A)** and the volume weight distribution **(B)** of PLHMGA microspheres loaded with EPO/inulin/Tween-80 (1/100/3.8 w/w). Microspheres were prepared with either w/o/w, s/o/w or s/o/o emulsification methods.

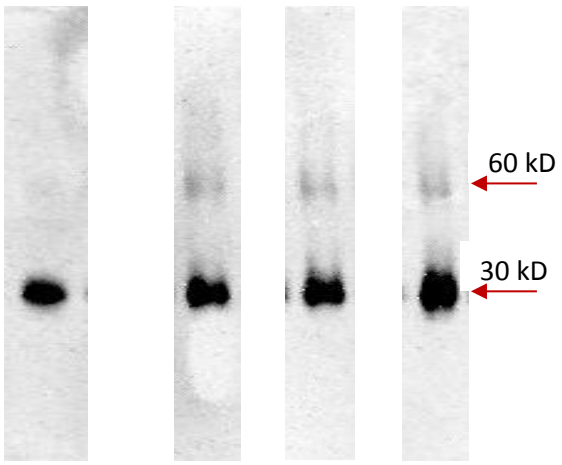

Figure 3. Western blot images of EPO extracted from PLHMGA microspheres prepared with w/o/w, s/o/w or s/o/o method. Percentage of EPO monomer and dimer were semi-quantified by ImageJ software and the results showed approximately 90% of EPO monomer and 10% of EPO dimer for all three formulations.

Table II. Characteristics of PLHMGA microspheres prepared with w/o/w, s/o/w and s/o/o methods (n=3); LE-loading efficiency

Microsphere formulations	Yield (%)	Vol-WT diameter (µm)	Vol-WT cumulative distribution range 10% - 90% of total particle volume (µm)	LE (%)
w/o/w	68 ±4	15 ±1	8-22	87 ±9
s/o/w	61 ±2	12 ±1	6-17	89 ±11
s/o/o	35 ±5	31 ±21	6-90	96 ±4

The loading efficiency and structural integrity of the encapsulated EPO was measured with Western blot after dissolving the PLHMGA microspheres in DMSO. All three microencapsulation methods produced microspheres with high loading efficiency (Table II). Around 88% of EPO was encapsulated using the two methods with an aqueous continuous phase whereas a loading efficiency of 96±4% of EPO was obtained for microspheres prepared with the s/o/o method. EPO dimers were detected in a low extent in all three types of PLHMGA microparticles (Figure 3)

with 7 ±2% of EPO dimers in microspheres prepared with s/o/o method and 11 ±1% in microspheres prepared with s/o/w and w/o/w methods. A high encapsulation efficiency in particles prepared using the s/o/o method has been reported before and is ascribed to the insolubility of protein in the outer oil phase [64], whereas using the s/o/w and w/o/w methods the loss of protein can occur due to extraction by outer water phase [65].

EPO-loaded SynBiosys microspheres were prepared with only s/o/o method and were obtained with a yield of around 70%. The obtained SynBiosys microspheres had a smooth surface with no visible pores (Figure 4). Microspheres prepared with 50CP10C20-LL40 had a mean particle size of 44 ±1 µm (average of two independently prepared batches; size distribution 18-72 µm), while microspheres prepared with 30CP15C20-LL40 co-polymer had a mean size of 27 ±3 µm (average of two independently prepared batches; size distribution 8-50 µm) (Figure 4 and Table III). The EPO loading efficiency was close to 100% in both formulations. Western blot images showed that EPO recovered from SynBiosys microspheres was mainly in its monomeric form with 2% of EPO dimers (Figure 5). Importantly, the three process methods used for the preparation of the different formulations did not differ in the amount of EPO dimers formed (between 7 and 11%). In different publications it was shown that EPO encapsulated in PLGA (and PLGA-type block copolymers) microspheres using a w/o/w method resulted in the substantial formation of dimers, trimers and high molecular weight aggregates when EPO was simply dissolved in water [26,27,29]. Therefore the low extent of dimers in PLHMGA microspheres prepared with w/o/w method in the current study may be due to the presence of inulin and Tween-80 in the inner water phase. Other authors have also shown that the addition of sugar excipients in the first emulsification step reduced aggregation of proteins in PLGA microspheres prepared with w/o/w method [19,66,67].

Table III. Characteristics of SynBiosys microspheres prepared with s/o/o method (n=2). The yield was around 70% for all batches; LE-Loading efficiency.

Type of copolymer	Vol-WT diameter (µm)	Vol-WT cumulative distribution range 10% - 90% of total particle volume (µm)	LE (%)
50CP10C20-LL40	44 ±1	18-72	97
30CP15C20-LL40	27 ±3	8-50	102

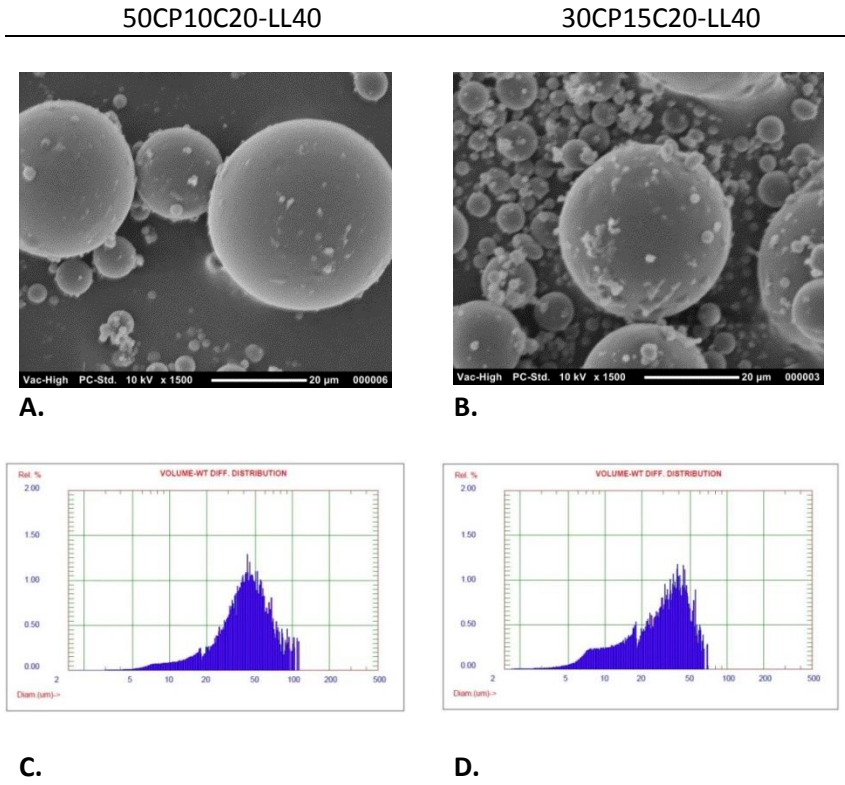

Figure 4. Representative SEM images **(A and B)** and the volume weight distribution **(C and D)** of SynBiosys microspheres loaded with EPO/inulin/Tween-80 (1/100/3.8, w/w) spray dried particles. Microspheres were prepared with s/o/o method.

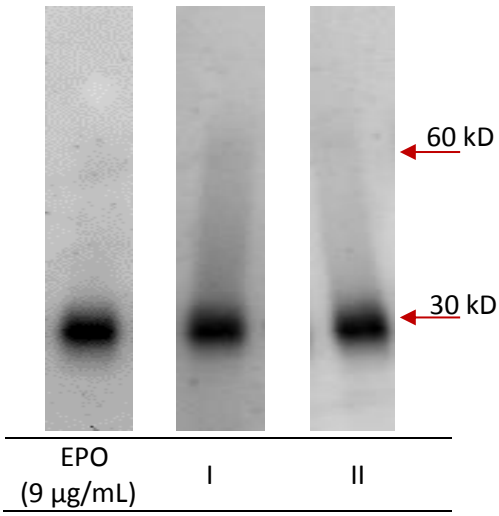

Figure 5. Western blot images of EPO extracted from microspheres prepared with SynBiosys copolymers: **I.** 50CP10C20-LL40 copolymer and **II.** 30CP15C20-LL40 copolymer.

3.4. In vitro release

The *in vitro* release of EPO from the different polymeric microspheres was measured with ELISA. The PLHMGA microspheres were dispersed in 100 mM phosphate buffer. Since we found later that EPO had the highest stability in a phosphate-glycine buffer (Supplemental Figure S1), the latter buffer was used for subsequent *in vitro* release experiments with SynBiosys microspheres. Figure 6 shows that EPO was primarily released during the first day upon incubation from all microsphere formulations. The burst release for the s/o/o PLHMGA microspheres was 29 ±4%, while for s/o/w and w/o/w it was only 8 ±3% and 0.7 ±1.1%, respectively. For SynBiosys microspheres, the burst release was 1.7 ±0.2% (for 30CP15C20-LL40 copolymer) and 2.4 ±0.1% (for 50CP10C20-LL40 copolymer). Western blot images showed the presence of EPO dimers (29/71 ratio monomer/dimer) in the burst release samples of PLHMGA microspheres (s/o/o), whereas mainly the EPO monomer was detected in the burst release samples of SynBiosys microspheres (Figure 7 and 8).

After the initial burst release negligible amounts (< 1%) of released EPO were detected with ELISA at later time-points from all formulations when incubated at 37°C. Western blot images of the release samples of PLHMGA microspheres prepared with s/o/o revealed that EPO dimer was present in the samples up to around 2 weeks while the monomeric EPO was lost after the first week of incubation (Figure 7). No bands were detected with Western blot in the release samples of SynBiosys microspheres (data not shown). Considering the surprising lack of further release after 24 h, the microsphere pellets that had been recovered from the *in vitro* incubations were also analyzed with Western blot. Unexpectedly, when the pellets of the different microspheres were dissolved in DMSO (for PLHMGA) or extracted with acetonitrile (for SynBiosys), no EPO was detected already after 1 day. The absence of EPO release after an initial burst was reported in earlier studies [26-28]. These studies showed an increase in covalent EPO aggregates inside PLGA microspheres during *in vitro* release experiments, as measured with Western blot. The amount of monomeric EPO detected inside microspheres decreased from 10% at day 1 to > 40% at day 32 during the *in vitro* release experiments, suggesting that EPO undergoes a moisture-induced aggregation [28].

As discussed earlier, EPO is quite sensitive to dimerization. As a result of conformational changes of the protein entrapped in polymeric particles that may have occurred during the *in vitro* release studies, the binding epitope might be masked for the monoclonal antibody used in the immunodetection of EPO with ELISA [68]. This could explain why low amounts (< 1%) of EPO were detected with ELISA in the release samples after the burst release.

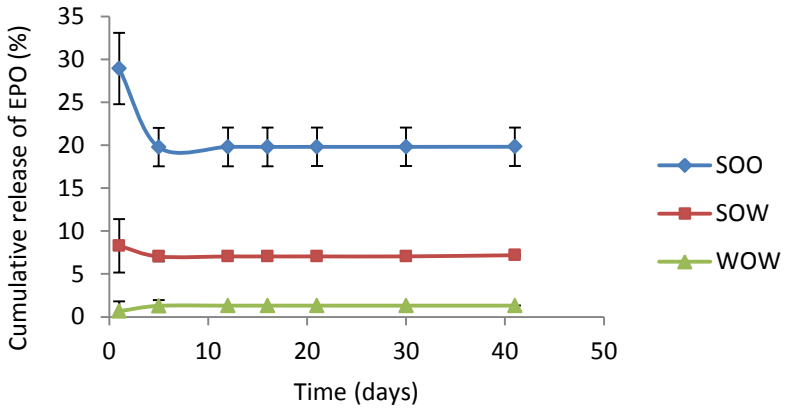

A.

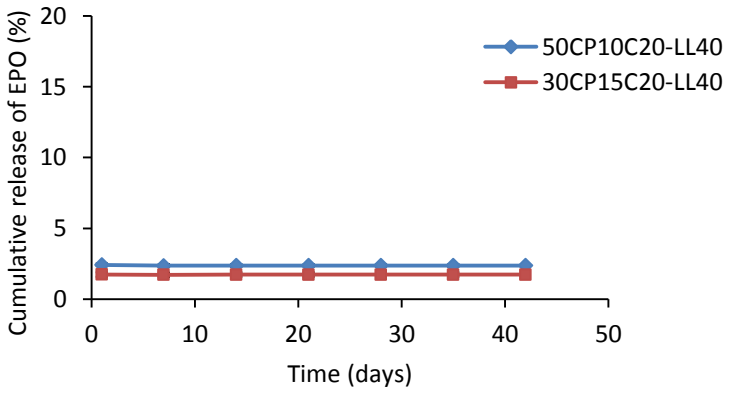

B.

Figure 6. Cumulative release of EPO from **A.** PLHMGA microspheres prepared with w/o/w, s/o/w or s/o/o method and **B.** SynBiosys microspheres prepared with s/o/o method.

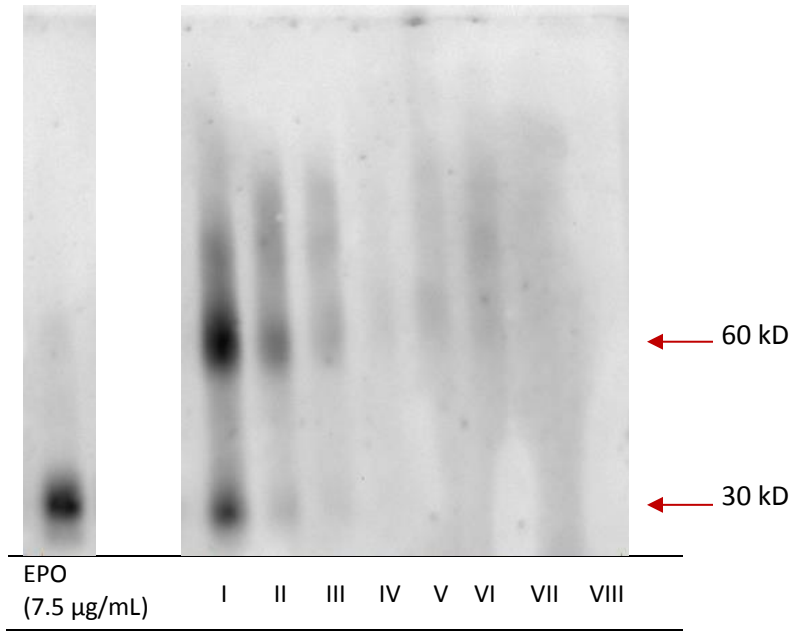

Figure 7. Western blot images of the *in vitro* release samples (supernatants) from PLHMGA microspheres prepared with s/o/o method. Lane **I** through **VIII,** from left to right: 1, 6, 10, 15, 20, 28, 30 and 42 days after incubation. No bands were visible from the extracted microsphere samples (data not shown).

These conformational changes in the structure of EPO might have occurred due to water absorption of the microspheres, which can cause moisture-induced aggregation of proteins loaded in polymeric matrices [27,28,69]. This might be more pronounced when hydrophilic copolymers are used for the encapsulation of the protein in microspheres which show high water absorption [27].

Interestingly, according to Burke *et al*. [70] administration of microspheres which did not show any detectable *in vitro* release of darbepoetin (a hyperglycosylated version of erythropoietin alfa) still yielded elevated serum levels of EPO when injected in rodents. These authors tested the *in vivo* release of the formulated darbepoetin and studied the changes in hemoglobin levels in rats. This *in vivo* study demonstrated the release of bioactive protein up to 4 weeks, as detected in the serum by ELISA, whereas hemoglobin levels remained elevated for over 7 weeks. Sytkowski et al [71] have reported that chemically crosslinked EPO monomers with accessible receptor binding domain resulted in biologically active dimer and trimer species (dimer having 10 times increased activity compared to monomer) with prolonged *in vivo* half-life (24 h compared to 4 h).

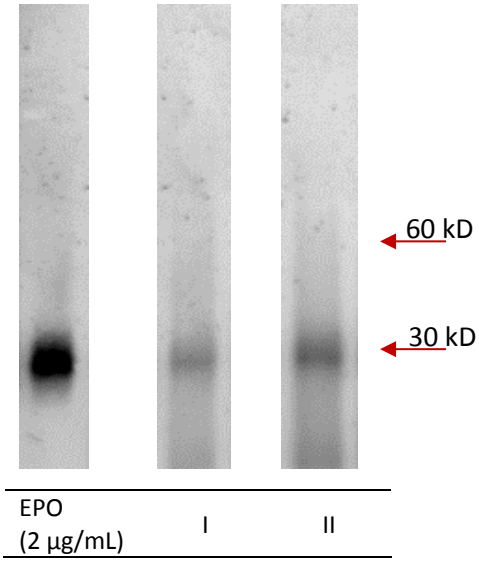

Figure 8. Western blot images of the in vitro burst release samples (supernatants) from SynBiosys microspheres prepared with s/o/o method. **I.** Samples from 50CP10C20-LL40 copolymer and **II.** Samples from 30CP15C20-LL40 copolymer. No bands were visible for later time points or from the extracted microsphere samples (data not shown).

These EPO dimers are thought to facilitate dimerization of the EPO receptor, which is believed to be necessary for generating EPO's intracellular activity [72]. Therefore it is possible that in the present study, the encapsulated EPO inside PLHMGA and SynBiosys microspheres underwent dimerization and multimerization induced upon the presence of water during *in vitro* release. The dimers and trimers of EPO were not measured with ELISA. However, it cannot be excluded that dimers and trimers are pharmacologically active since the EPO receptor is believed to dimerize.

Conclusion

The present study reports the challenges of encapsulating an aggregation prone therapeutic protein, EPO, into polymeric microspheres. Spray dried powder of EPO was encapsulated using three different methods: s/o/o, s/o/w and w/o/w. We demonstrated that no covalent aggregates of EPO were seen when spray dried with inulin and Tween-80 (100/1 molar ratio of Tween-80/EPO). After encapsulation into PLHMGA and SynBiosys microspheres, EPO mainly retained its native structure. However, during the *in vitro* release studies the monomeric form of EPO, detected by ELISA, was rapidly lost. This illustrates the current limitations in the area of polymeric microspheres when using a sensitive model protein, such as the limited sensitive methods for the detection and characterization of small

amounts of the protein. This hampers understanding of possible mechanisms underlying the dimerization and/or aggregation of the encapsulated protein.

Acknowledgments

This research forms part of the Project P3.02 DESIRE of the research program of the BioMedical Materials institute, co-funded by the Dutch Ministry of Economic Affairs.

References:

1. Sinha VR, Trehan A. Biodegradable microspheres for protein delivery. *J Control Release,* 90:261-280, 2003.
2. Gombotz WR, Pettit DK. Biodegradable polymers for protein and peptide drug delivery. *Bioconjug Chem,* 6:332-351, 1995.
3. Ye M, Kim S, Park K. Issues in long-term protein delivery using biodegradable microparticles. *J Control Release,* 146:241-260, 2010.
4. Chen PC, Kohane DS, Park YJ, Bartlett RH, Langer R, Yang VC. Injectable microparticle-gel system for prolonged and localized lidocaine release. II. In vivo anesthetic effects. *J Biomed Mat Res A,* 70:459-466, 2004.
5. Gaignaux A, Réeff J, Siepmann F, Siepmann J, De Vriese C, Goole J, Amighi K. Development and evaluation of sustained-release clonidine-loaded PLGA microparticles. *Int J Pharm,* 437:20-28, 2012.
6. Choi HS, Seo SA, Khang G, Rhee JM, Lee HB. Preparation and characterization of fentanyl-loaded PLGA microspheres: In vitro release profiles. *Int J Pharm,* 234:195-203, 2002.
7. Vaishya R, Khurana V, Patel S, Mitra AK. Long-term delivery of protein therapeutics. *Expert Opin Drug Deliv,* 12:415-440, 2015.
8. Vermonden T, Censi R, Hennink WE. Hydrogels for protein delivery. *Chem Rev,* 112:2853-2888, 2012.
9. Knipe JM, Chen F, Peppas NA. Enzymatic Biodegradation of Hydrogels for Protein Delivery Targeted to the Small Intestine. *Biomacromolecules,* 16:962-972, 2015.
10. Pisal DS, Kosloski MP, Balu-Iyer SV. Delivery of therapeutic proteins. *J Pharm Sci,* 99:2557-2575, 2010.
11. van de Weert M, Hennink WE, Jiskoot W. Protein instability in poly(lactic-co-glycolic acid) microparticles. *Pharm Res,* 17:1159-1167, 2000.
12. Estey T, Kang J, Schwendeman SP, Carpenter JF. BSA degradation under acidic conditions: A model for protein instability during release from PLGA delivery systems. *J Pharm Sci,* 95:1626-1639, 2006.
13. Bakker M, Van De Velde F, Van Rantwijk F, Sheldon RA. Lysozyme microencapsulation within biodegradable PLGA microspheres: Urea effect on protein release and stability. *Biotechnol Bioeng,* 70:270-277, 2000.
14. Schwendeman SP, Shah RB, Bailey BA, Schwendeman AS. Injectable controlled release depots for large molecules. *J Control Release,* 190:240-253, 2014.
15. Jain RA. The manufacturing techniques of various drug loaded biodegradable poly(lactide-co-glycolide) (PLGA) devices. *Biomaterials,* 21:2475-2490, 2000.
16. Ogawa Y, Yamamoto M, Okada H, Yashiki T, Shimamoto T. A new technique to efficiently entrap leuprolide acetate into microcapsules of polylactic acid or copoly(lactic/glycolic) acid. *Chem Pharm Bull,* 36:1095-1103, 1988.
17. van de Weert M, Hoechstetter J, Hennink WE, Crommelin DJA. The effect of a water/organic solvent interface on the structural stability of lysozyme. *J Control Release,* 68:351-359, 2000.
18. Sah H. Protein instability toward organic solvent/water emulsification: Implications for protein microencapsulation into microspheres. *PDA J Pharm Sci Technol,* 53:3-10, 1999.

19. Perez C, Castellanos IJ, Costantino HR, Al-Azzam W, Griebenow K. Recent trends in stabilizing protein structure upon encapsulation and release from bioerodible polymers. *J Pharm Pharmacol,* 54:301-313, 2002.
20. Müller M, Vörös J, Csúcs G, Walter E, Danuser G, Merkle HP, Spencer ND, Textor M. Surface modification of PLGA microspheres. *J Biomed Mater Res A,* 66:55-61, 2003.
21. Leach WT, Simpson DT, Val TN, Anuta EC, Yu Z, Williams III RO, Johnston KP. Uniform encapsulation of stable protein nanoparticles produced by spray freezing for the reduction of burst release. *J Pharm Sci,* 94:56-69, 2005.
22. Partridge J, Moore BD, Halling PJ. a-chymotrypsin stability in aqueous-acetonitrile mixtures: Is the native enzyme thermodynamically or kinetically stable under low water conditions? *J Mol Catal B Enzym,* 6:11-20, 1999.
23. Castellanos IJ, Crespo R, Griebenow K. Poly(ethylene glycol) as stabilizer and emulsifying agent: A novel stabilization approach preventing aggregation and inactivation of proteins upon encapsulation in bioerodible polyester microspheres. *J Control Release,* 88:135-145, 2003.
24. Costantino HR, Firouzabadian L, Hogeland K, Wu C, Beganski C, Carrasquillo KG, Córdova M, Griebenow K, Zale SE, Tracy MA. Protein spray-freeze drying. Effect of atomization conditions on particle size and stability. *Pharm Res,* 17:1374-1383, 2000.
25. Ruiz JM, Busnel JP, Benoit JP. Influence of average molecular weights of poly(DL-lactic acid-co-glycolic acid) copolymers 50/50 on phase separation and in vitro drug release from microspheres. *Pharm Res,* 7:928-934, 1990.
26. Bittner B, Morlock M, Koll H, Winter G, Kissel T. Recombinant human erythropoietin (rhEPO) loaded poly(lactide-co- glycolide) microspheres: Influence of the encapsulation technique and polymer purity on microsphere characteristics. *Eur J Pharm Biopharm,* 45:295-305, 1998.
27. Pistel KF, Bittner B, Koll H, Winter G, Kissel T. Biodegradable recombinant human erythropoietin loaded microspheres prepared from linear and star-branched block copolymers: Influence of encapsulation technique and polymer composition on particle characteristics. *J Control Release,* 59:309-325, 1999.
28. Morlock M, Koll H, Winter G, Kissel T. Microencapsulation of rh-erythropoietin, using biodegradable poly(D,L- lactide-co-glycolide): Protein stability and the effects of stabilizing excipients. *Eur J Pharm Biopharm,* 43:29-36, 1997.
29. Morlock M, Kissel T, Li YX, Koll H, Winter G. Erythropoietin loaded microspheres prepared from biodegradable LPLG-PEO-LPLG triblock copolymers: Protein stabilization and in-vitro release properties. *J Control Release,* 56:105-115, 1998.
30. Kendall RG. Erythropoietin. *Clin Lab Haematol,* 23:71-80, 2001.
31. Patel NSA, Sharples EJ, Cuzzocrea S, Chatterjee PK, Britti D, Yaqoob MM, Thiemermann C. Pretreatment with EPO reduces the injury and dysfunction caused by ischemia/reperfusion in the mouse kidney in vivo. *Kidney Int,* 66:983-989, 2004.
32. Sharples EJ, Patel N, Brown P, Stewart K, Mota-Philipe H, Sheaff M, Kieswich J, Allen D, Harwood S, Raftery M, Thiemermann C, Yaqoob MM. Erythropoietin protects the kidney against the injury and dysfunction caused by ischemia-reperfusion. *J Am Soc Nephrol,* 15:2115-2124, 2004.
33. Bahlmann FH, Fliser D. Erythropoietin and renoprotection. *Curr Opin Nephrol Hypertens,* 18:15-20, 2009.

34. Allison SD, Molina MDC, Anchordoquy TJ. Stabilization of lipid/DNA complexes during the freezing step of the lyophilization process: The particle isolation hypothesis. *Biochim Biophys Acta,* 1468:127-138, 2000.
35. Molina MDC, Armstrong TK, Zhang Y, Patel MM, Lentz YK, Anchordoquy TJ. The stability of lyophilized lipid/DNA complexes during prolonged storage. *J Pharm Sci,* 93:2259-2273, 2004.
36. Grasmeijer N, de Waard H, Hinrichs WL, Frijlink HW. A user-friendly model for spray drying to aid pharmaceutical product development. *PLoS One,* 8:e74403, 2013.
37. Hinrichs WL, Prinsen MG, Frijlink HW. Inulin glasses for the stabilization of therapeutic proteins. *Int J Pharm,* 215:163-174, 2001.
38. de Jonge J, Amorij JP, Hinrichs WLJ, Wilschut J, Huckriede A, Frijlink HW. Inulin sugar glasses preserve the structural integrity and biological activity of influenza virosomes during freeze-drying and storage. *Eur J Pharm Sci,* 32:33-44, 2007.
39. Adler M, Unger M, Lee G. Surface composition of spray-dried particles of bovine serum albumin/trehalose/surfactant. *Pharm Res,* 17:863-870, 2000.
40. Liu Y, Ghassemi AH, Hennink WE, Schwendeman SP. The microclimate pH in poly(D,L-lactide-co-hydroxymethyl glycolide) microspheres during biodegradation. *Biomaterials,* 33:7584-7593, 2012.
41. Stankovic M, Tomar J, Hiemstra C, Steendam R, Frijlink HW, Hinrichs WLJ. Tailored protein release from biodegradable poly(e-caprolactone-PEG)- b-poly(e-caprolactone) multiblock-copolymer implants. *Eur J Pharm Biopharm,* 87:329-337, 2014.
42. Ghassemi AH, Van Steenbergen MJ, Talsma H, Van Nostrum CF, Crommelin DJA, Hennink WE. Hydrophilic polyester microspheres: Effect of molecular weight and copolymer composition on release of BSA. *Pharm Res,* 27:2008-2017, 2010.
43. Ghassemi AH, van Steenbergen MJ, Barendregt A, Talsma H, Kok RJ, van Nostrum CF, Crommelin DJ, Hennink WE. Controlled release of octreotide and assessment of peptide acylation from poly(D,L-lactide-co-hydroxymethyl glycolide) compared to PLGA microspheres. *Pharm Res,* 29:110-120, 2012.
44. Stankovic M, De Waard H, Steendam R, Hiemstra C, Zuidema J, Frijlink HW, Hinrichs WLJ. Low temperature extruded implants based on novel hydrophilic multiblock copolymer for long-term protein delivery. *Eur J Pharm Sci,* 49:578-587, 2013.
45. Samadi N, Van Nostrum CF, Vermonden T, Amidi M, Hennink WE. Mechanistic studies on the degradation and protein release characteristics of poly(lactic-co-glycolic-co-hydroxymethylglycolic acid) nanospheres. *Biomacromolecules,* 14:1044-1053, 2013.
46. Leemhuis M, Van Nostrum CF, Kruijtzer JAW, Zhong ZY, Ten Breteler MR, Dijkstra PJ, Feijen J, Hennink WE. Functionalized poly(a-hydroxy acid)s via ring-opening polymerization: Toward hydrophilic polyesters with pendant hydroxyl groups. *Macromolecules,* 39:3500-3508, 2006.
47. Hissink CE, Steendam R, Meyboom R, Flipsen TAC. Biodegradable multi-block co-polymers. US Patent No. WO2005068533 A1, 2005.
48. Halim LA, Brinks V, Jiskoot W, Romeijn S, Praditpornsilpa K, Assawamakin A, Schellekens H. How bio-questionable are the different recombinant human erythropoietin copy products in Thailand? *Pharm Res,* 31:1210-1218, 2014.
49. Arakawa T, Philo JS, Kita Y. Kinetic and thermodynamic analysis of thermal unfolding of recombinant erythropoietin. *Biosci Biotechnol Biochem,* 65:1321-1327, 2001.

50. DePaolis AM, Advani JV, Sharma BG. Characterization of erythropoietin dimerization. *J Pharm Sci,* 84:1280-1284, 1995.
51. Alexander K, King CJ. Factors governing surface morphology of spray-dried amorphous substances. *Drying Technol,* 3:321-348, 1985.
52. Maa YF, Costantino HR, Nguyen PA, Hsu CC. The effect of operating and formulation variables on the morphology of spray-dried protein particles. *Pharm Dev Technol,* 2:213-223, 1997.
53. Walton DE. Spray-dried particle morphologies. *Dev Chem Eng Miner Process,* 10:323-348, 2002.
54. Webb SD, Golledge SL, Cleland JL, Carpenter JF, Randolph TW. Surface adsorption of recombinant human interferon-gamma in lyophilized and spray-lyophilized formulations. *J Pharm Sci,* 91:1474-1487, 2002.
55. Mumenthaler M, Hsu CC, Pearlman R. Feasibility study on spray-drying protein pharmaceuticals: recombinant human growth hormone and tissue-type plasminogen activator. *Pharm Res,* 11:12-20, 1994.
56. Macritchie F. Proteins at interfaces. *Adv Protein Chem,* 32:283-326, 1978.
57. Pinholt C, Hartvig RA, Medlicott NJ, Jorgensen L. The importance of interfaces in protein drug delivery - Why is protein adsorption of interest in pharmaceutical formulations? *Expert Opin Drug Deliv,* 8:949-964, 2011.
58. Lai PH, Everett R, Wang FF, Arakawa T, Goldwasser E. Structural characterization of human erythropoietin. *J Biol Chem,* 261:3116-3121, 1986.
59. Costantino HR, Langer R, Klibanov AM. Moisture-induced aggregation of lyophilized insulin. *Pharm Res,* 11:21-29, 1994.
60. Lai MC, Topp EM. Solid-state chemical stability of proteins and peptides. *J Pharm Sci,* 88:489-500, 1999.
61. Derby PL, Strickland TW, Rohde MF, Stoney K, Rush RS. Identification of the residues involved in homodimer formation of recombinant human erythropoietin. *Int J Pept Protein Res,* 47:201-208, 1996.
62. Endo Y, Nagai H, Watanabe Y, Ochi K, Takagi T. Heat-induced aggregation of recombinant erythropoietin in the intact and deglycosylated states as monitored by gel permeation chromatography combined with a low-angle laser light scattering technique. *J Biochem,* 112:700-706, 1992.
63. Ruiz JM, Tissier B, Benoit JP. Microencapsulation of peptide: a study of the phase separation of poly(d,l-lactic acid-co-glycolic acid) copolymers 50/50 by silicone oil. *Int J Pharm,* 49:69-77, 1989.
64. Carrasquillo KG, Carro JCA, Alejandro A, Toro DD, Griebenow K. Reduction of structural perturbations in bovine serum albumin by non-aqueous microencapsulation. *J Pharm Pharmacol,* 53:115-120, 2001.
65. King TW, Patrick Jr. CW. Development and in vitro characterization of vascular endothelial growth factor (VEGF)-loaded poly(DL-lactic-co-glycolic acid)/poly(ethylene glycol) microspheres using a solid encapsulation/single emulsion/solvent extraction technique. *J Biomed Mater Res,* 51:383-390, 2000.
66. Tomar P, Giri N, Karwasara VS, Pandey RS, Dixit VK. Prevention of structural perturbation and aggregation of hepatitis B surface antigen: Screening of various additives. *Pharm Dev Technol,* 17:421-428, 2012.

67. Pérez-Rodriguez C, Montano N, Gonzalez K, Griebenow K. Stabilization of a-chymotrypsin at the CH2Cl2/water interface and upon water-in-oil-in-water encapsulation in PLGA microspheres. *J Control Release,* 89:71-85, 2003.
68. Elliott S, Chang D, Delorme E, Dunn C, Egrie J, Giffin J, Lorenzini T, Talbot C, Hesterberg L. Isolation and characterization of conformation sensitive antierythropoietin monoclonal antibodies: Effect of disulfide bonds and carbohydrate on recombinant human erythropoietin structure. *Blood,* 87:2714-2722, 1996.
69. Schwendeman SP, Tobío M, Joworowicz M, Alonso MJ, Langer R. New strategies for the microencapsulation of tetanus vaccine. *J Microencapsul,* 15:299-318, 1998.
70. Burke PA, Klumb LA, Herberger JD, Nguyen XC, Harrell RA, Zordich M. Poly(lactide-co-glycolide) microsphere formulations of darbepoetin alfa: Spray drying is an alternative to encapsulation by spray-freeze drying. *Pharm Res,* 21:500-506, 2004.
71. Sytkowski AJ, Lunn ED, Davis KL, Feldman L, Siekman S. Human erythropoietin dimers with markedly enhanced in vivo activity. *Proc Natl Acad Sci U S A,* 95:1184-1188, 1998.
72. Livnah O, Stura EA, Johnson DL, Middleton SA, Mulcahy LS, Wrighton NC, Dower WJ, Jolliffe LK, Wilson IA. Functional mimicry of a protein hormone by a peptide agonist: The EPO receptor complex at 2.8 Å. *Science,* 273:464-471, 1996.

Supplemental data

Aim: To investigate the effect of different release buffers and different temperatures on the stability of EPO.

Method: EPO was first dissolved in a 100 mM phosphate buffer (pH 7.4) in a concentration of 16 µg /mL and incubated at 37°C for up to 4 weeks. In a second experiment EPO (1 µg/mL) was dissolved in a 100 mM phosphate buffer supplemented with 66 mM glycine and 0.23 mM Tween-80 and the samples were incubated at 37°C. The phosphate buffer had the following composition: 35 mM NaH_2PO_4, 65 mM Na_2HPO_4, 75 mM NaCl. At predetermined time-points one sample was removed, centrifuged (4,000 rpm for 5 min) and the supernatant was analyzed with ELISA and Western blot.

Results: The results obtained with ELISA and Western blot are given in Supplemental Figure S1. Within 2 weeks around 70% of EPO monomer was lost when incubated in 100 mM PBS buffer, whereas only 30% was lost when incubated in 100 mM PBS-glycine-Tween-80 buffers. Western blot images showed the presence of EPO dimers upon 1 week (100 mM PBS buffer) and 2 weeks (100 mM PBS-glycine-Tween-80 buffers) of incubation period.

Conclusion: After 2 weeks some dimerization of EPO occurs when incubated at 37°C in all tested buffers. Around 30% of EPO incubated in PBS-only and 70% of EPO incubated in 100 mM PBS-glycine-Tween-80 was detectable with ELISA within 2 weeks of the study period. These results show that addition of glycine and Tween-80 in a PBS buffer improved the stability of EPO monomer.

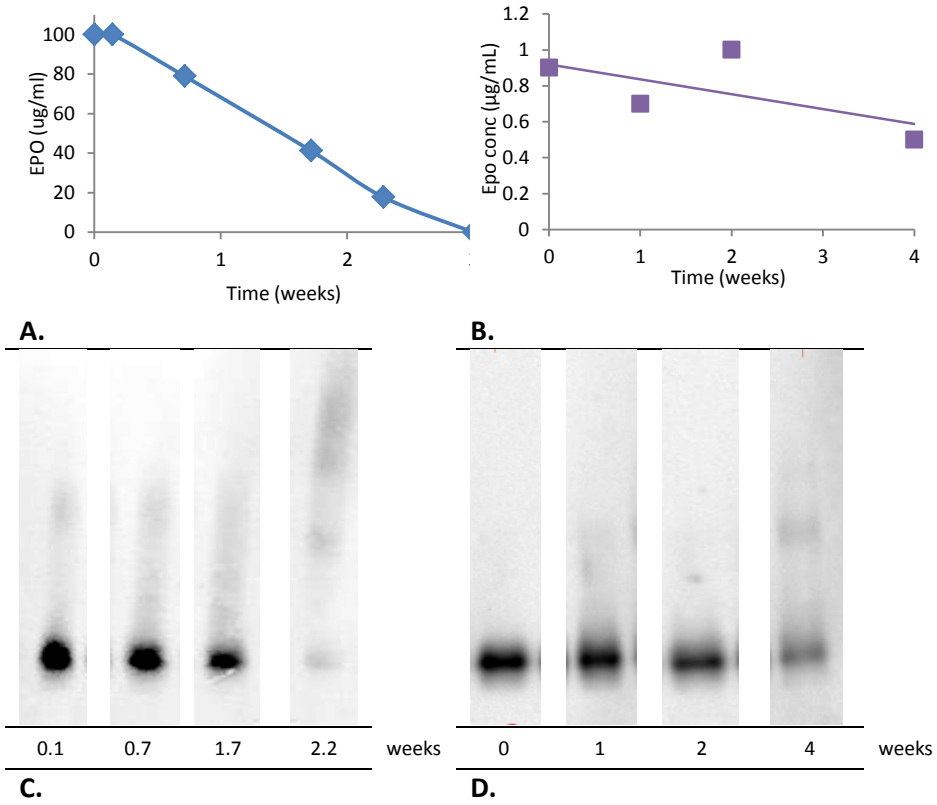

Supplemental Figure S1. Concentration of EPO over time measured with ELISA and Western blot when incubated at 37°C in **A and C.** PBS-only and **B and D.** PBS-glycine-Tween-80 buffer.

Chapter 6

Summary and Future Perspectives

1. Summary

The work described in this thesis was part of the project DESIRE (Device for Smart Intervention in Renal Repair), which was financed by Dutch public-private consortium BioMedical Materials. The aim of DESIRE was to develop a polymeric delivery system that can be injected under the kidney capsule and hence can deliver drug locally into the kidney. Such an approach is attractive for treatment of acute kidney injury, with the aim to prevent the development of chronic kidney disease. Among others, one of the research outputs of the DESIRE project was the subcapsular renal delivery of a small molecular weight drug, rapamycin, loaded in polymeric microspheres. Rapamycin administered in this way under the renal capsule of rats with unilateral ureter obstruction (UUO) showed a reduction in the influx of inflammatory cells in the kidney and inhibited the local fibrotic response in UUO model [1]. Most importantly, the adverse effects of rapamycin where reduced in comparison to the systemically administered rapamycin [1]. The conclusion of this work was that microspheres injected under the kidney capsule can be used for local delivery of antifibrotic small molecular drugs. Apart from small molecular weight drugs, anti-inflammatory therapeutic proteins can also be used for treatment of kidney diseases. Therefore, the delivery of therapeutic proteins encapsulated in polymeric microspheres to the kidney was the scope of the studies described in this thesis.

The advantages of protein therapeutics when compared to small-molecule drugs are significant. First and most important, proteins are characterized by a highly specific mechanism of action when interacting with pharmacological receptors. This implies a lower probability for a protein therapeutic to interfere with unintended biological processes and to cause severe side effects. Because many of the proteins that are intended to be used as therapeutics are endogenous compounds, they are often well tolerated and less likely to induce an immune response. For these and other reasons, research on protein therapeutics today is a key area of focus in development of new drugs [2]. Notwithstanding of their attractiveness, however, protein therapeutics also present some major challenges that need to be overcome. Generally speaking, proteins are structurally unstable and susceptible to conformational changes during their production, formulation and handling [3,4]. These conformational changes refer to a number of degradation mechanisms which may also negatively impact safety, since they can result in immune responses towards the protein [5,6]. Degradation mechanisms that can result in protein instability can be chemical (oxidation, deamidation, proteolysis, beta-elimination and disulfide scrambling) or physical (denaturation, aggregation, insoluble particle formation and adsorption at interfaces [3]. Furthermore, due to their low or absent bioavailability after oral delivery, proteins are mainly administered through parenteral routes (intravenous, intramuscular or subcutaneous) [7]. This is, however, inconvenient for the patient and therefore

needle-free alternative routes are being explored, including oral, transdermal, rectal, nasal and pulmonary [8-10]. Because of large size, hydrophilicity and poor permeability of proteins across biological membranes, non-invasive routes are however challenging for the delivery of proteins. Even dosing by parenteral administration can be challenging for proteins. Due to their sensitive and complex structure, proteins are susceptible to enzymatic degradation, which may result in short half-lives requiring frequent administrations to maintain therapeutic levels. In addition, small proteins (< 30 kDa) can undergo rapid renal elimination (from few minutes to hours). Frequent parenteral administrations are not patient compliant, especially in the treatment of chronic diseases. Drug delivery systems can be used to overcome the above mentioned challenges and issues [8,11]. This thesis focuses on polymeric microspheres as drug delivery systems and describes important characteristics required to encapsulate proteins. In addition, subcapsular renal injection is described as a possible local delivery method of therapeutic proteins to potentially treat kidney diseases.

An ideal drug delivery system should provide sustained drug levels of the therapeutic protein in blood and/or target tissue for an extended time-period following a single injection. In addition a suitable delivery system should ensure the stability of the encapsulated protein and maintain its biologically active conformational structure after being released. The most popular and extensively studied polymer for the preparation of protein-loaded microspheres is poly(lactic-co-glycolic acid) (PLGA). In **Chapter 2,** the influence of formulation parameters of PLGA microspheres on the release of a model macromolecule, blue dextran, is investigated. PLGA microspheres were prepared with a membrane emulsification method, which generates microspheres with a small size distribution (‘monodisperse’). A computer modelling assisted design artificial neural network (ANN) and gene expression programming (GEP) analysis was applied to design and formulate PLGA microspheres that would result in a continuous release of blue dextran from monodisperse PLGA microspheres. The results described in **Chapter 2** show that highly porous particles showed a sustained release of blue dextran, this was also associated with a high burst release (~20-40% of the total blue dextran loading) and low loading efficiency (< 50%). GEP analysis predicted the formulation characteristics (15% w/w of PLGA in the oil phase, 16% of the inner water volume and 3% of PVA in the continuous phase) that generated microspheres with a controlled porosity and an almost zero order release of blue dextran for a period of three months. The release was due to a combination of porosity (early stage) and degradation (late stage) of the particles. Importantly a high loading efficiency (70%) and low burst release (9%) were achieved. Cumulatively, this study provides information on the relationship between different formulation characteristics and particle porosity, and how to fine-tune them in order to obtain a desired release profile of an encapsulated macromolecule from monodisperse PLGA microspheres.

In our department poly(D,L-lactic-*co*-hydroxymethyl glycolic acid) (PLHMGA), a hydrophilic aliphatic polyester based on lactic acid and glycolic acid with pendant hydroxyl groups, has been developed and studied as an alternative for PLGA [12,13]. Nanoparticles and microspheres based on this polymer have been investigated for the loading and release of peptides and proteins [14-17]. **Chapter 3** describes the preparation of monodisperse PLHMGA microspheres with the above referred membrane emulsification method and by conventional single emulsion method. The biocompatibility of these PLHMGA microspheres (with either narrow or broad size distribution) was investigated after subcutaneous and renal subcapsular implantation in rats. The obtained results showed that microspheres prepared with membrane emulsification method had a volume weight mean diameter of 34 µm and a narrow size distribution (30-38 µm) compared to PLHMGA microspheres prepared with a conventional single emulsion method, which resulted in particles with a rather broad distribution (5-46 µm; volume weight mean diameter of 17 µm). Both microsphere formulations showed good cytocompatibility properties when incubated with skin fibroblasts (PK-84) as well as with kidney tubular and epithelial cells (HK-2 and PTECs). PLHMGA microspheres lead to only a mild foreign body reaction after subcutaneous injection in rats. It was further observed that microspheres degraded within 28 days post injection. The inflammatory reaction observed within this period had the character of a transient response to the implanted material and a fibrous capsule was not observed at the injection site.

In **Chapter 3**, the relation between the particle size distribution and intensity of the inflammatory reaction towards injected polymeric microspheres was also studied. The results demonstrate that polydisperse PLHMGA microspheres lead to a slightly increased recruitment of macrophages and increased vascularization compared to monodisperse PLHMGA microspheres upon subcutaneous implantation in rats. However, no significant differences were observed in the overall inflammatory reaction in the tissues injected with these two formulations. Similar to the reaction after a subcutaneous injection, when monodisperse PLHMGA microspheres were injected under the kidney capsule, a mild inflammatory reaction was observed. Importantly, the inflammatory cells were localized only at the implantation site between the cortex and the renal capsule. Cumulatively, the results of **Chapter 3** show that PLHMGA microspheres can be safely used *in vivo* as a drug delivery system after subcutaneous or subcapsular renal injection.

Subcapsular renal injection studied in **Chapter 3** is a relatively novel administration method being investigated for local delivery of therapeutics to the kidney. Moreover, it is also challenging to predict the fate of protein therapeutics released from subcapsular depots, as the studies conducted so far have mainly reported on pharmacological outcome and not on pharmacokinetic profiles. **Chapter 4** of this thesis investigates the feasibility of near-infrared imaging to

follow the sustained release of proteins from PLHMGA microspheres in the kidney and to study the subsequent redistribution of the released protein in the body. As a model protein, near infrared labeled BSA (NIR-BSA) was used. Since the aim was to evaluate the *in vivo* release profile of NIR-BSA from the PLHMGA microspheres, a protocol was established for quantification of 1) NIR-BSA isolated from intact microspheres in the kidney homogenates and 2) NIR-BSA that had been released into the kidney parenchyma and/or redistributed in the circulation or other organs. The results of this study show that the NIR signal from PLHMGA microspheres was visible at the injected site in the kidney for the 3-week study period. A continuous release of around 90% of NIR-BSA loading was observed from the injected depot within a period of 2 weeks. This was faster than what was measured *in vitro* (38% release in 2 weeks). SDS-PAGE analysis of the samples showed that mainly the intact protein was released from the injected PLHMGA microspheres. NIR-BSA was metabolized in the liver and subsequently the degradation products were cleared by the kidneys. In conclusion, this study shows that locally administered PLHMGA microspheres injected under the kidney capsule are characterized by a 2-week release period. As such they are an attractive system to deliver proteins locally to kidneys.

In order to test how the formulation and the *in vitro* release conditions of polymeric microspheres affect the aggregation of proteins, model proteins such as albumin or lysozyme are often used [18,19]. However, these model proteins are known to be relatively stable and therefore the results obtained might not be translated to cases where more sensitive therapeutic proteins are used. **Chapter 5** of this thesis describes the challenges in formulating an aggregation prone protein, erythropoietin (EPO), into polymeric microspheres. It is well known that EPO aggregates during w/o/w formulation into PLGA microspheres as a result of the presence of water in the first w/o emulsion where EPO tends to adsorb at the water/organic solvent interface [20-22]. Therefore, in **Chapter 5**, alternative methods were explored which avoid the use of water in the inner phase of the particles (s/o/w) or that are even completely water-free (s/o/o). In this study, EPO was first formulated into a dry powder by spray drying an aqueous solution of inulin (0.5% w/v) and Tween-80 (EPO/inulin/Tween-80 weight ratio of 1/100/3.8). The obtained sugar glass particles of EPO/inulin/Tween-80 were subsequently encapsulated into PLHMGA microspheres using w/o/w, s/o/w or s/o/o method. Concurrently the sugar glass particles of EPO were formulated into SynBiosys microspheres with s/o/o method. SynBiosys polymers are block co-polymers consisting of relatively short polylactide blocks intercalated with polyethyleneglycol/caprolactone blocks, which ensures a polymeric network controlling the release of the protein by swelling and erosion [23]. The obtained microspheres had a smooth surface with no visible pores. The mean particle size varied between 10-44 µm and a high loading efficiency was achieved for all formulations (between 88-100%). Only small amounts of EPO dimers (between 2-

11%) were formed during the three different preparation methods. The low dimer formation of EPO during w/o/w formulation observed in **Chapter 5** is likely to be explained by the stabilization of the protein in presence of inulin and Tween-80 in the inner water phase. When PLHMGA microspheres prepared with either of the three methods were incubated at 37°C in a PBS buffer, they showed only a burst release of EPO (between 1-30% of the protein loading) and no further release was detected with ELISA. Incubation of SynBiosys microspheres prepared with s/o/o method in a PBS-glycine buffer showed a similar release profile: around 2% of EPO was released as a burst and no further release was detected. A possible explanation for the lack of sustained EPO release is that upon hydration of microspheres during *in vitro* release studies, EPO can undergo a moisture-induced covalent aggregation resulting in the formation of dimers, trimers and higher-order oligomers. However, it is possible that as shown in literature [24], these higher order structures of EPO are pharmacologically active.

2. Future Perspectives

The results described in **Chapter 5** of this thesis show that it is possible to successfully encapsulate a therapeutic protein in polymeric microspheres. However, some further improvements should be pursued in future studies in order to preserve the stability of EPO upon encapsulation and release. For example, other additives, such as arginine and hydroxypropyl-β-cyclodextrin [21], could be added to improve the stability of EPO in the microspheres. As it was already discussed in **Chapter 5**, the aggregation of EPO is most likely to occur by forming covalent disulfide bonds. Therefore, one approach to reduce this aggregation could be limiting the formation of free thiols, which are likely formed during β-elimination of an intact disulfide bridge catalyzed by a hydroxide ion [25]. Lowering the pH prior to lyophilization of protein solution might be beneficial in reducing aggregation through disulfide interchange, as was reported elsewhere [25].

A significant number of proteins have been studied as potential drugs for the treatment of renal diseases. These include proteins such as IL-10 [26,27], BMP-7 [28,29], anti-TGFβ [30], interferon-γ [31] and EPO [32-34]. All these therapeutic proteins could serve as potential candidates for encapsulation into polymeric microspheres. A next step in assessing the feasibility of polymeric microspheres as drug delivery systems targeting kidney disease could be pharmacological studies in suitable animal models. Such studies would provide a proof of principle, in animals, that the treatment delivered in this manner is effective. A hint that subcapsular renal administration of polymeric microspheres results in a local therapeutic effect of the encapsulated drug is already provided by a study from Falke et al. [1]. It will be of great interest to obtain anti-inflammatory or antifibrotic effects in an animal model of renal disease with therapeutic proteins loaded in the polymeric microspheres discussed in this thesis. Eventually, if

pharmacology studies in rodents are successful, the feasibility of subcapsular renal implantation to treat acute kidney injury and chronic kidney diseases can subsequently be tested in larger animals and finally, in humans. In this respect, implantation of such a device under the kidney capsule can be done when the patient already undergoes surgery (i.e. during acute stenosis of the ureter). Other approach would be to identify minimally invasive surgical techniques that can be used for implantation under the kidney capsule. Some of the most recent techniques in renal surgery include imaging guided (ultrasound and magnetic resonance imaging) surgery and robotic laparoscopic surgery. These surgical methods show promising results in nephrectomy (surgical removal of tumor tissues in kidney), kidney biopsies and kidney transplantation [35-38].

3. Conclusion

PLHMGA microspheres are attractive delivery system of proteins for local administration in the kidney and can serve as a depot providing a continuous release of the protein in the kidney for several weeks. The subcapsular renal injection of this delivery system has the potential to reduce side effects of therapeutic proteins by increasing their presence at the site of injection and decreasing it elsewhere in the body.

References:

1. Falke LL, Van Vuuren SH, Kazazi-Hyseni F, Ramazani F, Nguyen TQ, Veldhuis GJ, Maarseveen EM, Zandstra J, Zuidema J, Duque LF, Steendam R, Popa ER, Kok RJ, Goldschmeding R. Local therapeutic efficacy with reduced systemic side effects by rapamycin-loaded subcapsular microspheres. *Biomaterials,* 42:151-160, 2014.
2. Leader B, Baca QJ, Golan DE. Protein therapeutics: A summary and pharmacological classification. *Nat Rev Drug Discov,* 7:21-39, 2008.
3. Jeong SH. Analytical methods and formulation factors to enhance protein stability in solution. *Arch Pharm Res,* 35:1871-1886, 2012.
4. Cicerone MT, Pikal MJ, Qian KK. Stabilization of proteins in solid form. *Adv Drug Deliv Rev,* 2015.
5. Hermeling S, Crommelin DJA, Schellekens H, Jiskoot W. Structure-immunogenicity relationships of therapeutic proteins. *Pharm Res,* 21:897-903, 2004.
6. Sauerborn M, Brinks V, Jiskoot W, Schellekens H. Immunological mechanism underlying the immune response to recombinant human protein therapeutics. *Trends Pharmacol Sci,* 31:53-59, 2010.
7. Patel A, Cholkar K, Mitra AK. Recent developments in protein and peptide parenteral delivery approaches. *Ther Deliv,* 5:337-365, 2014.
8. Patel A, Patel M, Yang X, Mitra AK. Recent advances in protein and peptide drug delivery: A special emphasis on polymeric nanoparticles. *Protein Pept Lett,* 21:1102-1120, 2014.
9. Kammona O, Kiparissides C. Recent advances in nanocarrier-based mucosal delivery of biomolecules. *J Control Release,* 161:781-794, 2012.
10. Milewski M, Manser K, Nissley BP, Mitra A. Analysis of the absorption kinetics of macromolecules following intradermal and subcutaneous administration. *Eur J Pharm Biopharm,* 89:134-144, 2015.
11. Škalko-Basnet N. Biologics: The role of delivery systems in improved therapy. *Biologics,* 8:107-114, 2014.
12. Leemhuis M, Van Nostrum CF, Kruijtzer JAW, Zhong ZY, Ten Breteler MR, Dijkstra PJ, Feijen J, Hennink WE. Functionalized poly(a-hydroxy acid)s via ring-opening polymerization: Toward hydrophilic polyesters with pendant hydroxyl groups. *Macromolecules,* 39:3500-3508, 2006.
13. Leemhuis M, Kruijtzer JAW, van Nostrum CF, Hennick WE. In vitro hydrolytic degradation of hydroxyl-functionalized poly(a-hydroxy acid)s. *Biomacromolecules,* 8:2943-2949, 2007.
14. Ghassemi AH, van Steenbergen MJ, Barendregt A, Talsma H, Kok RJ, van Nostrum CF, Crommelin DJ, Hennink WE. Controlled release of octreotide and assessment of peptide acylation from poly(D,L-lactide-co-hydroxymethyl glycolide) compared to PLGA microspheres. *Pharm Res,* 29:110-120, 2012.
15. Rahimian S, Fransen MF, Kleinovink JW, Christensen JR, Amidi M, Hennink WE, Ossendorp F. Polymeric nanoparticles for co-delivery of synthetic long peptide antigen and poly IC as therapeutic cancer vaccine formulation. *J Control Release,* 203:16-22, 2015.
16. Ghassemi AH, van Steenbergen MJ, Talsma H, van Nostrum CF, Jiskoot W, Crommelin DJA, Hennink WE. Preparation and characterization of protein loaded microspheres

based on a hydroxylated aliphatic polyester, poly(lactic-co-hydroxymethyl glycolic acid). *J Control Release,* 138:57-63, 2009.
17. Samadi N, Van Nostrum CF, Vermonden T, Amidi M, Hennink WE. Mechanistic studies on the degradation and protein release characteristics of poly(lactic-co-glycolic-co-hydroxymethylglycolic acid) nanospheres. *Biomacromolecules,* 14:1044-1053, 2013.
18. Bakker M, Van De Velde F, Van Rantwijk F, Sheldon RA. Lysozyme microencapsulation within biodegradable PLGA microspheres: Urea effect on protein release and stability. *Biotechnol Bioeng,* 70:270-277, 2000.
19. Estey T, Kang J, Schwendeman SP, Carpenter JF. BSA degradation under acidic conditions: A model for protein instability during release from PLGA delivery systems. *J Pharm Sci,* 95:1626-1639, 2006.
20. Pistel KF, Bittner B, Koll H, Winter G, Kissel T. Biodegradable recombinant human erythropoietin loaded microspheres prepared from linear and star-branched block copolymers: Influence of encapsulation technique and polymer composition on particle characteristics. *J Control Release,* 59:309-325, 1999.
21. Morlock M, Koll H, Winter G, Kissel T. Microencapsulation of rh-erythropoietin, using biodegradable poly(D,L- lactide-co-glycolide): Protein stability and the effects of stabilizing excipients. *Eur J Pharm Biopharm,* 43:29-36, 1997.
22. Bittner B, Morlock M, Koll H, Winter G, Kissel T. Recombinant human erythropoietin (rhEPO) loaded poly(lactide-co- glycolide) microspheres: Influence of the encapsulation technique and polymer purity on microsphere characteristics. *Eur J Pharm Biopharm,* 45:295-305, 1998.
23. Stankovic M, Tomar J, Hiemstra C, Steendam R, Frijlink HW, Hinrichs WLJ. Tailored protein release from biodegradable poly(e-caprolactone-PEG)- b-poly(e-caprolactone) multiblock-copolymer implants. *Eur J Pharm Biopharm,* 87:329-337, 2014.
24. Sytkowski AJ, Lunn ED, Davis KL, Feldman L, Siekman S. Human erythropoietin dimers with markedly enhanced in vivo activity. *Proc Natl Acad Sci U S A,* 95:1184-1188, 1998.
25. Costantino HR, Langer R, Klibanov AM. Moisture-induced aggregation of lyophilized insulin. *Pharm Res,* 11:21-29, 1994.
26. Deng J, Kohda Y, Chiao H, Wang Y, Hu X, Hewitt SM, Miyaji T, McLeroy P, Nibhanupudy B, Li S, Star RA. Interleukin-10 inhibits ischemic and cisplatin-induced acute renal injury. *Kidney Int,* 60:2118-2128, 2001.
27. Soranno DE, Lu HD, Weber HM, Rai R, Burdick JA. Immunotherapy with injectable hydrogels to treat obstructive nephropathy. *J Biomed Mater Res A,* 102:2173-2180, 2014.
28. Vukicevic S, Basic V, Rogic D, Basic N, Shih M-, Shepard A, Jin D, Dattatreyamurty B, Jones W, Dorai H, Ryan S, Griffiths D, Maliakal J, Jelic M, Pastorcic M, Stavljenic A, Sampath TK. Osteogenic protein-1 (bone morphogenetic protein-7) reduces severity of injury after ischemic acute renal failure in rat. *J Clin Invest,* 102:202-214, 1998.
29. Dankers PYW, Hermans TM, Baughman TW, Kamikawa Y, Kieltyka RE, Bastings MMC, Janssen HM, Sommerdijk NAJM, Larsen A, Van Luyn MJA, Bosman AW, Popa ER, Fytas G, Meijer EW. Hierarchical formation of supramolecular transient networks in water: A modular injectable delivery system. *Adv Mater,* 24:2703-2709, 2012.

30. Rodell CB, Rai R, Faubel S, Burdick JA, Soranno DE. Local immunotherapy via delivery of interleukin-10 and transforming growth factor ß antagonist for treatment of chronic kidney disease. *J Control Release,* 206:131-139, 2015.
31. Yao Y, Zhang J, Tan DQ, Chen XY, Ye DF, Peng JP, Li JT, Zheng YQ, Fang L, Li YK, Fan MX. Interferon-γ improves renal interstitial fibrosis and decreases intrarenal vascular resistance of hydronephrosis in an animal model. *Urology,* 77:761.e8-761.e13, 2011.
32. Vesey DA, Cheung C, Pat B, Endre Z, Gobé G, Johnson DW. Erythropoietin protects against ischaemic acute renal injury. *Nephrol Dial Transplant,* 19:348-355, 2004.
33. Johnson DW, Vesey DA, Gobe GC. Erythropoietin protects against acute kidney injury and failure. *Open Drug Discov J,* 2:8-17, 2010.
34. Bahlmann FH, Fliser D. Erythropoietin and renoprotection. *Curr Opin Nephrol Hypertens,* 18:15-20, 2009.
35. Greco F, Autorino R, Rha KH, Derweesh I, Cindolo L, Richstone L, Herrmann TRW, Liatsikos E, Sun Y, Fanizza C, Nagele U, Stolzenburg J-, Rais-Bahrami S, Liss MA, Schips L, Kassab A, Wang L, Kallidonis P, Wu Z, Young ST, Mohammed N, Haber G-, Springer C, Fornara P, Kaouk JH. Laparoendoscopic single-site partial nephrectomy: A multi-institutional outcome analysis. *Eur Urol,* 64:314-322, 2013.
36. Galloway Jr. RL, Duke Herrell S, Miga MI. Image-guided abdominal surgery and therapy delivery. *J Healthc Eng,* 3:203-228, 2012.
37. Tsai MK, Lee CY, Yang CY, Yeh CC, Hu RH, Lai HS. Robot-assisted renal transplantation in the retroperitoneum. *Transplant Int,* 27:452-457, 2014.
38. Uppot RN, Harisinghani MG, Gervais DA. Imaging-guided percutaneous renal biopsy: Rationale and approach. *Am J Roentgenol,* 194:1443-1449, 2010.

Appendices

Nederlandse Samenvatting
Acknowledgments
List of Publications
Curriculum Vitae

Nederlandse Samenvatting

Nierziektes komen tegenwoordig steeds meer voor in samenhang met de algemene stijging van andere ziektes zoals diabetes en hart- en vaatziektes. Behandeling van nierziekte richt zich allereerst op het op het wegnemen van de onderliggende oorzaak, maar daarnaast ook op het behouden van een goede nierfunctie. De nieren spelen een belangrijke rol bij het filteren van afvalstoffen uit het bloed, het reguleren van de bloeddruk en in de productie van rode bloedcellen in het lichaam. Wanneer de nieren hun functie verliezen, accumuleren afvalstoffen in het lichaam en dit kan weer tot levensbedreigende problemen leiden. Als nierziekten niet goed behandeld worden kan dit uiteindelijk leiden tot een volledig verlies van de nierfunctie (nierfalen). Dan resteert vaak nog slechts vervanging van de nierfunctie, door nierdialyse of een niertransplantatie. Beide opties hebben hun eigen nadelen en resulteren in een lage kwaliteit van leven van patiënten. Er is daarom een grote behoefte aan nieuwe behandelstrategieën die de progressie van nierziekten stoppen en nierfalen kunnen voorkomen.

Dit proefschrift beschrijft de ontwikkeling van polymere microsferen voor de gereguleerde afgifte van therapeutische eiwitten onder het nierkapsel. Er zijn verschillende therapeutische eiwitten die gebruikt kunnen worden bij de behandeling van nierziektes. Doorgaans worden dit soort farmaca toegediend als intraveneuze injecties, wat zeker bij herhaalde toediening belastend is. Polymere microsferen kunnen dienen als depotpreparaat voor geneesmiddelafgifte, zowel voor kleine moleculen als voor grote moleculen zoals eiwitten. Een depotinjectie van polymere microsferen toegediend onder het nierkapsel kan het eiwit gedurende meerdere weken afgeven. De lokale werking in de nier zal het aantal benodigde injecties sterk verminderen. De studies beschreven in dit proefschrift zijn onderdeel van het project DESIRE (Device for Smart Intervention in Renal Repair), dat werd gefinancierd door het Nederlandse publiek-private consortium BioMedical Materials (BMM). Het doel van DESIRE is om een nieuwe behandelmethode voor nierziektes te ontwikkelen, gebaseerd op lokale geneesmiddelafgifte onder het nierkapsel.

Het copolymeer van melkzuur en glycolzuur (poly(lactic-co-glycolic acid; PLGA) is een van de meest onderzochte biomaterialen voor gecontroleerde geneesmiddelafgifte. Er zijn al diverse depotpreparaten ontwikkeld die met PLGA gemaakt zijn, vooral voor afgifte van kleine geneesmiddelen en peptiden. De moleculen die ingesloten zijn in dit type microsferen worden vrijgelaten in drie fasen: de eerste snelle vrijgifte heet het ”burst-effect”en wordt gekenmerkt door een snelle afgifte binnen de eerste 24 uur; deze wordt vaak gevolgd door een fase zonder vrijgifte (de ”lag-fase”) die bij veel PLGA systemen ongeveer 1 maand duurt. Dan volgt tot slot de vrijgiftefase. Deze gefaseerde afgifte leidt tot verschillende geneesmiddelspiegels in de loop van de afbraak van de deeltjes. Een meer constante en continue afgifte zorder burst en lag-fase heeft doorom de

voorkeur. In **Hoofdstuk 2** hebben we geanalyseerd hoe we PLGA microsferen met zo'n verbeterd afgifteprofiel kunnen maken. De microsferen werden gemaakt met een relatief nieuwe methode, zogeheten membraan-emulsificatie, waarbij een niet met water mengbare oplossing van het polymeer via een membraan wordt geëmulgeerd in water met daarin andere hulpstoffen. Een voordeel van deze membraan-emulsificatie techniek is dat de gevormde druppeltjes en uiteindelijk ook de microsferen allemaal dezelfde grootte hebben, wat gunstig is voor de injecteerbaarheid van het depotpreparaat. In plaats van een therapeutisch eiwit hebben we een model-molecuul gebruikt, namelijk een blauw gekleurd macromolecuul (dextraan-blauw). De eigenschappen van de polymere microsferen hebben we met een artificiële neuraal-netwerk benadering geanalyseerd, waarmee we een relatie konden leggen tussen de formuleringscondities, de eigenschappen van de microsferen en de afgifte van het ingesloten dextraan-blauw. De verkregen resultaten toonden aan dat vooral de porositeit van de microsferen belangrijk was voor een continue afgifte van dextraan-blauw. Het maken van dit type deeltjes kon vervolgens gestuurd worden door de juiste formuleringscondities vooraf goed af te stemmen.

In **Hoofdstuk 3** werden microsferen gemaakt met PLHMGA (poly(D,L-lactic-co-hydroxymethyl glycolic acid), een nieuw type polymeer dat afgeleid is van polymelkzuur. PLHMGA heeft meer hydrofiele eigenschappen dan PLGA waardoor het beter geschikt is voor de afgifte van eiwitten. In dit hoofdstuk wordt beschreven hoe PLHMGA microsferen gemaakt kunnen worden met de membraan-emulsificatie methode en met een gewone emulsificatie methode waarbij de gevormde deeltjes niet allemaal een gelijke grootte hebben. Beide soorten PLHMGA mirosferen zijn getest op hun biocompatibiliteit, ofwel hoe goed dit soort materialen verdragen worden als ze in contact gebracht worden met cellen (in vitro) of na toediening aan ratten (in vivo). Bij het testen in ratten hebben we zowel subcutane toediening onderzocht als de injectie onder het nierkapsel. De microsferen werden goed verdragen door de gekweekte cellen (in vitro) en in de proeven met ratten. PLHMGA microbolletjes werden gedegradeerd binnen 28 dagen na de injectie en veroorzaakten slechts een milde ontstekingsreactie in het geïnjecteerde gebied. Met deze resultaten wordt aangetoond dat PLHMGA microsferen veilig kunnen worden gebruikt in dierstudies.

De injectie onder het nierkapsel is een relatief nieuwe manier om geneesmiddelen lokaal af te geven aan de nieren. Er is daarom slechts weinig bekend over de farmacokinetiek van eiwitten na zo'n soort toediening. In **Hoofdstuk 4** van dit proefschrift hebben we de afgifte van een eiwit vanuit PLHMGA microsferen onder het nierkapsel onderzocht. In deze studie hebben we een gelabeld albumine als modeleiwit in PLHMGA microsferen ingesloten. Het label dat aan albumine gekoppeld was kan middels nabij-infrarode fluorescentie spectroscopie worden aangetoond, een gevoelige detectiemethode waarmee het

gelabelde eiwit zowel in bloed als in organen zonder ingewikkelde zuiveringsmethodes gemeten kan worden. We hebben een protocol ontwikkeld waarmee we verder onderscheid kunnen maken tussen gelabeld eiwit dat nog in intacte PLHMGA microsferen aanwezig is in de weefsels en gelabelde albumine afgegeven aan het nierparenchym. De resultaten van deze studie tonen aan dat PLHMGA microsferen het gelabelde albumine gedurende twee weken vrijgeven, en dat het eiwit na vrijgifte in de nieren wordt afgegeven aan het bloed en vervolgens in de lever gemetaboliseerd wordt. De afbraakproducten verschijnen uiteindelijk in de urine. Deze studie laat zien dat PLHMGA microsferen als zodanig dus in staat zijn om eiwitten gedurende een aantal weken lokaal af te geven in de nieren.

Vaak worden modeleiwitten gebruikt om de formuleringscondities van polymere microsferen te testen. Deze modeleiwitten zijn echter relatief stabiel in vergelijking met therapeutische eiwitten. **Hoofdstuk 5** van dit proefschrift beschrijft de uitdagingen bij het formuleren van een model-therapeutisch eiwit dat wel gevoelig is voor aggregatie. Dit eiwit is erytropoëtine (EPO). Het is bekend dat EPO aggregeert tijdens emulsificatie in PLGA microsferen en dat de aanwezigheid van water in de microsferen daarbij een rol speelt. Daarom hebben we alternatieve methoden voor het maken van polymere microsferen onderzocht waarbij het water in de inwendige fase van de deeltjes is vervangen door andere hulpstoffen. EPO werd eerst geformuleerd in een droog poeder door het te sproeidrogen met inuline, met Tween-80 als stabilisator. De verkregen suikerglasdeeltjes werden vervolgens in polymere microsferen verwerkt met verschillende emulsificatiemethodes. Behalve PLHMGA polymere microsferen werden ook microsferen gemaakt met SynBioSys® blokcopolymeren. De stabiliteit van het EPO tijdens de verschillende bereidingstappen werd onderzocht door niet-geaggregeerd EPO en dimeren van elkaar te scheiden middels gel-electroforese en vervolgens op een Western blot met immunodetectie te kwantificeren. Deze analyses lieten zien dat het EPO grotendeels intact was in de uiteindelijke formuleringen. Er werden slechts kleine hoeveelheden EPO dimeer aangetoond in de suikerglasdeeltjes en de polymere microsferen. Wanneer de polymere microsferen bij 37°C geïncubeerd werden voor het bestuderen van de EPO afgifte, werd er echter alleen een snelle burst-afgifte gemeten gedurende de eerste dag, variërend van 1-30% van de belading afhankelijk van de formuleringsmethode. De verdere verwachte continue afgifte werd niet waargenomen, ook niet bij microsferen die geen burst-afgifte lieten zien. Een mogelijke verklaring voor het ontbreken van EPO afgifte is dat EPO alsnog in de microsferen is gaan aggregeren onder invloed van water dat de deeltjes in is gediffundeerd tijdens het afgifte experiment.

Samenvattend kan gesteld worden dat polymere microsferen aantrekkelijke afgiftesystemen zijn voor de lokale toediening van eiwitten. Subcapsulaire injectie van PLHMGA microsferen lijkt een interessante manier om gedurende enkele weken een therapeutisch eiwit lokaal af te geven, zodat er een

sterke werking in de nieren is en potentieële bijwerkingen elders in het lichaam kunnen worden voorkomen.

Acknowledgments

My PhD story started one day when Agon came with some brochures from the Utrecht University. Among these was the Drug Innovation master course brochure which caught my eye immediately. After a few months I found myself in Utrecht driving a second hand bike under a heavy October rain. When I first came to the Netherlands for a Master's degree, I felt lost with all the new and advanced research methods. I remember our master study coordinator Ed Moret asking, in one of his lectures, how many of us will continue PhDs. Because I always wanted to do a PhD, I caught myself raising a hand and being skeptical at the same time. Upon finishing this book now, I cannot stop thinking how far I have come. For this I am grateful to a lot of people from which I have learned along the way.

In the end of 2009 I started my PhD studies in the Department of Pharmaceutics under the supervision of Wim, Robbert Jan and Rene. All three of them continually suggested, recommended, criticized and guided my research project. Wim, with his critical thinking and his "why's", always made me look for the answer and understand the details of everything that I did. Rene was helpful with his knowledge about synthesis and preparation of microspheres, and Robbert Jan was always there to discuss several ups and downs of our project. I will be eternally grateful to all three of you because you made it possible for me to be in an exciting and interesting project where I had the opportunity to learn, conduct state of the art research and collaborate with many other researchers.

I started to work in the lab within the first weeks of my PhD. Here, I cannot continue without thanking Mies, our head technician, whom I called every time something was broken, missing or when I was simply lost. Therefore, I did not dare to complain about the loud music when his Friday afternoons come. Whenever I needed to work at weekends, I remember him saying that my planning is improper. In future, he can use a quote I heard recently "If you're working day and night you ain't doing it right".

In the lab, I joined Hajar, a then third year PhD student teaching synthesis to Kimberley, who I have to thank for introducing me to the process of combining chemicals and for the fun chats and talks that we had afterwards. I remember her sitting next to the column and collecting samples from morning till evening. These were very long days when you would dream of joining your bed and pillow. Unfortunately, Hajar didn't see days of the ready-columns and automatic sample collector as she had finished her PhD by then. My following tutor was Amir G, another last year PhD student, who taught me how to prepare microspheres. By then, I realized that almost all the last year students were pretty stressed. And no wonder; I remember during the first meetings when I joined Amir G at a big round table with Wim, Daan, Here, Robbert Jan, Rene, Amir, Amir's two students Kiara and Manish, and I. Any further explanation is needless. During that time there were other last year PhD students as well, Marina, Amir V, Albert, Emmy, Roberta,

to name but a few, and we would learn from them about many different challenges of doing a PhD.

Synthesis and microspheres carried on until in one of the meetings Wim inquired about my first article. This is how we came up with the idea to study the microsieve technology, where I worked with Audrey, Sergio and Gert from Nanomi. Located in the far east of the Netherlands (reached by couple of trains, a bus and 20 minute walk), it was the most comfortable lab I have worked in. These people taught me their unique techniques for preparation of microspheres with PLGA. I am sort of proud that I quickly reached their daily record for preparation of batches. As they were professional in the preparation of round and uniform spheres, it was difficult to convince them that some of my batches had to have polydisperse and broken microspheres. This work resulted in a total of 32 batches, separated into around 400 Eppendorf vials and each of them analyzed for more than 20 different characteristics. This large amount of information was difficult to handle, but we were fortunate to have Mariana Landin, a professor from Spain, in our department working specifically with bunch of data. I have to thank her for making everything easier to explain and understand. This enabled us to finish the study which resulted in the first published article of this PhD.

Meanwhile, we continued with new experiments, this time in Groningen, in the far north of the country. With the group of Eliane Popa we studied the biocompatibility of our PLHMGA polymer. For this we needed grams of polymer and this meant more synthesis and more columns. There were lots of fluctuations with this research but thanks to Eliane's genuine support and with the help of Jurjen and Roel we, finally, answered the very essential question "Is your polymer safe?".

Things got more and more exciting in the third year. We planned our third experiment, an *in vivo* study, to obtain some important answers for our project. For this we did not go very far but stayed in Utrecht, thanks to the group of prof. Roel Goldschmeding in the UMCU. Stefan and Dione were in the operating room, Ebel, Farshad and I were collecting samples. The writing following the experiment took some more time than expected, as I had my first daughter, Eda. This was when we needed all the help that we could get and I had to thank our parents which made it a bit easier to catch up with the new routine. Interestingly, Maryam was also pregnant and we had a lot of things to chat about. And by now Stefan was also an experienced dad.

Working pregnant in a synthesis lab is not an easy task, but I am very thankful to all my considerate colleagues who warned me of dangerous smells and noises. This thoughtfulness carried on at the lunch table with advices on what to eat, drink, stay calm and relax. According to Edu, I had to get ready for many sleepless nights, but I was also lucky to have Mehrnoosh around as an experienced PhD-mom. The lunch table was something we looked forward to in between work with all the internationals, and Merel. There was Luis telling about Portugal, Yang

drinking tea with only hot water, Andhyk giving healthy tips, Anastasia with her exotic travelling, Sima my neighbor from Mazandaran, Neda my other neighbor from Tehran, Rachel with her perfect English and Mereltje our Dutch friend. In few occasions Işıl and Burçin would also join us for lunch. Thanks to these ladies, I really did not miss talking in my own language. And please don't ask me anymore how I know Turkish, it's just complicated.

In the following year and the last experiment in this project, it was exciting and at times nerve-wrecking to go for the most difficult task, encapsulation of an unstable protein. For this we went back to Groningen in the group of prof. Erik Frijlink and Wouter Hinrichs. I thank Niels for being helpful in the preparation of particles with spray drying and the chats while waiting for the equipment. I would also like to thank Rob and Christine from Innocore for their part with the Synbiosis polymers. Everybody knew that this was challenging and additionally, because I had to move to another country I was unable to finish everything that I planned. Luckily a former PhD from Utrecht, Marco van de Weert, was already working in Copenhagen University, and I have to thank him for letting me join his group to continue finishing this last chapter of my project. With many new and future mom and dads I fitted in nicely in his department. Thanks to Marco and his experience, we managed to finish this chapter with some very valuable research findings. I was also lucky to have Andhyk and Jurjen back in Utrecht for their support.

In the middle of writing the thesis book, Stina was born and we had to readjust to the new routine again through the help of our parents. However, thanks to my supervisors we could find means to overcome the distance and finally set a date for my defence. So after 4 and a couple of years, it seems that time has come to part ways with Utrecht, but again I can and will always find an excuse to come back. Some excuses I already have: I have to come back for Sima's wedding, Işıl has a new house and Marcus still has to send his mom's recipe for the cheesecake. Besides this I can't forget Audrey who moved to the beautiful Montpelier and also Sun with whom we are sharing the same birthday and passion for food.

And what would I do without Barbara's help! All the forms, mails, papers, everything passes through the hands of this lovely lady. I look forward to her next visit to Denmark and hope by then my children will be friendlier with dogs. Lastly, I wish to mention Sima and Rachel who are my paranymphs and my second hands. I am really happy to walk with you in this last day of my PhD. Hope to see you more often as I miss our chats a lot.

I am glad we chose to come to Utrecht and I would choose it again anytime. Now I remember with a delight the day when Agon and I set on the airport with huge bags waiting for our flight to be announced. Without saying anything we were both thinking about this huge step that we were about to take without knowing where it will lead us. I just want to say thank you Agon for being there with me as whatever I do it is easier when you are around. "..një jetë me ty

dhe asgjë u bë gjithçka papritur, e dua një jetë me ty.” Last but not least, a special thanks to our daughters Eda and Stina, I hope that one day you will have as much fun in your graduate studies as your parents did.

I will never forget these years in Utrecht and I thank all of you for taking part in them. I hope our paths will cross again in the future.

List of Publications

- **Kazazi-Hyseni** F, van Vuuren SH, van der Giezen DM, Pieters EH, Ramazani F, Rodriguez S, Veldhuis GJ, Goldschmeding R, van Nostrum CF, Hennink WE, Kok RJ. Release and pharmacokinetics of near-infrared labeled albumin from monodisperse poly(D,L-lactic-*co*-hydroxymethyl glycolic acid) microspheres after subcapsular renal injection. *Acta Biomaterialia*, 22:141-154, Aug 2015.

- Ramazani F, Hiemstra C, Steendam R, **Kazazi-Hyseni** F, Van Nostrum CF, Storm G, Kiessling F, Lammers T, Hennink WE, Kok RJ. Sunitinib microspheres based on [PDLLA-PEG-PDLLA]-*b*-PLLA multi-block copolymers for ocular drug delivery. *European Journal of Pharmaceutics and Biopharmaceutics*, doi: 10.1016/j.ejpb.2015.02.011.

- Falke LL, van Vuuren SH, **Kazazi-Hyseni** F, Ramazani F, Nguyen TQ, Veldhuis GJ, Maarseveen EM, Zandstra J, Zuidema J, Duque LF, Steendam R, Popa ER, Kok RJ, Goldschmeding R. Local therapeutic efficacy with reduced systemic side effects by rapamycin-loaded subcapsular microspheres. *Biomaterials*, 42:151-160, Feb 2015

- **Kazazi Hyseni** F, Zandstra J, Popa ER, Goldschmeding R, Lathuile AA, Veldhuis GJ, Van Nostrum CF, Hennink WE, Kok RJ. Biocompatibility of poly(D,L-lactic-*co*-hydroxymethyl glycolic acid) microspheres after subcutaneous and subcapsular renal injection. *International Journal of Pharmaceutics*, 482:99-109, Mar 2015.

- **Kazazi Hyseni** F, Landin M, Lathuile A, Veldhuis GJ, Rahimian S, Hennink WE, Kok RJ, van Nostrum CF. Computer modelling assisted design of monodisperse PLGA microspheres with controlled porosity affords zero order release of an encapsulated macromolecule for 3 months. *Pharmaceutical Research,* 31:2844-2856, Oct 2014.

- **Kazazi-Hyseni** F, Beijnen JH, Schellens JHM. Bevacizumab. *Oncologist*, 15:819-825, 2010.

- **Kazazi Hyseni** F, Halkes SBA, Quarles van Ufford HC, Beukelman CJ, van den Berg AJJ. Remming van de activiteit van xanthine-oxidase door Filipendula-soorten. *Nederlands tijdschrift voor fytotherapie*, 23:17-18, 2010.

List of Abstracts

- **Kazazi Hyseni** F, van Vuuren SH, van der Giezen DM, Pieters EHE, Ramazani F, Rodriguez S, Veldhuis GJ, Goldschmeding R, van Nostrum CF, Hennink WE, Kok RJ. The fate of a protein encapsulated in polymeric microspheres after subcapsular renal administration. *Wetenschappelijk najaarssymposium, Nederlandse Federatie voor Nefrologie,* Oct 2013, Utrecht, The Netherlands.

- **Kazazi Hyseni** F, Kok RJ, Landin M, Lathuile A, Veldhuis GJ, Rahimian S, Hennink WE, van Nostrum CF. Membrane emulsification method: designing monodisperse particles with optimal release profile. *Dutch Polymer Days*, Mar 2013, Lunteren, The Netherlands.

- **Kazazi Hyseni** F, Kok RJ, Landin M, Lathuile A, Veldhuis GJ, Rahimian S, Hennink WE, van Nostrum CF. Designing monodisperse particles with optimal release profile by changing the particle porosity. *Annual Meeting & Exposition, Controlled Release Society*, Jul 2013, Honolulu, Hawaii.

- **Kazazi Hyseni** F, Lathuile A, Veldhuis GJ, Landin M, Hennink WE, van Nostrum CF, Kok RJ. Optimization of monodisperse microparticles by ANN. *FIGON Dutch Medicine Days*, Oct 2012, Lunteren, The Netherlands.

- **Kazazi Hyseni** F, Lathuile A, Veldhuis GJ, Hennink WE, van Nostrum CF, Kok RJ. Membrane emulsification method: designing monodisperse particles with optimal release profile. *12th European Symposium on Controlled Drug Delivery,* Apr 2012, Egmond aan Zee, The Netherlands.

- **Kazazi Hyseni** F, Lathuile A, Veldhuis GJ, Hennink WE, Kok RJ, van Nostrum CF. Monodisperse microspheres of biodegradable poly(lactic-*co*-hydroxymethyl-glycolic acid) for controlled release of proteins. *Dutch Polymer Days*, Mar 2012, Lunteren, The Netherlands.

- **Kazazi Hyseni** F, van Nostrum CF, Kok RJ, Hennink WE. Biodegradable poly(lactic-co-hydroxymethyl glycolic acid) microspheres for controlled release of anti-inflammatory drugs in the treatment of renal diseases. *i-Polymer Materials*, May 2010, Rolduc, The Netherlands.

Curriculum Vitae

Filis Kazazi Hyseni was born on 24 November 1979 in Prizren, Kosovë. She graduated from the Faculty of Pharmacy in Pristina University and obtained her Master of Pharmacy diploma in June 2005. Thereafter she worked as a pharmacist in a pharmacy in Peje and as a Medical Representative for Hoffman La Roche in Pristina. In September 2007 she moved to the Netherlands to study Masters in Drug Innovation in Utrecht University, where she recieved the Utrecht Excellence Scholarship. During this time, she performed scientific research at the Medicinal Chemistry Department in Utrecht University and in Schering Plaugh in Oss. She obtained her Master's diploma in 2009. Thereafter, in November of the same year she started her doctorate studies at the Pharmaceutical Department in Utrecht University in a BMM project named DESIRE. The results of this project are described in this thesis.